UNIVERSITÄT DUISBURG-ESSEN
LEHRSTUHL FÜR TECHNISCHE CHEMIE II

Microfiltration Membranes via Electrospinning of Polyethersulfone Solutions

Dissertation

zur Erlangung des akademischen Grades

Dr. rer. nat.

der Fakultät für Chemie

der Universität Duisburg-Essen

vorgelegt von M.Sc. BINTASAN KWANKHAO

geboren am 27.02.1979 in Thailand

Essen 2013

Microfiltration Membranes via Electrospinning of Polyethersulfone Solutions

By

M. Sc. Bintasan Kwankhao

Thesis submitted to the Department of Chemistry of University of Duisburg-Essen, in partial fulfillment of the requirements of the degree of
Dr. rer. nat.

Approved by the examining committee on
Chair: Prof. Dr. Christian Mayer
Advisor: Prof. Dr. Mathias Ulbricht
Reviewer: Prof. Dr. Jochen S. Gutmann
Date of oral examination: 12.11.2013

Abstract

Nanofibers or nanowebs produced by electrospinning have several prominent properties such as high surface area to volume ratio, high porosity and pore size in nanorange. As the porosity of electrospun nanoweb is more than 90%, they are candidates for air filters and liquid filtration membranes. However, the application of electrospun nanofibers membranes has yet to make breakthrough in other avenues of separation than air filtration, especially in pressure-driven liquid separations, such as ultrafiltration (UF) or nanofiltration (NF).

In this project, the preparation of polyethersulfone (PES) membranes by electrospinning was studied. The influence of processing parameters, i.e., polymer concentration, applied voltage, flow rate, spinneret-to-collector distance, relative humidity, were investigated. The treatment of the proto-membrane formed by immersion in an aqueous coagulation bath was also studied. More comprehensive characterizations of the nanofiber membranes, including fiber diameter, pore size, porosity, thickness, basic weight and tensile strength as well as air and water permeability were investigated. Thereby, we expect that this work will open up the avenue toward the use of nanofibers for very important applications of separation technology. Of particular interest are membranes in water purification, e.g., pre-filters to minimize contaminations and fouling prior to ultra- or nano-filtration.

PES (Ultrason 6020P) was dissolved in N-methyl-2-pyrrolidone (NMP) at concentrations of 9%, 15%, 22%. The polymer solution was electrospun under processing conditions i.e., a spinneret-to-collector distance of 10 cm, an applied voltage of 30 kV, a flow rate of 20 µL/min, and a spinneret diameter of 0.8 mm, stationary substrate set-up, aluminum foil and PET nonwoven served as the substrate. The first results showed that the 22% PES solution can be electrospun into well-defined nanofiber. The overall morphology of the membranes obtained is changed from a fiber network into spherical particles connected by fibers with the decrease of the polymer concentration in the solution used for electrospinning. The properties of nanofiber can be measured on aluminum foil or PET nonwoven as substrate. Image analyses gave a mean fiber diameter of 489 ± 142 nm but under stationary spinning conditions that leads to a 3 dimensional fiber web on the substrate.

When the 22% PES solution was electrospun membrane using a moving substrate under processing conditions i.e., applied voltage of 18 kV, a spinneret-to-collector distance of 10 cm, a flow rate of 20 µL/min, a spinneret diameter of 0.8 mm, a speed of substrates moving of 2.2 cm/min, 65% RH and served the PET nonwoven as substrate, yielded a more planar and homogeneous membrane. The thickness of membrane was 200 µm. The image analyses gave a mean fiber diameter of 800 nm. However, the proto-membrane which had been treated by immersion

into the water bath lead to a pronounced porosity on the nanofiber surface which will be useful, for instance, for increasing binding capacity to the fiber surface. In addition, the membranes which had been electrospun under processing condition at high humidity resulted in irregular fiber formation.

All test results for membranes showed that the fiber diameter and membrane structure and, consequently, membranes properties were clearly affected by applied voltage and spinneret-to-collector distance. The electrospun membrane was prepared by an applied voltage 18 kV at distance spinneret-to-collector of 10 cm, a flow rate of 20 µL/min, a spinneret diameter of 0.8 mm, a speed of substrates moving of 2.2 cm/min, 65% RH and served the PET nonwoven as substrate exhibited the pore size of 1.8 µm, the porosity of 93% and basic weight of 0.169 mg/cm^2. All membranes showed similar and high contact angle. The electrospun membranes prepared by applying higher voltage have lower flux than membranes prepared with lower voltage. The electrospun membranes which were prepared by increasing distance between spinneret-to-collector (kept other conditions) exhibited high water flux and clear correlation between structure and performance that decreasing of mean pore size leads to decreasing water flux of electrospun membranes. However the results suggested that PES electrospun nanofiber membranes are excellent materials for high water flux MF applications.

Regarding nitrogen gas flow through electrospun membranes, the membranes which were prepared by increasing applied voltage showed decreasing gas permeability. Moreover with the DEHS aerosol, with particles size of 400 - 1000 nm, filtration performance of electrospun nanofiber web was much greater than that of the 4 layers commercial nonwoven (Novatexx 2429) with pore size of 8 µm. This result clearly demonstrated the potential of electrospun nanofiber in the development of filter material against aerosol nanoparticles.

The filtrate fluxes of commercial membrane (Membrana MicroPES; pore size 1 µm) was much smaller than the filtrate fluxes of PES electrospun membrane with pore size ranging between 1.7 - 4.5 µm. Overall, PES electrospun membrane showed greater water flux than commercial membrane both before and after separation of silica nanoparticles (size 35 nm). The water flux before separation of all membrane was higher than after silica nanoparticles separation. The PES electrospun membranes had higher particles rejection than PES commercial membrane. Besides, the rejection of electrospun membranes was well above 90%, while commercial membrane rejected the nanoparticles by only 85% in the beginning of the filtration. Moreover, the PES electrospun membranes exhibited the rejection above 98% at the end of rejection experiment run. Such the results showed, electrospun nanofiber PES membranes can be used in various applications such as removal of nano or microparticles from waste-water, e.g., pre-filters to minimize contaminations and fouling prior to UF or NF.

This dissertation is dedicated with love to

my parents (Siri & Yong Kwankhao)

for their encouragement, support and

endless love over four years during

my doctorate study.

This work was performed during the period from February 2010 to March 2013 in the Institute of Technical Chemistry II (Lehrstuhl für Technische Chemie II), Faculty of Chemistry, University of Duisburg-Essen and Deutsche Textilforschungszentrum Nord-West e.V. (DTNW), Krefeld, under the supervision of Prof. Dr. Mathias Ulbricht.

I declare that this dissertation represents my own work, except where due acknowledgement is made.

Bintasan Kwankhao

Bintasan Kwankhao
08 July 2013, Essen

Acknowledgements

This dissertation could not have been completed without the support and help of many people and organizations that are gratefully acknowledged here.

At the very first, i would like to express my deepest gratitude to my supervisor, Prof. Dr. M. Ulbricht for the support, supervision and giving me the great opportunity to work in his research group. He always offered me the valuable suggestions and ideas with his knowledge and research experiences.

Secondly, i would like to give best thanks as well to Dr. T. Bahners for giving me the opportunity to work in his research group at Deutsche Textilforschungszentrum Nord-West e.V. (DTNW), Krefeld. He always supported me through the difficulties of my research work and encouraged me. I am greatly grateful Dr. A. Wego for the help, support and very valuable discussions on my work.

I would like to thank Prof. Dr. C. Mayer for being the head of examination committee and to Prof. Dr. J. S. Gutmann for being the co-referents of my work.

I am very thankful to Ministry of Science and Technology of Thailand for financial support and Rajamangala University of Technology Thanyaburi, Thailand for providing me the five-year scholarship to support my Ph.D. study in Germany. I would like to thank Office of Education Affairs, Berlin for the help of scholarship arrangements and extension.

I also wish to acknowledge I. Danielzik, C. Schenk, R. Nordmann-Silberg, T. Kallweit for their support. I would like to express my appreciation to C. Bettray. She always helped me and paid attention to my private life when i lived in Germany during the study. I would like to thank to U. Fehrenschild for the help with electrospinning set-up, B. Gebert for contribution to SEM observation. E. Daueber (Institut fuer Energie- und Umwelttechnik e.V.) for air filtration measurement, Dr. Z. Pei for the helps and suggestions, S. Frost for support with water filtration measurement and to all members of our research group at Lehrstuhl für Technische Chemie II, Universität Duisburg-Essen.

I would like to thank S. Salehi, Dr. V. Ameri, Dr. A. Farouk and Dr. N. Mohamed for the nice time we spent together at DTNW, Krefeld. Furthermore, i am grateful to all my colleagues at DTNW, Krefeld for the nice discussion and environment.

Special thanks to W. Sae-Lai for encouragement through the difficult moments of my Ph.D. study and to J. Breuer and her family, who are giving me a warm and familial atmosphere in Germany.

Finally, i wish to express my special thanks to my family in Thailand for support, encouragement and giving me all their endless love from far away.

Contents

List of Figures

List of Tables

Chapter 1
Introduction

1. Introduction

1.1. Background and motivation

Ultrafiltration (UF) and microfiltration (MF) membranes have become the main focus as promising separation tool in several industrial processes, covering fractionation and concentration steps in the food, pharmaceutical and biotechnological industries, in pure water production and in water and wastewater treatments. Although many methods have been proposed to improve the separation performance, the heart of UF and MF processes is the membrane itself. Important characteristics for achieving high performance UF and MF are high flux in combination with desired selectivity and low fouling. Because of their mechanical strength, thermal and chemical stability as well as excellence film forming properties, sulfone polymers, e.g., polyethersulfone (PES), have been used very often for the fabrication of high performance commercial MF membranes [1-4].

Nowadays, electrospinning has become a multipurpose technique which is able to generate fibers with diameters ranging from less than 100 nm to several μm by creating a continuous filament. The extremely fine electrospun nanofibers make them very useful in a wide range of advanced applications, covering the following main application areas: selective liquid filtrations, affinity membranes, e.g. for recovery of metal ions, tissue engineering scaffolds, sensors, or barrier materials for energy storage applications. However, nanofiber membranes produced by electrospinning have several prominent properties such as high surface area to volume ratio, high porosity and pore size in nanorange. Therefore, electrospun nanofibers membranes normally impart high efficiency in filtration at relatively small decrease in water or air permeability without any permanent fouling. As the porosity of electrospun nanowebs is more than 90%, they are candidates for air filters and liquid filtration membranes. Moreover, the application of electrospun nanofibers membranes has yet to make breakthrough in other avenues of separation than airfiltration, especially in pressure-driven liquid separations, such as ultrafiltration (UF) and nanofiltration (NF) [5-8].

Thus, in this study, the preparation of polyethersulfone (PES) membranes by electrospinning technique was studied and nanofiber membranes were produced in order to compare the properties and performance with commercial MF membranes. The influence of processing parameter and the treatment of the proto-membrane formed by electrospinning under different conditions were investigated. Thereby, we expect that this work will open up the avenue toward the use of nanofibers for very important applications of separation technology. Of particular interest are membranes in water purification, e.g., pre-filters to minimize contaminations and fouling prior to UF or NF.

1.2 Objectives of the research

The objectives of this research are:

1.2.1 To establish and optimize the preparation of nanofiber and electrospun membranes.

1.2.2 To investigate the influence of polymer concentration, electrical potential, spinneret-to-collector distance, relative humidity in electrospinning process on the resulting membrane properties and performance.

1.2.3 To study the treatment of the proto-membrane formed by electrospinning under different conditions, i.e., drying at controlled relative humidity and temperature or immersion in an aqueous coagulation bath.

1.2.4 To test and characterize electrospun membrane properties and separation performances in air and water filtration.

1.3 Scope of the thesis

The structure of this Ph.D. thesis consists of 5 chapters including:

Chapter 1 – Introduction

Chapter 2 – Theory and literature review: including the brief contents regarding electrospinning technique and the influence of parameters in process and application of electrospun nonafiber. However, this chapter will be focused on filtration application area.

Chapter 3 – Experimental: the experimental part of the study including preparation of electrospun nanofiber membranes and characterization the properties and performance of electrospun membranes.

Chapter 4 – Results and discussion: this chapter mainly deals with the results of the optimization of the electrospun nanofiber membranes including the influence of various parameters in electrospinning process on the resulting membrane properties and performance as well as the results of the characterization the properties and performance of electrospun membranes.

Chapter 5 – Conclusions and outlook: the results of this study will be summarized. Furthermore, the outlook of the current Ph.D. study is to modify the PES nanofiber membranes surface by macromolecular additives to the electrospinning solution.

Chapter 2
Theory and Literature Review

2. Theory and literature review

2.1 Electrospinning process background

Electrospinning process can produce the diameter of polymeric fibers from micrometer (10-100 µm) to sub-microns or nanometer (0.01 - 0.1 µm). That led to create some special characteristics such as high surface area to volume ratio (as large as 10^3 times of microfiber), high porosity and pore size in nanorange. The extremely fine electrospun nanofibers make them very useful in a wide range of advanced applications, covering the following main application areas: selective liquid filtrations, affinity membranes, e.g. for recovery of metal ions, tissue engineering scaffolds, sensors, or barrier materials for energy storage applications. Figure 2.1 shows electrospun nanofiber compared to a normal human hair and Figure 2.2 shows electrospun PES nanofiber compared to PET conventional microfibers.

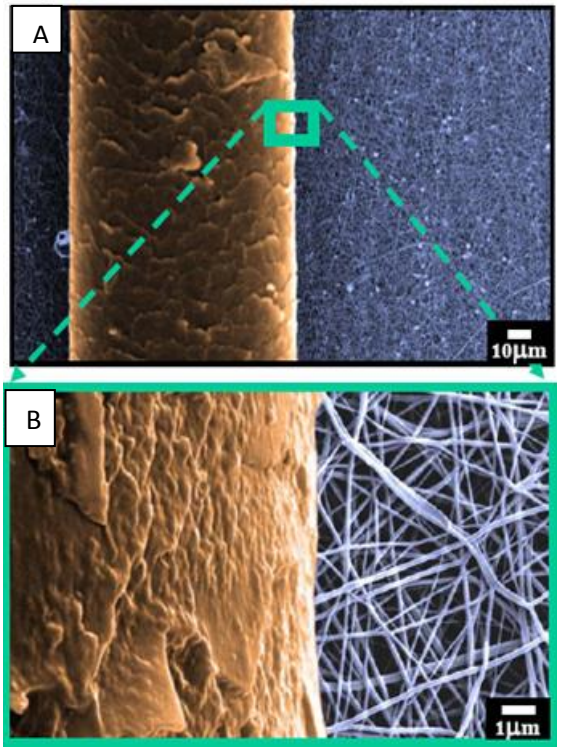

Figure 2.1 Size comparisons of TiO_2/PVP nanofibers and a normal human hair [9].

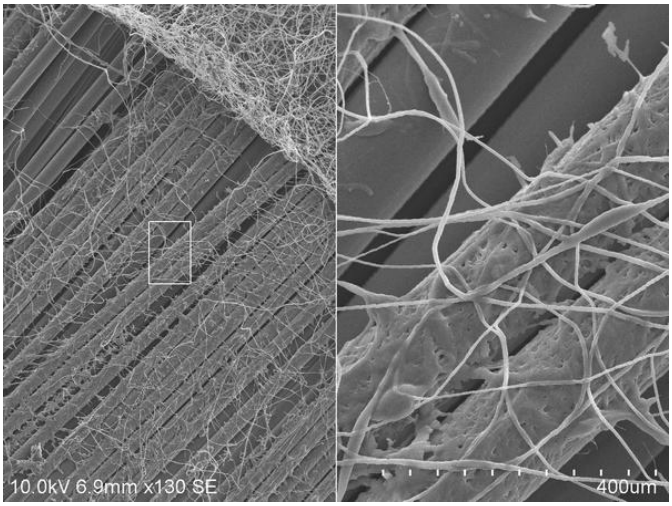

Figure 2.2 Electrospun PES nanofibers compared to PET microfiber [result of experiment during this Ph.D. project].

The basic electrospinning instruments include of a power supply, a spinneret or needle of small diameter, an electrode collector and a capillary tube for polymer as presented in Figure 2.3

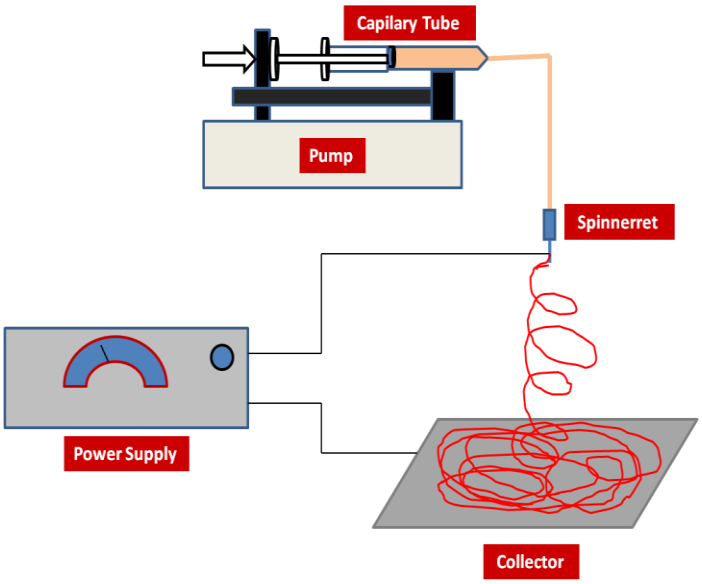

Figure 2.3 Schematic view of electrospinning instrument.

In the electrospinning process a high voltage power supply is used in order to create an electric field between a polymer solution held by its surface tension at the end of a capillary tube and an electrode collector. A charge is induced on the surface of the polymer solution by electric field. As the intensity of the electric field increases, the hemispherical surface of the solution at the tip of the capillary tube

elongates to form a conical shape known as Taylor cone. When the electric field increases and reaches a critical value at which the repulsive electric force overcomes the surface tension force, a charged jet of the solution is ejected from the tip of the cone, as the jet flies in air, its diameter decreases as a result of the stretching and solvent evaporation, resulting in a nonwoven web of randomly oriented fibers with diameters on the nanometer scale [10-19].

(a) (b)

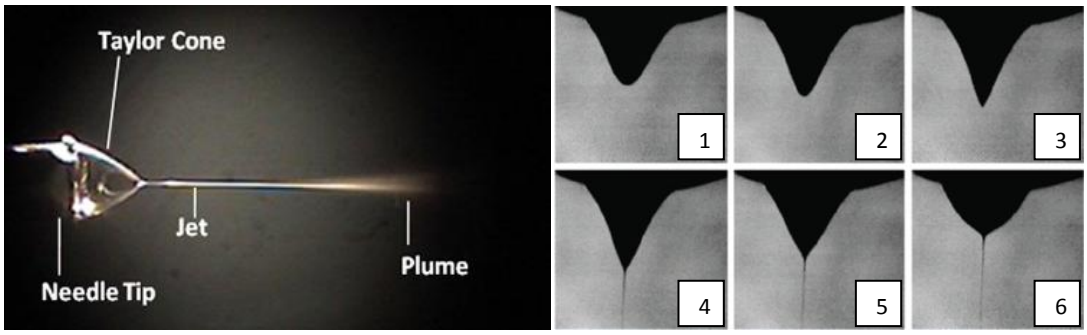

Figure 2.4 The development of the cone-jet in electrospinning, (a) photograph of polyvinyl alcohol solution showing a fiber being electrospun from a Taylor cone [12], (b) the evolution of the shape of a meniscus of polyethylene oxide–water solution under an electric field [18]. The meniscus is first transformed to a conical shape by the applied electric potential (b.1, b.2). The rounded tip then becomes sharper (b.3), and a jet is finally emitted from the tip of the cone (b.4). Then, the shape of the cone was changed back to a new, stable rounded shape (b.5), which persists as long as the solution carried away by the jet is replaced by fluid flowing into the meniscus (b.6).

2.2 Influence of parameters in electrospinning process

The polymer is generally processed in the molten state at temperatures 30 – 50 °C above the melting point and the most thermoplastics have low melting temperatures (100 – 200 °C). Basically, the polymer is heated to the melt state by the screw extruder and then shaped under high pressure and finally cooled down to room temperature (below Tg or Tm) to preserve its shape. In addition, the melt viscosity is an important factor in polymer processing [13].

An alternative is electrospinning of polymer solutions. For electrospinning process, many parameters (e.g., polymer solution, electrical potential, distance between spinneret and collector, humidity and temperature) can influence to properties and performance of electrospun nanofiber. It is possible to create nanofibers with different morphology, pore size, thickness and etc. by varying these

parameters. The influences of parameters in electrospinning process on the fiber morphology are summarized in Table 2.1.

Table 2.1 Influences of parameters in electrospinning process on the fiber morphology [18-44,102].

Parameter	**Effect on fiber morphology**
Viscosity (polymer solution) ↑	Fiber diameter ↑ (from beads to beaded fibers to smooth fibers)
Surface tension ↑	Number of beaded fibers and beads ↑
Solution conductivity ↑	Fibers diameter ↓
Evaporation of solvents↑	Fibers exhibit microtexture (pores on fiber surfaces)
Applied voltage ↑	Fiber diameter ↓ initially, then fiber diameter↑ (not monotonic)
Spinneret to collector distance ↑	Fiber diameter ↓ (beaded morphologies occur if the distance between the capillary and collector is too short
Humidity ↑	Fiber diameter ↓ (pores on fiber surfaces), then fiber diameter ↑
Flow rate ↑	Fiber diameter ↑ (beaded morphologies occur if the flow rate is too high)

2.2.1 Electrospinning from polymer solution

2.2.1.1 Polymer concentration

Generally, the molecular weight of the polymer influences the viscosity of the solution and when a polymer of a lower molecular weight was dissolved in a solvent, its viscosity will be lower than a polymer of a higher molecular weight. One of the conditions necessary for electrospinning to occur where fibers are formed is that the solution must consists of polymer of sufficient molecular weight and the solution must be of sufficient viscosity [14]. During electrospinning when the jet leaves the needle, the polymer solution is stretched as it deposits towards the collector plate. However, increasing the polymer concentration led to increasing the viscosity of the polymer solution, an increased in the concentration results in greater

polymer chain entanglements of the solution that is essential to maintain the continuity of the jet during electrospinning [15]. Furthermore, the chain entanglement of polymer had a significant impact on whether resultant breaks up electrospun beads-fiber form or fibers with small droplets [15,16]. Besides, increasing viscosity of polymer solution at too high values, it will make difficult to pump the solution through the capillary tube as well as the polymer solution will dry at the tip of the needle before begin electrospinning process [15,17].

In the literatures, there are several experiments that have shown that the viscosity of solution at a low values led to beads or spherical particles connected by fiber. Whereas, increasing the viscosity of polymer solution led to the shape of the beads change from spherical to spindle-like until well-defined nanofiber is achieved [18 – 26,31].

Figure 2.5 shows SEM images of polyurethane fibrous membranes which were electrospun from 6 %, 8 % and 10% (w/v) solution in tetrahydrofuran (THF) and N,N-dimethyl formamide (DMF).

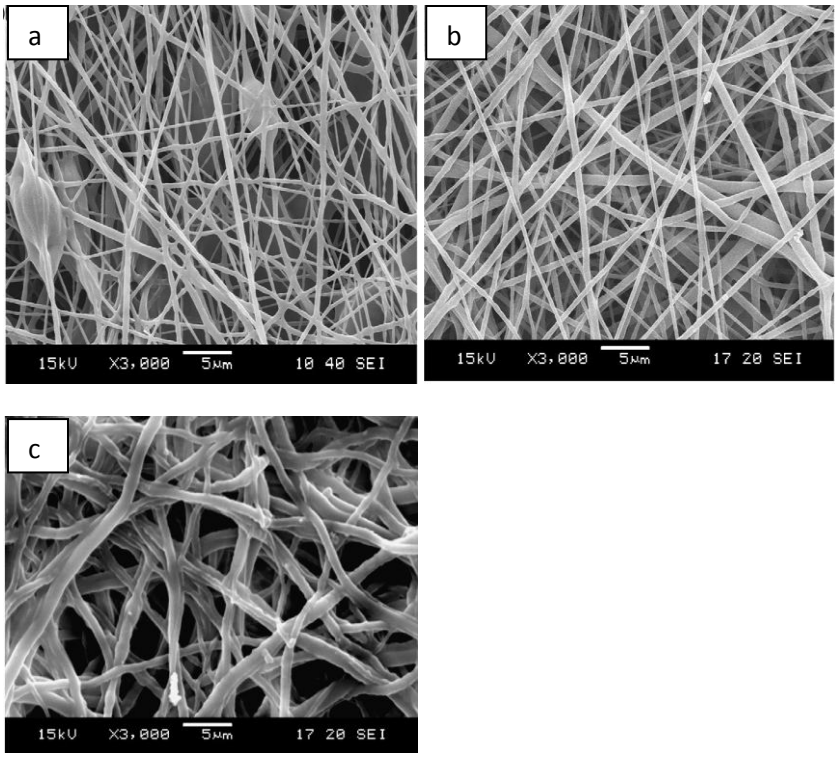

Figure 2.5 SEM images of polyurethane fibrous membranes which were electrospun from (a) 6 %, (b) 8 % and (c) 10% (w/v) solution in tetrahydrofuran (THF) and N,N-dimethyl formamide (DMF) [21].

The results from their study showed that at PU concentration of 6% (w/v), morphology of membrane resulted a bead-on-string with several big beads. At PU

concentration of 8%, the shape of the beads became spindle like and the fibers were smooth and homogeneous without beads in fiber. Nevertheless, when PU concentration increased from 8% to 10% (w/v), the electrospun membrane became thicker and resulted a film-like structural as shown in Figure 2.4 [21]. Furthermore, the electrospinning solution parameter affects to the diameter of nanofiber as well. When the viscosity increased with increasing of polymer concentration led to the average fiber diameter increased. Therefore, the viscosity of polymer solution was the main factor affecting the average diameter of nanofibers as well as the formation of fiber [21,25 - 28].

Tang et al. [24] have investigated the influence of polyethersulfone concentration in electrospinning as PES was dissolved in a mixture of DMF and NMP. Thereafter, the 18% and 20% PES solutions was electrospun by using condition electrospinning, i.e., voltage of 30 kV, distance between spinneret and rotating drum collector of 10.5 cm. The result indicated that when the PES concentration increased from 18% to 20%, the average of fiber diameter increased from 134 nm to 183 nm, respectively.

2.2.1.2 Surface tension

In electrospinning, the charges on the polymer solution must be high enough to overcome the surface tension of the solution. As the solution jet accelerates from the tip of the source to the collector, the solution is stretched while surface tension of the solution may cause the solution to breakup into droplets [15]. However, some solvent such as ethanol was a low surface tension thus it can be added to promote the formation of good fiber geometry [19]. Another way is to add surfactant, which is a powder, to the polymer solution. The polymer solution was added the powder surfactant resulted more uniform nanofiber and the diameter of fibers are also improved [19,29].

2.2.1.3 Polymer solution conductivity

The polymer solution conductivity determines the charge carrying capacity in a jet and thus influences the tensile forces exerted on the jet by the electric field. A higher stresses on the jet induced by higher conductivities generally result in reduced fiber diameters. The increased amount of charge forces the jet to elongate as a consequence of columbic repulsion. These forces act against surface tension, hence suppressing the Rayleigh instability favoring formation of non-beaded fibers. Salt additives in electrospinning solutions create migrating ions in solution that

transport charges and on tribute to higher conductivities [17,31]. Zong et al. [17] investigated also the effect of ions by adding ionic salt on the morphology and diameter of electrospun fibers. The results shown that PDLA fibers with adding ionic salts, here KH_2PO_4, NaH_2PO_4, and NaCl, produced beadless fibers and the diameter of fiber was ranging from 200 to 1000 nm. While, Baumgarten et al.[30] found that the jet radius varied inversely as the cube root of the electrical conductivity of the solution.

2.2.1.4 Evaporation of solvents

During elctrospinning process, when most of the solvent has evaporated before the jet reaches the collector, thereafter, the fibers or nanofiber webs are formed. However, if the rate of evaporation of the solvent is too low, the fibers may not be formed and a thin film is deposited on the collector. Nevertheless, the evaporation rate of a solvent depend on several factors such as vapor pressure, specific heat, surface tension of liquid, air movement over the liquid surface etc. Megelski et al. [31] demonstrated the structure of electrospun fibers with respect to the physical properties of mixed solvents. They found that influence of vapor pressure was pronounced when PS fibers were electrospun with different THF/DMF combinations, resulted in nanostructure morphology at high solvent evaporation and microstructure morphology at lower solvent evaporation. Lee et al. [32] studied the effect of the solvent ratio on the morphology and fiber diameter of electrospun PVC fibers. The results indicated that average fiber diameters decreased with an increase in the amount of DMF in the THF/DMF mixed solvent. While, Bognitzki et al. [33] found that the use of highly evaporation solvents such a dichloromethane resulted in PLLA fibers with average diameter of 250 nm.

2.2.1.5 Flow rate

An important parameter in electrospinning process is the flow rate of the polymer from the syringe that affects the polymer solution transfer rate and the evaporation of the jet. For the preparation of PS fibers, Megelski et al. [31] found that the mean pore size and the fiber diameter increased with an increase in the polymer flow rate. When the flow rate more increased from 20 to 30 µL/min, fibers had pronounced beaded morphology and the mean pore size increased from 90 to 150 nm.

2.2.2 Electric field

The electric field (applied voltage) is a parameter of electrospinning processing that could influence behavior. In this context, Fridrikh et al. [34] and Bahners et al. [35] reported a model for the stretching of a viscous charged fluid in an electric field. The model predicts that there is a limiting diameter for the fluid jet, which arises from a force balance between surface tension and electrostatic charge repulsion. Charge separation in the polymer and acceleration is induced by the force [35];

$$F = qE \tag{2.1}$$

Where *F* is the force

q is the charge

E is the electric field strength

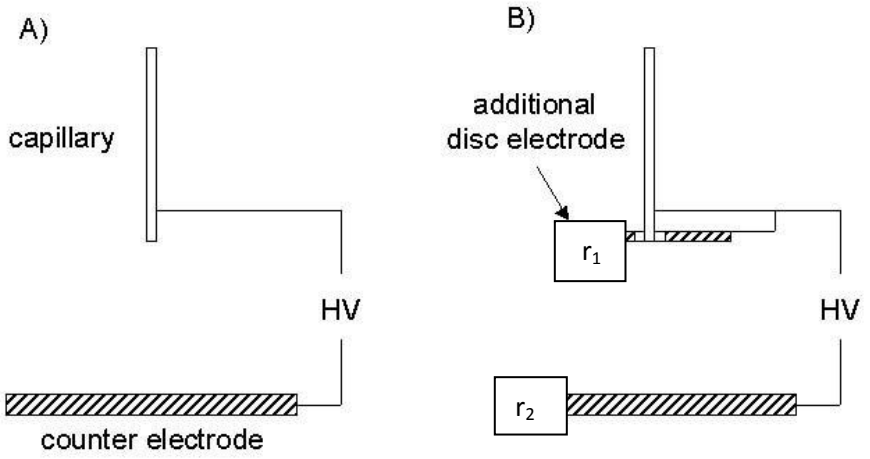

Figure 2.6 Conventional electrical setup for electrospinning as, (a) reported by Fridrikh et al. [34] and (b) modified setup for more homogeneous field geometry as studied by Bahners et al. [35].

In order to estimate the charge separation force in the case of the tip-collector-geometry, as show in Figure 2.6(a), one needs to calculate the local field strength E_1 at the surface of a droplet of polymer solution at the capillary tip.

$$E(r) = \frac{1}{4\pi\varepsilon_0} \int \frac{\sigma(x,y,z)}{r^2} \, . dx \, . dy \, . dz \qquad (2.2)$$

In general, $\sigma(x,y,z)$ is a charge distribution

r is effects in a distance

ε_0 is the permittivity

If a point charge is assumed in the center of the spherical droplet at the capillary,

$$E_1(r) = \frac{Q}{4\pi\varepsilon_0 r^2} \qquad (2.3)$$

Where Q is the total charge

r is the distance from the tip

Hence, the field E_1 is very large near the tip, i.e. r ----> 0. In the actual experiment, a droplet of radius r_d will form at the capillary. The radius r_d depends on the diameter of the capillary (radius r_c), the surface tension and the flow of the solution. The flow is often driven by gravitation force. If a droplet of a radius $r_d = r_c$ is assumed in a first approximation, the field E_1 at the surface of the droplet can be estimate to,

$$E_1(r_c) \approx \frac{Q}{4\pi\varepsilon_0 r_c^2} \qquad (2.4)$$

In order to calculate the total charge, one has to consider the field at the counter electrode. For the plate geometry, Bahners et al. [35] explained that the field can be assumed to be near homogeneous, i.e.,

$$E_2 = \frac{Q}{2\varepsilon_0 A_2} \cong const. \qquad (2.5)$$

At the plate, respectively, A_2 denotes the area of the plate of the plate, i.e. $A_2 = \pi r_2^2$ for a disc electrode of radius r_2. If the distance d between capillary tip and plate is large compared to the disc diameter and V is the voltage, E_2 is given by V/d and

$$Q = \pi\varepsilon_0 \left(r_2^2 \frac{V}{d}\right) \tag{2.6}$$

Using eq. (2.4) and eq. (2.6), the field strength at the surface of the droplet can be estimated to

$$E_{1\,(r_c)} \cong \frac{1}{4}\left(\frac{r_2}{r_c}\right) . \left(\frac{r_2}{r_c}\right)\frac{V}{d} \tag{2.7}$$

Obviously, E_1 will be very large for fine capillaries and the electric field strongly inhomogeneous. This can be visualized in a graphical presentation of the distribution of the electric potential $V(r) = dE(r) / dr$ shown in Figure 2.7.

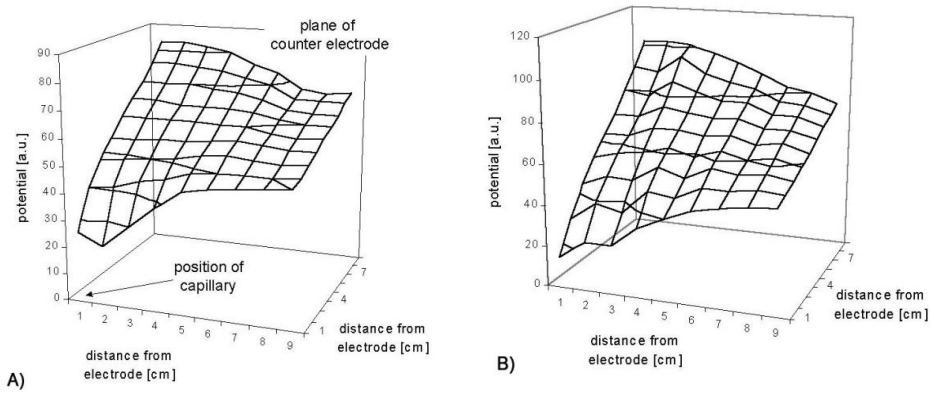

Figure 2.7 (a) Distribution of the electrical potential in tip-collector-geometry and (b) tip-collector-geometry with additional disc electrode around the capillary tip [35].

One way to reduce E_1 and the resulting force is to increase the size of the capillary or the size of the droplet by increasing flow rate and/or by decreasing the surface tension of the solution [33].

In order to discuss a collector-collector-geometry, the circular collector electrodes with radii r_1 and r_2 were considered. The capillary is positioned in the center of one of the collector, as shown in Figure 2.7 (b). Neglecting boundary effects, the field E_1 at the capillary opening in collector 1 can be approximated with an expression similar to eq. (2.5) giving

$$E'_1(r_c) \cong \left(\frac{r_2}{r_1}\right) . \left(\frac{r_2}{r_1}\right) \frac{V}{d} \qquad (2.8)$$

According to eqs. (2.7) and (2.8), E'_1 is smaller than E_1 by a factor $4\left(\frac{r_c}{r_1}\right) . \left(\frac{r_c}{r_1}\right)$. The reduced inhomogenity of the field is accordingly mirrored in the distribution of the potential of the electric potential $V(r) = dE(r) / dr$ (Figure 2.6b). For disc electrode of identical diameter as investigated by Fridrikh et al. [32], i.e. $r_2 = r_1$, the field is completely homogeneous. It is increasingly inhomogeneous with decreasing radius ratio r_2/r_1 .

In addition, Bahners et al. [35] have been investigated the effect of the field geometry to fiber diameter of polycaprolactone nanofibers by using a setup model in Figure 2.5 (a) and (b). A first electrospinning experiments was set by using the tip-collector-geometry and a 0.45 mm capillary was used in the process. The counter electrode was a disc with a diameter of 60 mm. The results showed that fiber diameter of 350 nm were obtained with a concentration of 14%, an applied voltage of 14 kV and a distance (*d*) of approximately 16 cm, i.e. E_2 = 0.875 kV/cm (cf. eq. 2.5). In case of a droplet of the polymer solution of a diameter equal to the capillary size is assumed, eq. 2.5 gives field strength at the surface of the droplet of approximately 15,000 kV/cm. Using these experimental parameter was employed for the plate-plate-setup (cf. Figure 2.6 (b)). Around the capillary, disc electrodes of various diameters were employed, which ranged from 20-60 mm and diameter of the counter electrode was 66 mm. The morphology presented very fine fiber with the modified field geometry. Due to the more homogeneous electric field near the capillary tip, a constant flow without sudden breakage is obtained. As a consequence, the fiber diameter is nearly constant over great lengths. However, the optimum diameter of the disc electrode turned out to be 20 mm and the experimental parameters were varied for optimization. The best results were obtained with a concentration of 6% PCL in methylene chloride, at 20 kV and a distance of 15 cm from capillary tip to counter electrode. Neglecting boundary effect, the field at the capillary is only E_1 = 12 kV/cm in this case.

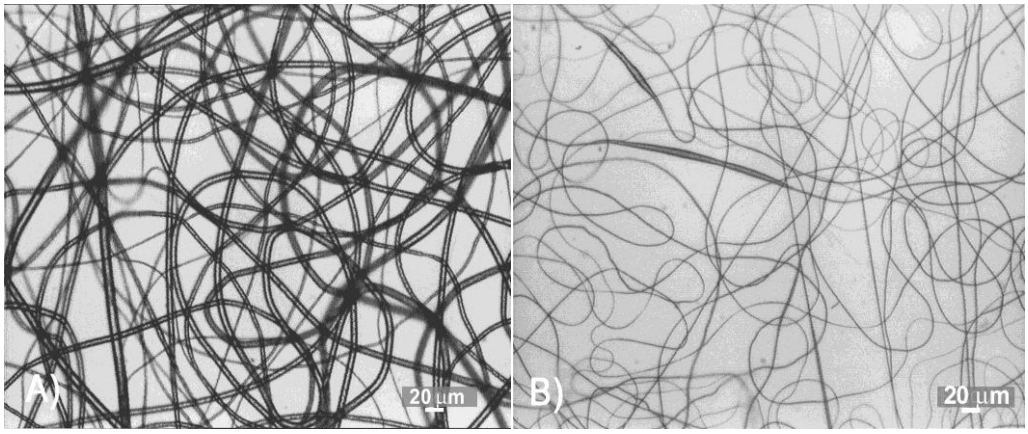

Figure 2.8 Optical micrographs of electrospun PCL fibers. Spinning condition were: 13% PCL in methylenchoride, 16 kV and 19 cm distance from capillary tip to counter electrode. (a) tip-plate-geometry and (b) with additional disc electrode around the capillary tip [35].

Generally, at applied voltage of more than 6 kV, the solution drop at the tip of the needle can be changed to become deformed into the Taylor Cone shape [36]. Increasing electric charge will cause the jet to accelerate faster and more volume of solution will be drawn from the tip of needle. This may yield in smaller Taylor cone shape [37]. Most results indicated that high voltage lead to greater stretching of the polymer solution due to the stronger electric field. These have the effect of decreasing the diameter of fiber [14,31,38-40]. Figure 2.9 shows SEM images and fiber size distribution of electrospun Nylon 6,6 fiber produced at various applied voltage. As clearly seen in Figure 2.8, when Nylon 6,6 was electrospun under processing condition with an applied voltage of 20 kV, the fiber size distribution peak existed in 400 nm. In the case of 30 kV, the number of fibers smaller than the peak size was increased even though the peak was located at the same range with that of the case of 20 kV. On the other hand, when applied voltage increasing to 50 kV, finer fibers was obtained and the peak fiber diameter was in 300 nm [39]. This result is in line with the explanation of Megelski et al. [31], who have been investigated the voltage dependence on the fiber diameter using polystyrene (PS). The fiber diameter of PS increased from about 10 µm to 20 µm with a decrease in voltage from 12 kV to 5 kV.

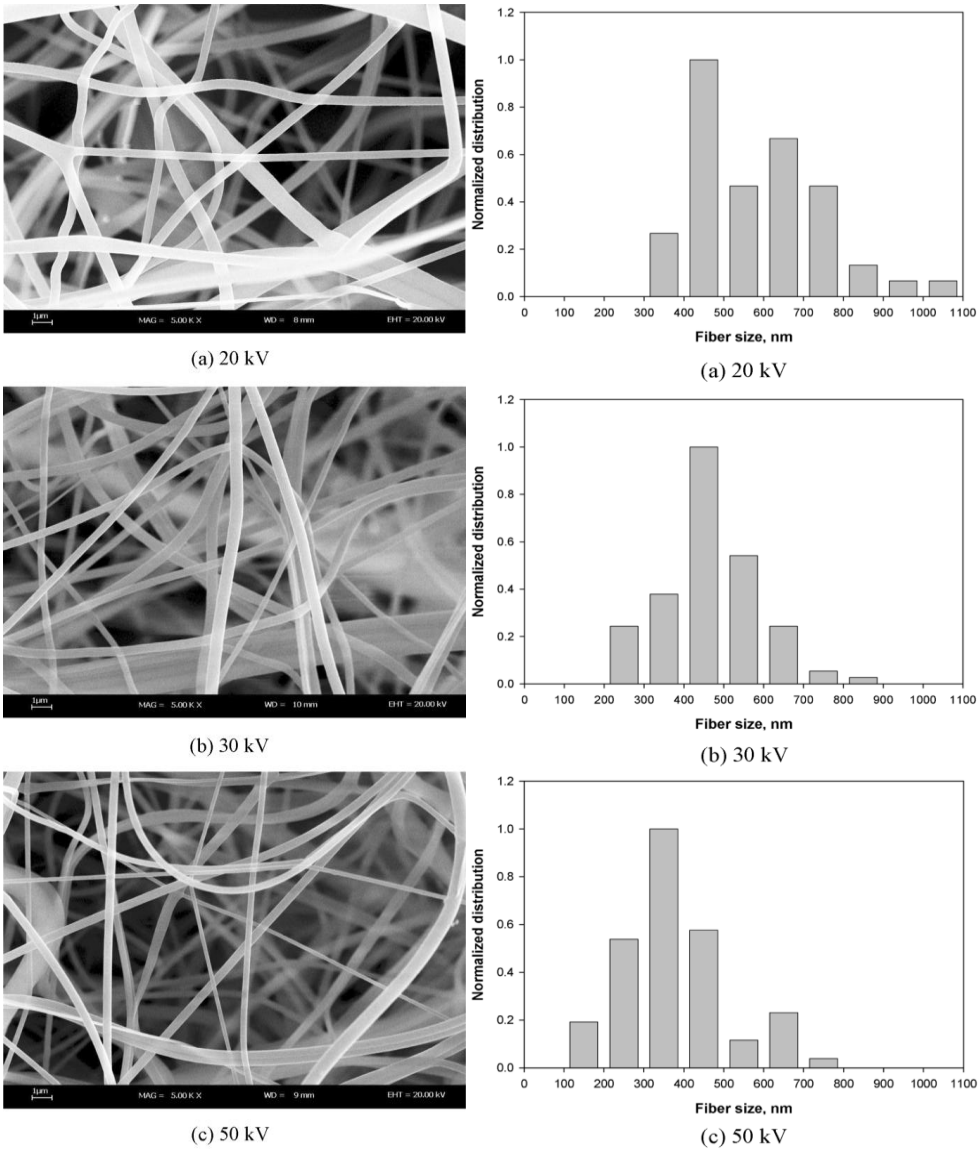

Figure 2.9 SEM images and fiber size distribution of electrospun Nylon 6,6 fiber produced at various applied voltage: (a) 20 kV, (b) 30 kV, (c) 50 kV [39].

2.2.3 Tip-to-collector distance

The tip-to-collector distance affected the structure and morphology of electrospun fibers because of their complementing on the deposition time, evaporation rate of polymer solution and the electric field strength. For fibers to form, the electrospinning jet must have enough time for the evaporation of the solvent in polymer solution. When the distance between tip and collector was decreased, the jet will have a shorter distance to travel before it reaches the collector plate as well as the electric field strength was increased (cf. 2.2.2). Buchko et al.[14] have been investigated the influence of variations in the distance between the tip and the collector plate to the morphology of Nylon 6,6 electrospun fibers.

However, decreasing the distance between tip and collector has the similar influence as increasing the applied voltage in process and led to increasing electric field strength as well. Megelski et al. [31] noted that bead formation in electrospun PS fibers decreased with increasing the tip to collector distance, while the ribbon shaped morphology would be maintained, when the tip to collector distance was decreased. Furthermore, Zhang et al. [26] found that when chitosan/PVA was electrospun at distance between tip and collector of 10 cm, the average diameter of fibers was 114 ± 35 nm. While with distance between tip and collector of 15 cm, the amount of beads decreased and the image analyze gave the average diameter of fiber of 99 ± 21 nm. Thereby, increasing the distance in electrospinning process resulted in a decrease of the average fiber diameter. Nevertheless, when the distance was too large resulted ribbon shaped morphology or no fibers deposit on the collector [41]. That is due to the electrostatic field strength in process is too low.

2.2.4 Humidity

The humidity of the electrospinning environment has an influence in the polymer solution during electrospinning. At higher humidity leads to more water molecules are between the tip and collector. These molecules will increase the conductivity of this region, therefore, changing the properties of the electric field strength in electrospinning process due to the polarization of water molecules [24,42]. Hence, the electrospun fiber became thick-diameter due to lose electric field strength and smaller draw-down force at higher humidity [24,43]. Tang et al. [24] investigated influence of relative humidity in electrospinning of PES to the average diameter of fiber and the adhesion strength. They found that high humidity led to large fibers as the fiber diameter increased from 266 nm (45% RH) to 492 nm (70% RH) (cf. Figure 2.10) and humidity also affected to the adhesion strength of PES nanofibers membrane and nonwoven substrate. At low humidity (<45%), the PES membrane – nonwoven adhesion was low (2.6 psi) and when the humidity was increased to 50%, the PES membrane – nonwoven adhesion increased to 40.5 psi. In case of acrylic nanofibers, Baumgarten [44] noted that acrylic fibers electrospun in an atmosphere of more than 60% relative humidity and resulted to ribbon shaped morphology.

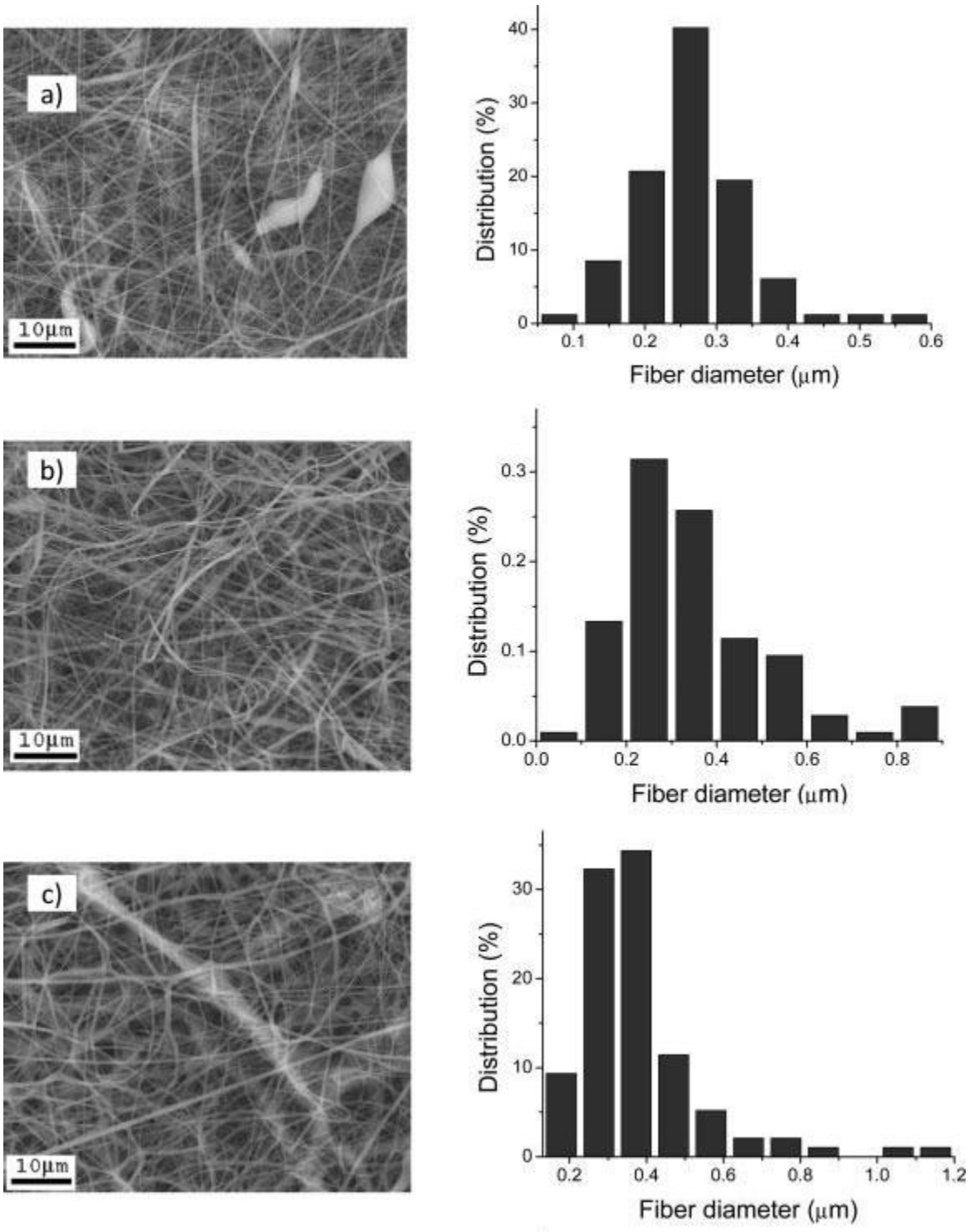

Figure 2.10 SEM image and nanofiber diameter distribution of electrospun nanofibers of PES/DMF/NMP solution at different relative humidity; a) 45% RH, mean diameter 266 nm, b) 50% RH, mean diameter 349 nm and c) 60% RH, mean diameter 382 nm [24].

2.3 Application of electrospun nanofibers

The electrospun nanofiber webs have several prominent properties such as high surface area to volume ratio, high porosity and pore size in nanorange. These make them very useful in a wide range of applications, covering the following main application areas, as present in Figure 2.11, such as tissue engineering scaffolds, wound healing, release control, sensor, affinity membrane and recovery of metal ions and the most important ones is filtration applications [45-48], However, this thesis will focus on the researches of filtration application.

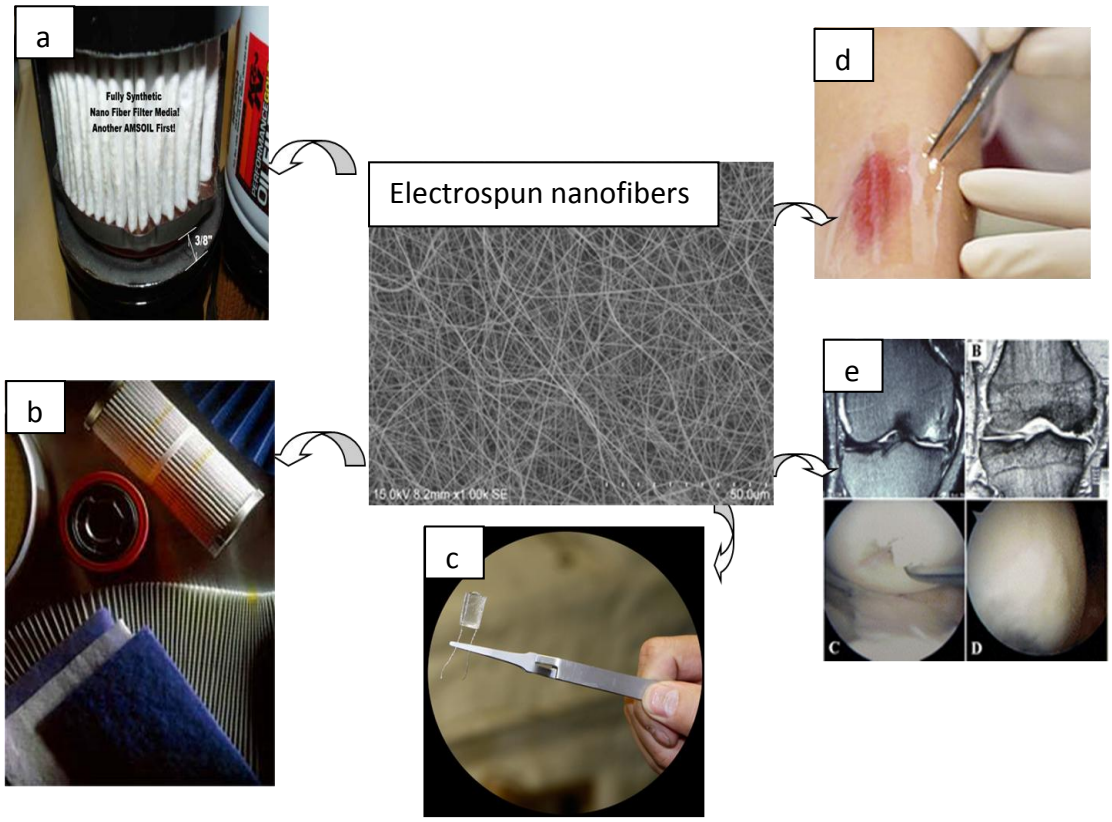

Figure 2.11 Main applications of electrospun nanofiber: (a) oil filtration [49], (b) air filtration [50], (c) sensor [51], (d) wound healing [53] and (e) tissue engineering scaffolds [54].

2.3.1 Filter structure and function

Filter media can be classified as depth filters, surface filters of adsorptive filters. The depth filter consists of a fibers web with a wide pore size distribution and a very open three-dimensional structure. Larger particles become trapped within the tortuous path created by the maze of fiber. As particles become lodged within the

depth filters structure, the openings or channels become narrower and begin to trap finer and finer particles. Depth filters become more efficient as particles are trapped within its structure. Moreover, depth filters have high dirt holding capacities, nominal efficiencies, low initial pressure drops and long life. Compared to surface filter, it consists of a non-woven with a two-dimensional structure and a uniform or narrow pore size distribution will generally form a filter cake on its surface. As the cake forms it performs the majority of the mechanical filtration. As more and more solids are loaded on the surface of the filter, the pressure drop increases and the filter becomes more efficiency [55,56].

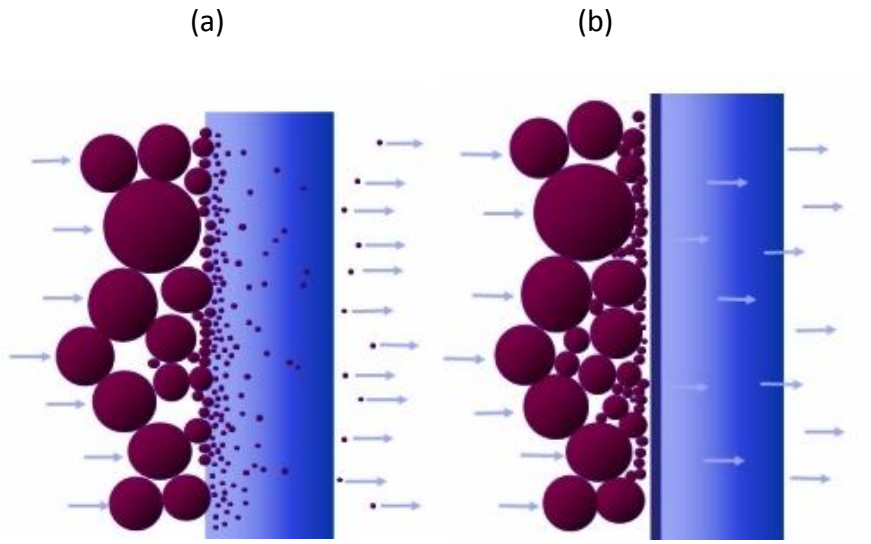

Figure 2.12 The cartoon shows an example for the combination of depth and surface filtration, the large particle are separated via surface filtration in both cases. Differences are seen for the smallest particles which are trapped (partially) in the depth (a) and completely on the surface (b) [57].

In general, textile fabrics of varying construction, e.g., woven, knitted, nonwovens, pile and combinations thereof, find increasing application in fluid filtration on the background of their complex pore system. This characteristic pore structure of textile fabrics effect particle separation through different mechanisms, so called 'geometric separation' and 'impact separation'. In addition, the rather open geometry of a textile allows for high flow rates. Accordingly, the use of a textile offers various means to 'tune' the separation performance of a filter. Characterized by the separation function T(d), which gives the percentage of separated particles of a given size d, the separation performance can be affected by the choice of fabric construction (yarn geometry, fineness, weave etc.), by combination of fabrics of similar of differing geometry as well as the flow direction [62,63].

For nanofibers filter, the mechanisms of particles removal are captured by the large particles are blocked on the filter surface due to the sieve effect and the particles which are smaller than the surface-pores would penetrate into the nanofibers filter, as collected by fibers [5,58]. However, nanofibers web as the membranes can improve separation efficiency, low fouling, accompanied by higher permeability i.e. lower energy consumption [59-61]. Figure 2.13 presents the SEM images of electrospun PAN/PET membrane after filtration by using the 0.20 μm particles suspension. Normally, the filtration efficiency is dependent on nanofiber physical structure (e.g., thickness, pore size, porosity on surface, fiber diameter, etc.), surface chemical characteristic and fiber surface electronic properties. Moreover, the filter media efficiency of the applications is evaluated by pressure drop and flux resistance as well.

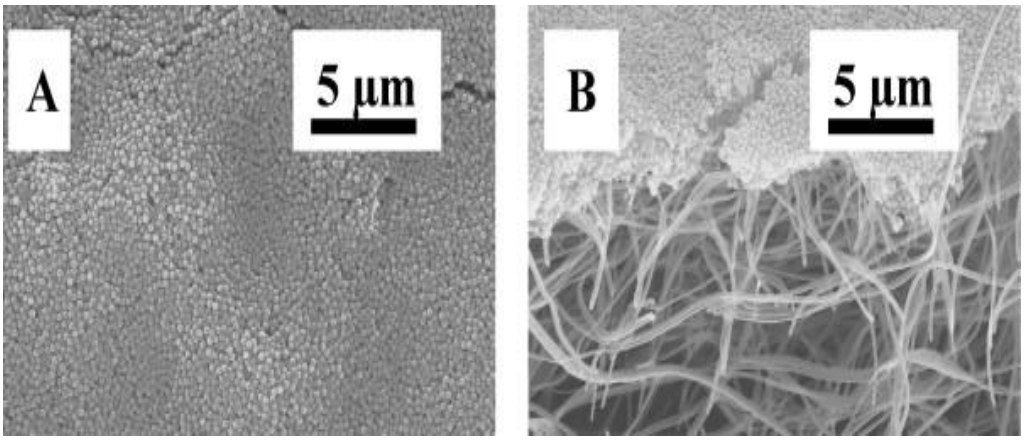

Figure 2.13 SEM images of electrospun PAN/PET membrane after filtration by using the 0.20 μm particles suspension from (A) surface and (B) cross-section views [58].

Geometric separation refers to the separation of particles lager than the textile mesh, i.e. pore size, just because of their physical dimension. A good efficiency of the geometric separation effect with, at the same time, low flow resistance can be achieved by using a textile fabric with a distribution of pore size or the combination of differing fabrics. On the other hand, impact separation is affected by the complex flow through the fabric, which forces the medium of gas or fluid and the particles to travel around fibers following complex stream lines ('labyrinth effect'). Particle with certain inertia, however markedly smaller than the mesh of the textile may leave the stream lines and impact on fiber surface as is sketched in Figure 2.13. The determining quantity of this effect is the Stokes number (*St*) of a particle, which is given by

$$St = C_m \,.\, \rho_p . d_p^2 \,.\, U_\infty \,/\, 9 \,.\, \mu \,.\, d_f \qquad (2.9)$$

In eq. (2.9), where d_p and d_f are the relevant diameters of particle in question and the fiber of the textile filter respectively and ρ_p is the particle density. The μ is the air viscosity and U_∞ is the undisturbed air velocity. C_m is the so called Cunningham correction term, which takes account of gas slip at the particle surface. Using assumptions made by Fuchs [64], Pflueger et al. [65] and Bahners et al. [66] for practical conditions in air filtration, eq. (2.9) can be written as

$$St = 3.12 \,.\, d_p^2 / d_f \qquad (2.10)$$

Where d_p and d_f are in µm. Particle trajectories for different values of St are sketched in Figure 2.14 showing that the probability of impact separation increases with increasing Stokes number. Obviously this is the case with increasing particle diameter, but also with decreasing fiber diameter.

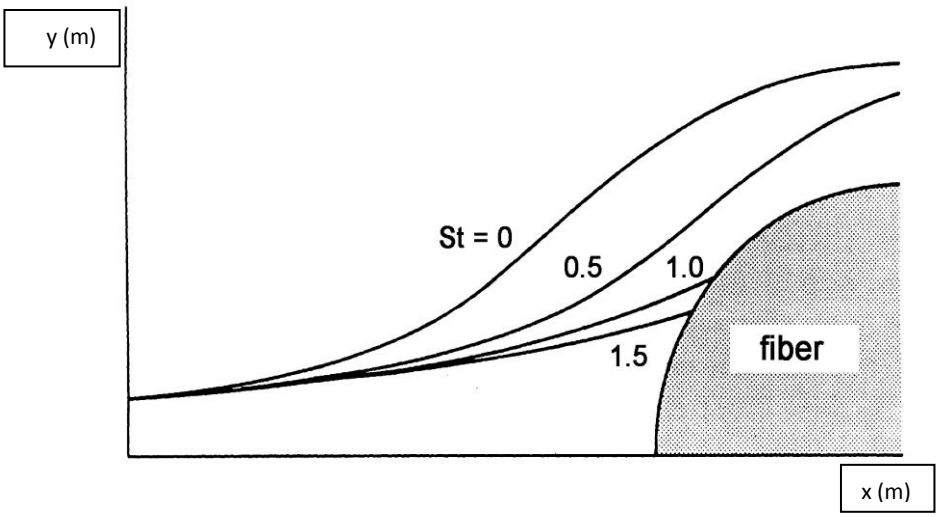

Figure 2.14 Particle trajectories around a cylindrical fiber for particle of different Stokes number (St). A zero Stokes number denotes the actual stream line of the transport [66].

One important aspect for the efficiency of impact separation is the adhesion of an impacted particle on the fiber surface, i.e. the resistance to be taken up by the flow of the gaseous of liquid transport medium. The adhesion of a particle is

governed by van der Waals interaction, electrostatic force and H-bonding forces, the hierarchy of these interactions varying with medium and particle size [66].

Bahners et al. [66,67] reported the effect of impact separation by increasing particle adhesion following surface modification, e.g., micro-roughening by means of laser treatment. The results of wet filtration efficiency as well as dust separation in industrial filter facility showed that particle capture especially in the micron-range could be enhanced by the characteristic surface topography, a rather regular roll-like structure in the micrometer scale, created by an UV laser treatment of PET fibers. In SEM analyses of the filter as shows in Figure 2.15, it was observed that a large amount of very fine grain particles was captured, which would normally not be captured on the smooth surfaces of commercial filter, which was attributed to very high adhesion forces acting in the groves of the roll-like surface structure.

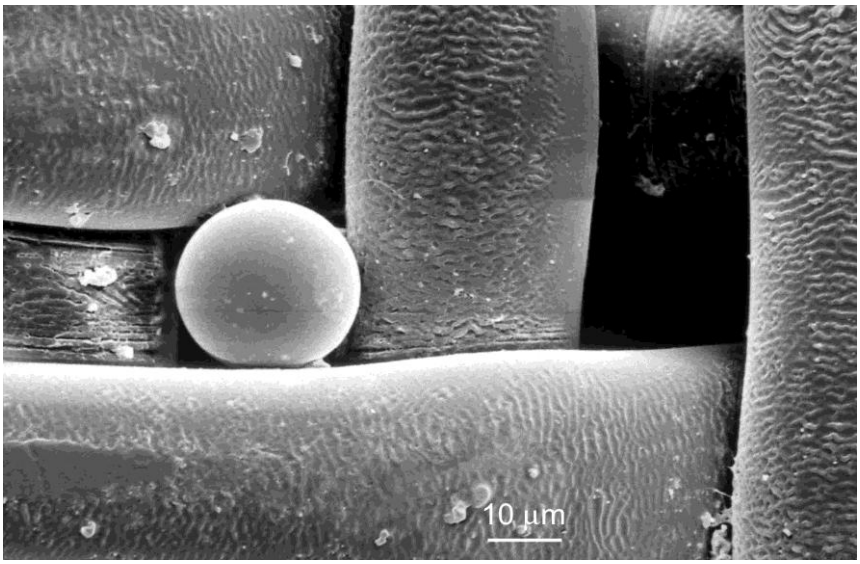

Figure 2.15 SEM micrograph of a laser-treated textile filter, PET sieving fabric with a mesh opening of 10 µm, after wet filtration process [67].

2.3.2 Air filtration

Because the nanofibers filtration is pronounced by higher inertial impaction and interception than with conventional filtration microfibers, it is offering more optimum filtration efficiency. In case of air filtration application, the main reason for increasing attention for usability is its very high surface area of the nanofibers facilitating adsorption of dust or contaminant from the air [68]. For a commercial air filter is produced by Donaldson company (Figure 2.16).

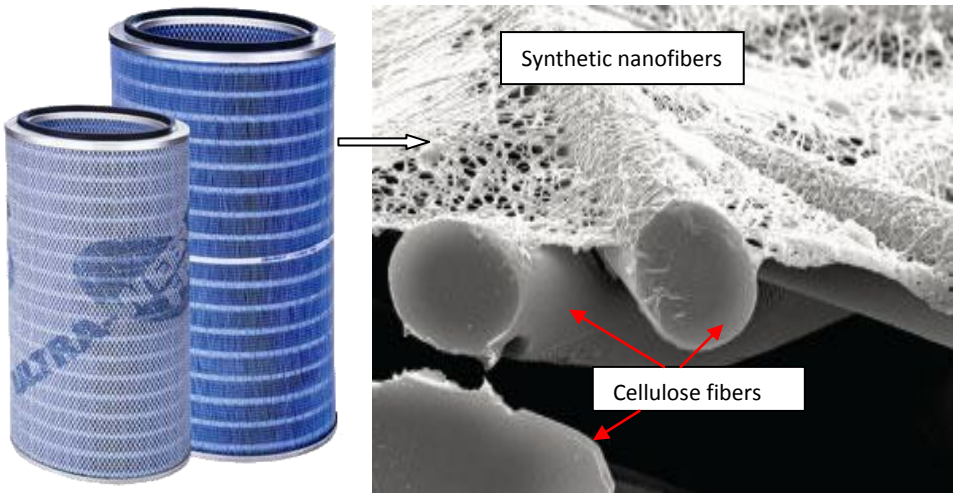

Figure 2.16 Commercial air filter is produced by Donaldson company [69].

Aerosol filtration is most widely applied for sampling and air cleaning. It is also utilized in a variety of industries such as air cleaning of smelter effluents, processing of nuclear and hazardous materials, respiratory protection and particle collection in clean rooms [70-72]. In particular, nanofibers filters have been widely used to separate aerosol particles/solid from air flow stream because of their low material cost [71], high filtration efficiency, maintaining a relative low resistance to the air flow [72], lower energy consumption [73], longer life and easy maintenance [74].

Several studies have investigated the filtration efficiency of electrospun nanofiber as filter media and they found that the possible ways to improve filtration efficiency are (i) to fabricate fine fiber with diameter down to nano-scale, (ii) to produce the multiple thin layer of nanofiber filter and (iii) to control the orientation distribution on filter structure [73-78]. Leung et al. [79] reported that under continuous loading of sub-micron aerosol, filtration efficiency of nanofiber filter was much better than microfiber filtration as well as the pressure drop of nanofiber filter rises much faster than microfiber filtration. Polyacrylonitrile (PAN) nanofibers with mean diameters in 270 – 400 nm rang were produced by Yun et al. [72] in order to compare to commercial filters made of polyolefin fiber and glass fiber. The performance of PAN nanofiber filters were tested the penetration of mono-disperse NaCl nanoparticles (below 80 nm in size) through the filters. The results showed that the penetration of nanoparticles through PAN electrospun filters reduced by increasing the diameter of nanofibers as well as decreasing filter thickness. However, the penetration of nanoparticles through PAN electrospun filter was in better agreement with theoretical predictions than was the measured penetration through commercial filters. Recent study by Leung et al. [80] presented that the PAN nanofiber filter, with fiber diameter of 98 – 300 nm, have higher efficiency and

quality factor than microfiber filter at clean state. On the other hand, microfiber filter, which was much thicker, has higher NaCl nanoparticles holding capacity under continuous loading of sub-micron aerosol, as justified from its much lower pressure drop increase rate than nanofiber filter. The multi-layer of microfiber filter reduced the pressure drop over time compared to a layer of PAN nanofiber. The novel alumina nanofiber for effective removal and retention of Escherichia coli bacteriophage (MS2) aerosol was demonstrated by Li et al. [77]. They found that the physical removal efficiency of alumina nanofiber was 94.3% with diameter of MS2 aerosol in the 10 - 400 nm range. While it is viable removal efficiency was 98.8% and yielding higher filter efficiency than HEPA commercial filter. However the pressure drop of HEPA commercial filter was higher than alumina nanofiber and the viruses were effectively retained in the nanofiber filter due to electrostatic attraction. Furthermore, the performance of alumina nanofiber was not affected by RH change.

In order to improve the filtration performance, several recent studies the filtration efficiency of multiple layers of nanofiber, Podgorski et al. [73] have developed melt-blown technique for producing nanofiber filter (made by the fibers diameter of 300 nm) in order to improve the filtration efficiency of the most penetrating aerosol particles (MPPS) in fibrous filters and the nanofiber filters and commercial filter were measured the pressure drop and efficiency of removal of aerosol particles with diameter 10 - 500 nm. Their results confirmed the many-layer nanofibers filter combined with a single microfibers backing layer filter have significantly increased efficiency at the MMPS and the pressure drop rises moderately as compared to conventional microfiber filter. Vaisniene et al. [82] have electrospun nanofiber from 8% polyvinyl alcohol (PVA) for gas filtration. Thereafter, three types of samples of PP nonwoven material without nanofiber filter, PP nonwoven material with different of thickness of nanofiber filter (the mean thickness of nanofiber of 250 nm and 300 nm, respectively) were chosen for measuring air permeability and gas filtration of cigarette smoke. They reported that nonwoven material with different of thickness of nanofiber filter have a lower air permeability than without nanofiber filter. A higher fiber diameter of nanofiber filaments makes the filter more effective. The PVA nanofiber filter, as for cigarette application, was effective for holding organic compound with polar O-H or N-H groups, carbonyl group (>C=O) containing compounds, ether (C-O) and compounds with C-N bonds. IR spectrum of nonwoven without a PVA nanofiber filter before cigarette smoke filtering was similar after filtered. It indicated that those nonwovens are not effective with respect to the efficiency of filtration. Zhang et al. [76] improved the filtration performance by using multiple thin layers of PAN nanofiber mats. The filtration test results showed that the multi-layer nanofiber mat structure had a filter efficiency factor much higher than the single thick layer nanofiber mat tested under the same conditions. In particular, the sandwiched multi-layer of PAN

nanofiber mat exhibited a higher quality than the conventional glass fiber HEPA (high efficiency particulate air) filter.

Effect of face velocity, nanofiber packing density and thickness on filtration performance and pressure drop of filters was investigated by Leung et al. [83]. For the experimental, they fabricated the nanofiber filters by electrospinning polyethylene oxide (PEO) nanofiber (mean fiber diameter of 208 nm) on microfiber substrate, thereafter, the nanofiber layer of the same packing density but different thickness was designed. The filtration performance of nanofiber filters decreases, when face velocity was increased from 5 to 10 cm $s^{-1}$and the reduction became lager at smaller particle size especially for the particles size below 100 nm. However, the most penetrating particle size decreased from 140 to 90 nm when nanofiber packing density increased from 3.9 to 36 x 10^{-3} g/cm^3. In addition, the effect of nanofiber layer thickness has less prominent effect on most penetrating particle size than that of nanofiber packing density and the filtration efficiency increases in a decreasing rate with respect to pressure drop. It indicated that nanofibers being deposited into single layer elevate the pressure drop without improving the filtration performance of filters. However, the efficiency of filters and reducing pressure drop can be improved by distributing the same amount of nanofibers thinly through stacking up multiple filter, called as “multi – layering”. Recently, Pantanaik et al. [74] also composited PEO nanofiber mat with a microfiber nonwoven by sandwiching structure of filters. They found that the filtration efficiency was decreased and the pressure drop was increased after cyclic compression for the PEO nanofiber deposited over nonwoven, whereas, changes were not significant in composite PEO nanofiber mat with a microfiber nonwoven by sandwiching structure. Composite PEO nanofiber by sandwiching structure showed high efficiency for long term application. Wang et al. [83] combined a microfiber mat with a nanofiber (fiber diameter of 150 nm) mat to a micro/nanocomposite fibrous filter structure. The microfiber nonwoven used as the nanofiber support and the nanofiber mat acted as the collection layer facing the airstream containing aerosols particles and four nanofiber mat with different solidities (packing densities) were used in this structure. The filtration efficiency of the combined microfiber mat with a nanofiber presented close to conventional HEPA or HVAC filters. Besides when collecting the aerosol particles of 300 nm resulted to have a better filtration efficiency than those conventional filters.

Alternatively, recent researches [73,84] has also reported an advanced melt-blown technique for better nanofiber filters production. The main advantages of this technique are well-defined fiber structure, higher production rate, lower emission of toxic vapor wastes and higher filtration quality at lower basis weight of filters. In one recent study by Hassan et al. [84], the polypropylene polymer was fabricated by using melt-blown technique. They reported the polypropylene nanofibers with an

average fiber diameter in the range of 300 - 500 nm by using melt-blown technique were obtained. Thereafter, those nanofiber mats were measured the fiber diameter, air permeability and aerosol (dioctylphtalate, the particles diameter range of 10 - 800 nm) filtration efficiency, respectively. Airflow through nanofibers mats resulted much higher air permeability as well as these nanofiber filters exhibited a higher quality filtration, at low basic weight, than the commercial fiber glass filter.

2.3.3 Water filtration

2.3.3.1 Membrane classification

A membrane is a selective barrier between two phases [85]. Depending on the application, different membrane morphologies will be used. Several types of membrane separation mechanisms exist. In membrane applications where the solution diffusion mechanism plays the major role, the membrane material is chosen based on the selective sorption and diffusion properties, membrane morphology will be not the main factor to affect the selectivity but it is still important as regarding to total flux. A schematic representation of various morphologies is given in Figure 2.17.

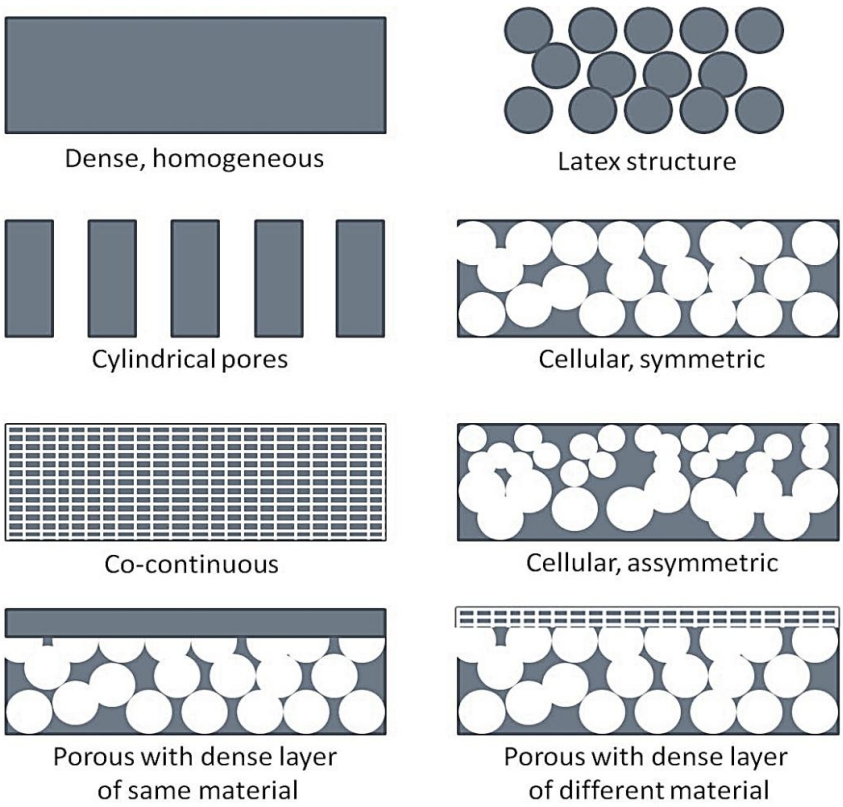

Figure 2.17 Schematic representation of different membrane morphologies [85].

In all the membrane processes, driving force is essential to deliver the energy to separate the feed molecules or particles; commonly applied driving force differences in pressure, concentration, partial pressure, temperature or electrical potential. The most widely used pressure driven processes are generally classified as microfiltration (MF), ultrafiltration (UF) and hyperfiltration, which is normally subdivided in reverse osmosis (RO) and nanofiltration (NF). Nevertheless, the difference between the processes is not always so sharp, as presents in Table 2.2, summarizing the main characteristics of various membrane processes, in which, typical permeability is for a typical permeate stream, i.e., with rejected species on the retentate side of the membrane.

Table 2.2 Pressure driven membrane processes [85].

Membrane process	Typical pressure (bar)	Typical permeability ($l/(m^2 \cdot h \cdot bar)$)	Morphology of the selective layer
Microfiltration	0.1-2	>50	Porous
Ultrafiltration	1-5	10-50	Porous
Nanofiltration	5-20	1.4-12	Porous/Dense
Reverse Osmosis	10-100	0.05-1.4	Dense

2.3.3.2 Electrospun microfiltration membranes

According to the Baker's definition: "Microfiltration refers to filtration process that use porous membranes to separate suspended particles with diameter between 0.1 and 10 µm" [70]. The electrospun nanofibers membranes could be good candidate for water microfiltration membrane due to these nanofibers membranes have a pore size distribution from sub-micron to micrometers. The viability of developing high surface area pre-filter through electrospinning has been explored by Gopal et al. [6]. Polysulfone nanofibers were electrospun into membranes and their ability to remove micro-particles from solution was investigated. The nanofiber membranes possess high porosity together with high surface area to produce high flux pre-filters with high loading capacity. The membranes had a bubble-point of 4.6 µm and were able to remove above 99% of 10, 8, and 7 µm particles without any permanent fouling. However, the membranes were observed to foul irreversibly by 2 and 1 µm particles with a cake layer forming on the outer membrane surface. Below 1 µm, the membrane behaved as a depth filter with 0.5 and 0.1 µm particles being attracted onto the nanofiber surface. Such

nanofiber pre-filters could be used in various applications such as removal of microparticles from waste-water, prior to UF or NF.

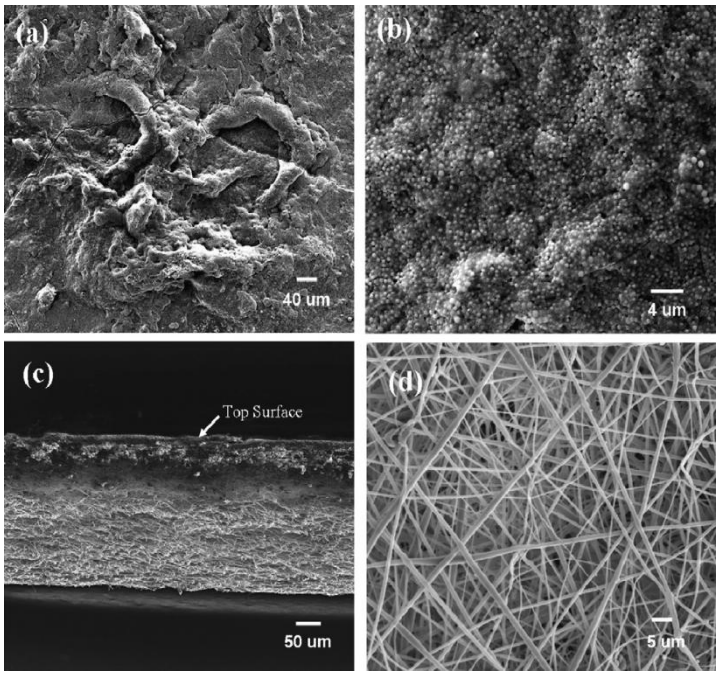

Figure 2.18 PSU electrospun membrane after particle–challenge (polystyre with paticle size ranging between 0.1 – 10 µm) test, a) & b) top surface, c) cross-section and d) bottom surface [6].

The filtration of PVDF electrospun nanofiber membranes were investigated by Gopal et al. [7] and Kaur et al. [86], their performances were compared with commercial microfiltration membrane. For filtration performance experiment of both membranes in equal conditions i.e., the similar pore size by heat-treating of proto- electrospun membrane [5] or by grafting with methacrylic acid on top layer of the electrospun membranes [86] in order to reduce its pore size to the range of the commercial microfiltration membrane. The results indicated an up two times higher flux for the PVDF electrospun membrane than commercial microfiltration membrane at the same pore size distribution and applied pressure and the rejection of PVDF electrospun membrane resulted more than 90% of the micro-particles from solution. The higher flux for PVDF electrospun membrane confirms the better performance and efficiency of the electrospun microfiltration membranes leading to lower energy consumption. Recently, Zhuang et al. [87] fabricated the PVDF nanofibers membrane by a new process so-called “solution blowing”. The nanofibers membranes were electrospun by this process exhibited the fiber diameter mostly of 60 - 280 nm and the porosity of membrane of 95.8%. The microfiltration performance of the hot-pressed membrane showed retention ratio more than 90%

against 1.0, 5.0 and 10 µm particles and presented high pure water flux at low pressure. Meanwhile, a heat treated electrospun PAN nanofiber membrane for particle separation from water with average fiber diameter of 165 ± 16 nm, the porosity of 91.7%, pore size in the diameter range of less than 2 µm and specific surface area near 40 $m^2g^{-1}$was obtained by Bazargan et al. [88]. The PAN nanofiber membranes were post-heated treatment exhibited high performance such as the mechanical strength was 4.87 MPa with 23% elongation, the water permeability was 225.6 kg/m^2h and the contact angles were equal to zero. It can be concluded that the heat treated electrospun PAN nanofiber membrane was completely hydrophilic. For filtration efficiency, the membrane has high ability to remove more than 90% of microparticles in the range of 1-20 µm from water.

In particular, the application of electrospun poly(ethylene terephthalate) nanofiber membrane for apple juice filtration was demonstrated by Veleirinho et al. [89]. Poly(ethylene terephthalate) nanofibers were electrospun into membranes as the average fiber diameter was 420 nm and the electrospinning process was performed until the membrane reaches the similar thickness to the ultrafiltration membrane of 0.20 mm. The PET nanofibers membranes showed a higher flux performance than commercial microfiltration or even ultrafiltration membrane. However, the apple juice was obtained from PET electrospun nanofibers membranes presented the better physic-chemical characteristic, i.e., more pronounced reduction of free sugars, decreasing the apple juice color, low protein content, comparable to the apple juice obtained by commercial microfiltration or by ultrafiltration membrane. Although the protein content of the apple juice was very low, however it will not be reduced the nutritional values of apple juice. On other hand, that can be useful to improve juice stability as well as reduce turbidity in apple juice. In additions, microfiltration membrane is also used for antibacterial filter application. Cooper et al. [90] reported the development of chitosan - polycaprolactone (PCL) nanofibers membranes. These membranes were prepared from PCL and chitosan content of 25, 50 and 75% and utilized the natural antibacterial property of chitosan for antibacterial water filtration. The performance of chitosan-PCL resulted the fiber diameter of 200 – 400 nm and 25% chitosan-PCL nanofiber membrane showed highest water flux of 6926 $L/h/m^2$ with 100% removal of 300 nm particles, while the 25% chitosan-PCL nanofiber membrane exhibited a similar water flux to that of the PCL membrane (≈ 2756 $L/h/m^2$). In a series of bacterial test, electrospun chitosan-PCL nanofibers membrane can be reduced *Staphylococcus aureus* adhesion compared to PCL nanofiber membranes.

Because PES can be considered as a model membrane material as it is widely use for commercial MF and UF as well as its high chemical, thermal resistance and also its appropriate mechanical properties. The preparation polyethersulfone (PES) electrospun nanofiber membrane for MF applications had been reported by

Homaeeigohar et al. [91,92]. The membrane was electrospun from 20 wt% PES solution, which PES was dissolved in N,N-dimethylformamide (DMF), by using the electrospinning conditions i.e., applied voltage of 20 kV, feed rate of 0.5 ml/h, spinning distance of 25 cm, inner diameter of the needle of 0.8 mm and using PES nonwoven as substrate. Thereafter, a set of samples was heated in the oven at temperature of 190 °C for 6 h. and then the membrane was slowly cooled in the oven. The surface morphology of PES electrospun nanofibers membrane showed relatively smooth and no beads or even droplet and the image analysis gave the average fibres diameter of 260 nm. The membrane properties exhibited the thickness of 200 µm, areal density of 0.2 -0.3 g/cm^2, mean flow pore diameter of 2 µm. Moreover, in term of membrane performance, the water flux measurement indicated that the membrane possess a high initial flux while retention test with polystyrene suspension showed that the filtration efficiency of PES electrospun membrane was highly dependent on size distribution of the suspended particles. When in feed was the particle over 1 µm in size, the rejection of the particles was performed within the first hour of the measurement with highly flux. On other hand, in case of a feed containing only nanoparticles, the rejection was accomplished within first hour as consequent of surface pore blocking and leading to the flux decreased. However, the PES electrospun membrane has potential to be used in pre-treatment of water or one step before UF and NF membranes.

Separation of polystyrene micron to sub-micron particles from water of electrospun Nylon-6 nanofiber membranes were investigated by Aussawasathien et al. [100]. The electrospun Nylon-6 nanofiber membrane, which fiber diameter in range of 30 - 110 nm, membrane thickness of 0.15 mm, pore size of 6.0 µm, had separated all particle size from 10 µm down to 1 µm unless separation efficiency was about 90% for 0.5 µm. Nevertheless, at the smaller the particle size, the flux was low due to the particles were able to pack closely together on the membrane surface, so called “layer effect” and thereby reducing the effective pore size of electrospun membrane at the surface. Furthermore, this dense “cake layer” acted as the separation layer for electrospun membrane, leading to high filtration efficiency for high content of ultra-small particles and the fouling mainly occurred within the surface of electrospun membrane due to the particles were mostly retained on the surface of the membrane. Therefore, electrospun Nylon-6 nanofiber membrane was able for using as pre-filters prior to ultrafiltration or nanofiltration to increase the filtration efficiency. In addition, the properties and performance of electrospun microfiltration membranes are summarized in Table 2.3.

Table 2.3 Properties and filtration performance of electrospun microfiltration membranes.

Polymer	Fiber diameter (nm)	Pore size (µm)	Thickness (µm)	Permeability ($l/m^2.h.bar$)	Filtration performance (%)	Particle size (µm)	Ref.
Nylon 6	30-110	6.0	150	9500	90	1.0	[100]
PAN-PET	100	0.22	200	2189	97	0.5	[58]
PCL-Chitosan	300	2.8	N.A.	17536	99	0.3	[90]
PES	280	2.0	200	2080	98	1.0	[92]
PET	420	2.5	N.A.	N.A.	96	N.A. (apple juice)	[89]
PSU	470 ± 150	2.1	135	13333	94	1.0	[6]
PVA	100 ± 19	0.21	100	23529	98	0.2	[103]
PVDF	380 ± 106	4.1	300	4000	91	5.0	[7]

2.3.3.3 Electrospun ultrafiltration membranes

Ultrafiltration is a filtration process discriminating a diverse range of particulates, such proteins, colloids, emulsions and viruses, as big as approximately 1 to 100 nm in the liquid environment [3]. This implies that, in order to use electrospun nanofibers web directly for ultrafiltration, the pore size of the electrospun nanofibers web needs to be less than 0.1 µm. Although it is possible to produce electrospun nanofibers web with such small pore size, this is not a practical solution for ultrafiltration membranes due to the rapid fouling of these webs. The rapid fouling rate in neat nanofiber membranes leads to high replacement frequency, which in turn leads to increased cost [97].

Conventional UF membranes are based on multi-layer composite structures [82,93], including an asymmetric porous membrane (see Figure 2.17) to give filtration functions and a nonwoven (fiber diameter of sub-micron) support to provide structure integrity and mechanical strength. Nevertheless, the porosity in these membranes usually results in a relatively low flux rate and high fouling tendency due to geometric structure of pore and the corresponding pore size distribution [94-96] and undesirable macro-void formation of pore across the membrane thickness [95,96].

Thereby, Yoon et al. [93] proposed a new concept to fabricated high flux UF membranes, involving to use of electrospun nanofiber membrane to replace the asymmetric porous membrane. Their demonstration system consists of a three-tier composite structure: (i) a non-porous hydrophilic top-layer by coating chitosan, (ii) an PAN electrospun nanofiber membrane as mid layer and (iii) a conventional

polyester nonwoven microfiber as substrate support, the schematic structure of three-tier approach to fabricate high flux and low-fouling ultrafiltration membranes as presents in Figure 2.19. The membranes, which assembled of electrospun PAN nanofiber membrane with average fiber diameter from 124 to 720 nm and porosity of 70%, was coated a chitosan top layer with a thickness of 1 µm. The results showed that these membranes had higher flux than commercial nanofiltration membranes in 24 h of operation (e.g. NF 270 from Dow), while maintaining the same rejection efficiency, more than 99% for oily waste-water filtration.

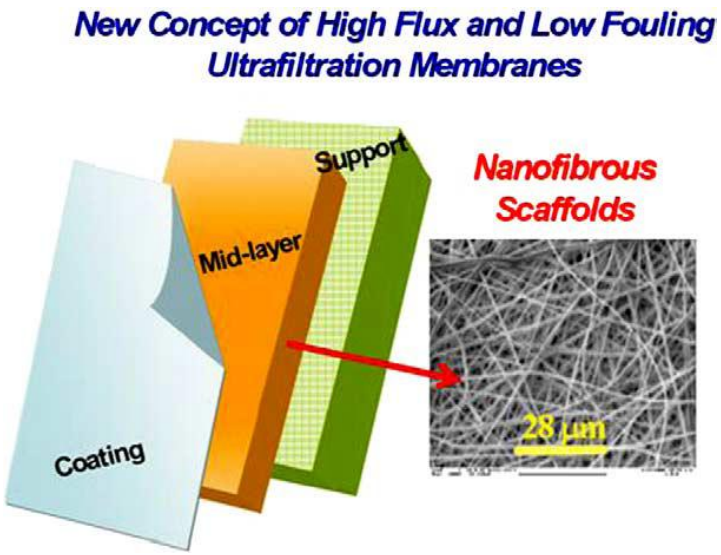

Figure 2.19 Schematic structure of three-layer approach to fabricate high flux and low-fouling for ultrafiltration membranes [82].

Wang et al. [27] prepared the hydrogel PVA in order to coat on top of nanofiber PVA scaffold. Results indicated that hydrogel PVA-PVA TFNC membrane exhibited a flux rate, more than 130 L/m^2 h, significantly higher than commercial UF membranes but with similar filtration efficiency of 99% for oily waste-water filtration. In addition, the mechanical property before and after cross linking of hydrogel PVA of the electrospun scaffold fabricated by 96% hydrolyzed PVA with relatively high molecular weight in range of 85,000-124,000 g/mol exhibited the similar performance.

A new kind of TFNC ultrafiltration membrane was developed by You et al. [98]. The TFNC membranes were used as an ultrafiltration membrane for oil/water emulsion separation at low feed pressure, which TFNC membrane consisted of a PVA thin hydrophilic barrier layer (thickness of 0.5 µm), electrospray PVA nanofiber (fiber diameter of 250 nm) and using electrospun PAN nanofibers (fiber diameter of 300 nm) as supporting substrate. The performance of PVA/PAN TFNC membrane resulted high flux (347 L/m^{2}h) with high rejection rate (99.6% for oil/water emulsion

separation) at very low feed pressure (0.2 MPa). Tang et al. [99] reported that the water flux of the curing of UV-PVA barrier layer on cross-linked PVA electrospun nanofiber scaffold of TFNC membrane was 70 L/m^2h with oil rejection during filtration of oil/water of 99.5% under the operation pressure of 0.21 MPa. It indicated that the performance of electrospray PVA/PAN TFNC membrane was better than the UV cured PVA TFNC membrane. Besides, the water flux of electrospray PVA/PAN TFNC membrane maintained at 309 L/m^2h and kept the rejection of oil/water emulsion separation of 99.5% and good anti-fouling property after 12 h filtration treatment. Nevertheless, ultrafiltration membranes cannot be achieved from a layer of electrospun nanofiber.

Chapter 3
Experimental

3. Experimental

3.1 Materials and chemicals

Commercial polyethersulfone (PES) (Ultrason E 6020 P) donated by BASF was used and dried at 120 °C for at least 4 hours before use and N-methyl-2-pyrrolidone (NMP) was purchased from Merck in order to prepare the electrospinning solutions. Nanoparticles base on silicon dioxide of 35 nm purchased from sigma-aldrich chemie GmbH were used for water filtration experimentation. In order to test air filtration, Di-Ethyl-Hexyl-Sebacat (DEHS) was purchased from Topas GmbH. Water purified with a milli-q system from millipore was used for all experiments. A polyethylene terephthalate nonwoven (Type, Novatexx 2429) served as the substrates donated by Freudenberg Filtration Technologies KG.

3.2 Experiments

3.2.1 Viscosity measurement

Polyethersulfone was dissolved in N-methyl-2-pyrrolidone at concentrations of 9%, 15% and 22% for 24 hours. The viscosity of the dope polymer solutions were measured with Anton Paar (Germany) model Physica MCR 301 digital rheometer. A CP25 – 2/TG cone-plate sensor was selected. The viscosity measurements as a function of the shear rate were performed at 25 °C. Each flow curve was obtained as an average of at least five measurements.

3.2.2 Preparation of nanofiber membranes

The electrospinning set-up was used for preparation of nanofiber membranes is shown in Figure 3.1. A power supply (model PNC 30000-40 UMP) was purchased from Heinzinger electronic GmbH. A solution pump (model KDS 100) was purchased from K.D. Scientific Inc., Holliston, MA, USA. Omnifix® solo plastic syringe and a needle of inner diameter 0.8 mm were purchased from B.Braun GmbH. A tube (Tygon Inert SE-200, size 3.2 X 6.4 mm.) was purchased from Pro Liquid-Scan. A steel plate was used as the electrode collects the nanofiber membranes.

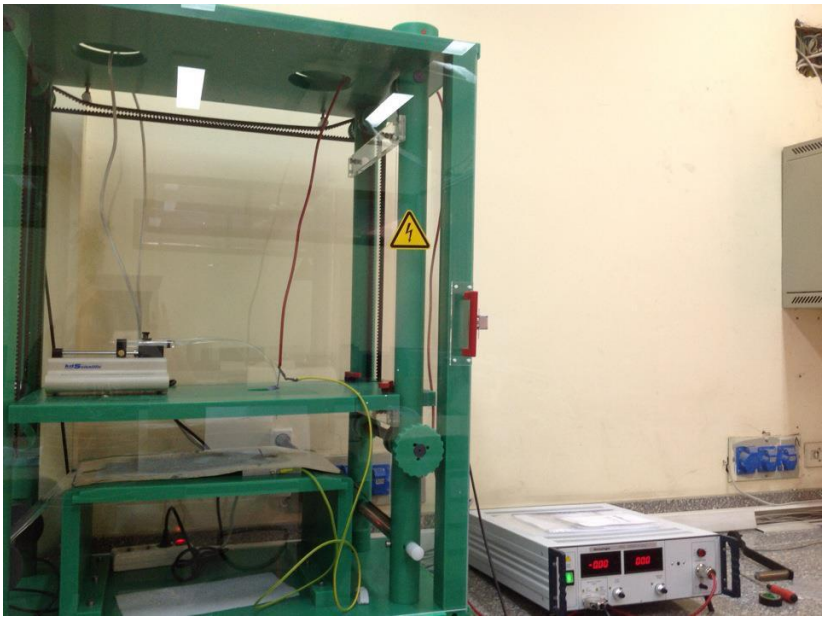

Figure 3.1 Experimental set-up for preparation of PES nanofiber membranes.

The PES solutions were electrospun under processing conditions with an applied voltage of 8, 10, 12, 14, 15, 16, 18 and 30 kV, a spinneret-to-collector distance of 5, 10, 15 or 20 cm, a flow rate of solution of 20 µL/min, a spinneret diameter of 0.8 mm and stationary or moving substrate with a speed of substrates moving of 2.2 cm/min. Either aluminum foil or polyethylene terephthalate nonwoven served as the substrates. The environmental humidity was varied, i.e., 50%, 65%, 70% and 80% RH.

The proto-membranes formed by electrospinning were treated under two conditions, i.e., drying at room temperature for 24 hours before characterization of membrane and immersion into water as coagulation water bath for 30 minutes and then washed before drying. Thereafter, the nanofiber membranes were placed in an oven at 60 °C for 24 h for drying.

3.2.3 Membranes characterization

3.2.3.1 Morphology

The top surface and cross section morphology of the nanofiber membranes was observed by using a Quanta 400 FEG (FEI) environmental scanning electron microscope (ESEM) at standard high-vacuum conditions. A K550 sputter coater (Emitech, U.K.) was used in order to coat the outer surface of the sample with gold/palladium. At least five different locations were observed to obtain surface morphology as well as cross section for one membrane sample.

3.2.3.2 Fiber diameter

The diameters of the fibers were determined by using an engage software program. At least five SEM pictures were used and the diameters of 100 fibers were measured and calculate the mean values for one condition nanofiber membrane.

3.2.3.3 Membranes thickness

The membrane thickness was measured by Coolant Proof Micrometer IP 65, Mutico Co., Japan and at least five measurements from different nanofiber membrane samples were averaged.

3.2.3.4 Porosity of membranes

The electrospun membranes maintained in distilled water was weighed after mopping superficial water with filter paper. The wet membrane was placed in an air-circulating oven at 60 °C for 24 h and then further dried in a vacuum oven at 60 °C for 24 h before measuring the dry weight. From the two weights (wet sample weight and dry sample weight), the porosity of membrane was calculated using equation following:

$$P\ (\%) = [\ (Q_0 - Q_1)/A.T\ ] \times 100 \quad (3.1)$$

Where P is the porosity of membrane, Q_0 the wet sample weight (g), Q_1 the dry sample weight (g), A the square of membrane (cm^2) and T is the thickness of membrane (cm).

3.2.3.5 Basic weight

Due to the delicate handling and the compressibility of the membranes, conventional methods for weight determination as, e.g. standard textile tests, were expected to be not applicable. Instead, the basic weight was estimated using two approaches. In a first approach the weight was calculated from the total polymer mass deposited over the membrane area. The basic weight of electrospun membranes can then be calculated as follows:

Basic weight (mg/cm^2) = (m-dot . τ) / A (3.2)

Where m-dot = mass flow (mg/min)

τ = residence time (min) = size of membrane in the direction of substrate movement (cm) / speed of substrates (cm/min)

A = area (cm^2)

In a second approach to estimate the basic weight, the specific volume of fibers in a unit area (1 cm^2) was calculated from the measured (mean) thickness, which was measured at five spots over the membrane area and averaged, and the porosity, which was determined as described in section 3.2.3.4. The basic weight is given by:

Basic weight (mg/cm^2) = A . T . ρ . (1 - P) (3.3)

Where A = unit area (1 cm^2)

T = thickness (cm)

ρ = density of PES polymer (1.37 g/cm^3)

P = porosity of membrane

3.2.3.6 Pore size of membranes

Pore size of electrospun membranes was determined by liquid dewetting of membrane pores using the Capillary Flow Porometer CFP-34RTG8A-X-6-L4 (PMI Inc., Ithaca, NY, USA). Membrane samples with a diameter of 25 mm were characterized via the “Dry up / Wet up” method. For the “Wet up” part, the membranes were wetted with 1,1,2,3,3,3-hexafluoropropene Galwick). The maximum transmembrane pressure for the air flow measurements was 3 bar. The mean pore was estimated using the PMI software.

3.2.3.7 Mechanical property

Electrospun membranes were tested for tensile strength by using an Zwick Roell material testing instrument (Test Expert® II, Germany) with a 10 N load cell at 25 °C and 65 ± 5% RH. The samples was cut, the size of samples was 2 cm of a width and a length of 10 cm. A cross-head speed of 50 mm/min was used and five samples were measured for each condition of electrospun membranes and then the mean values were calculated.

3.2.3.8 Contact angle

Sessile drop static contact angle (CA) of electrospun membranes were determined by using an optical contact angle measurement system (OCA 15 Plus; Dataphysics GmbH, Filderstadt, Germany). The water of 5 µL was dropped on the electrospun membrane surface from a microsyringe with a stainless steel needle in room temperature approximately 21 ± 3 °C. In order to determine, at least five measurements of drops at different location were averaged to obtain CA for one membrane sample.

3.2.4 Characterization of membranes performance

3.2.4.1 Gas permeability

Gas permeability of electrospun membranes were determined by using the Capillary Flow Porometer CFP-34RTG8A-X-6-L4 (PMI Inc., Ithaca, NY, USA). The maximum transmembrane pressure for the gas flow measurements was 3 bar, permeability of membranes were calculated by Darcy's law such that;

$$K_D = (\mu.Q / A)(T / \Delta p) \quad (3.4)$$

Where K_D is the permeability constant (m^2), µ the gas viscosity (17.85×10^{-6} kg m^{-1} s for N_2 at 20 °C), Q the total volumetric flow rate (m^3/s), A the area of membranes samples (m^2), T the thickness (m) and Δp the pressure drop across membrane samples (Pa).

3.2.4.2 Air filtration (Aerosol collection efficiency)

Aerosol particles were produced from di-ethyl-hexyl-sebacat (DEHS) by a pneumatic aerosol generator. In this study, aerosol of 400, 600, 800 and 1000 nm in diameter were used. The concentration of aerosol particles was monitored with scanning mobility particle sizer (Welas 2000 with Sensor 2100 (Palas)) and the aerosol particles was feed through the electrospun membrane samples by Feeder (AGF 2.0 (Palas)). The flow velocity through the electrospun membrane samples was 10 cm/s. The sample test area clamped in the holder exposed a circular diameter of 150 mm to the aerosol stream. The electrospun membranes were measured the upstream and downstream concentration of aerosol particles (DEHS), and then calculated the aerosol collection efficiency, E, of electrospun membranes using equation following:

$$E = (C_p - C_f) / C_p \quad (3.5)$$

Where C_f is the concentration downstream of the filter test sample and C_p is the aerosol particle concentration upstream.

3.2.4.3 Water flux

All electrospun membranes were characterized the water permeability by using a dead-end stirred cell filtration system (Amicon cell, model 8010) equipped with a reservoir (~450 mL) and pressurized by nitrogen from gas tank. The diameter of the membrane samples were 25 mm. Nanofiber membranes compaction were performed by filtration of pure water at 0.03 bar. The membranes were firstly compacted for at least 30 min. At least three measurements with the same pressure (0.03 bar) from different membrane sample were averaged for one membrane condition.

3.2.4.4 Water filtration

Silica nanoparticles of 35 nm were used for water filtration measurement. For preparation feed solution, a calibration curve was determined for each nanoparticles feed solution using Particlemetrix Stabisizer model 200CS. All the water filtration measurements were carried out using a dead-end stirred cell

filtration system connected to a reservoir and pressurized by nitrogen from gas tank at 0.1 bar. The flux of pure water was first determined, followed by separation of silica particles solution and feed solution concentration of 1.5 %. The stirring rate was 300 rpm. The separation flux was measured for every 5 cm^3 of permeate collected. The separation experiment was stopped at 50 mL or cm^3 of permeate was collected. The remaining nanoparticles solution was removed and the cell rinsed without removing the membrane. The cell was refilled the pure water and the water flux was determined again. Presence of any silica nanoparticles in permeate was detected with Particlemetrix Stabisizer model 200CS. The rejection (R, %) was determined using the formula following:

$$R = (1 - C_p / C_f) \times 100 \quad (3.6)$$

Where C_p and C_f are the silica solution concentration of permeate collected and the original solution feed, respectively.

Chapter 4
Results and Discussion

4. Results and discussion

The results in this work are shown in following parts: i. optimization of the nanofibers, ii. optimization of the nanofiber membranes, iii. nanofiber membranes properties and iv. nanofiber membranes performance.

4.1 Optimization of PES nanofibers

The polyethersulfone solution was electrospun into nanofibers under investigation the influence of parameters on electrospinning process with the stationary substrate set-up. The PES nanofibers were firstly observed the morphology. Thereafter, the diameters of fibers were measured.

4.1.1 Influence of polymer concentration

Figure 4.1 shows the morphology of electrospun nanofiber membranes with variation of polymer concentration.

(a)

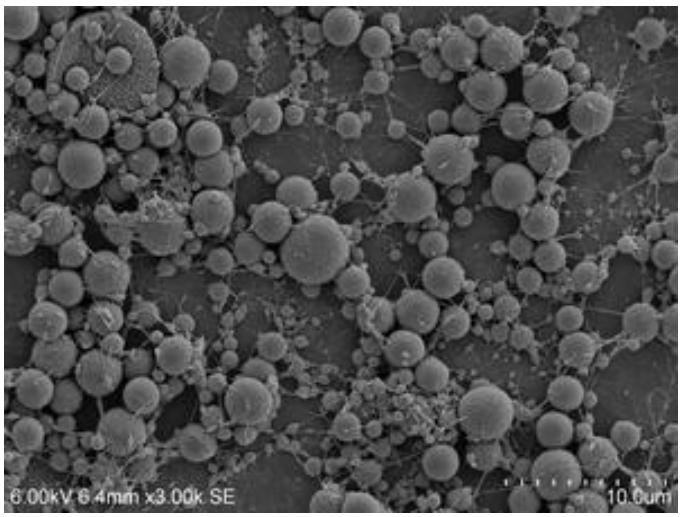

(b)

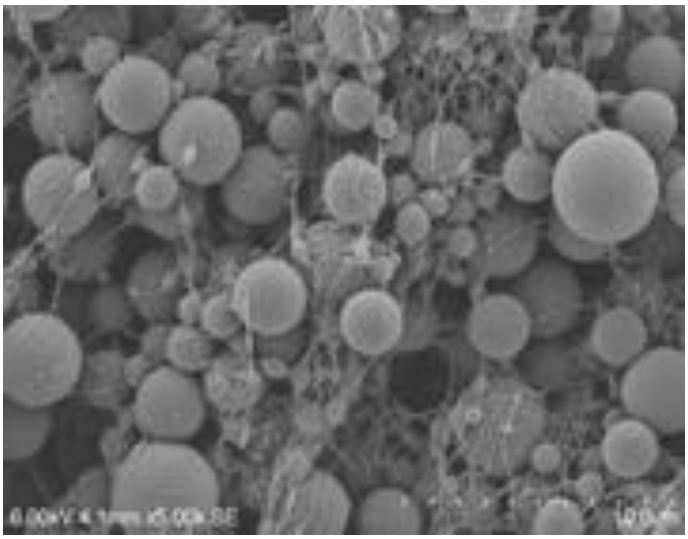

(c)

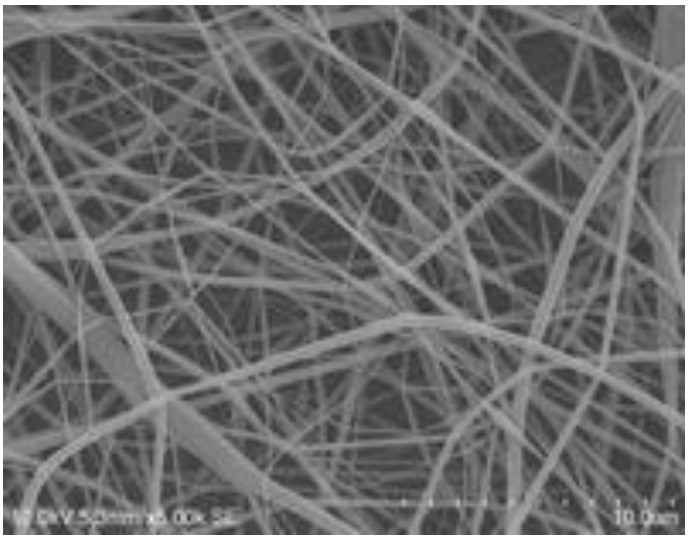

Figure 4.1 SEM images of nanofiber membranes from (a) 9% PES, (b) 15% PES and (c) 22% PES, in NMP using the conditions, i.e., a spinneret-to-collector distance of 10 cm, an applied voltage of 30 kV, a flow rate of 20 µL/min, a spinneret diameter of 0.8 mm, stationary substrate set-up and PET nonwoven served as the substrate.

The influence of PES concentration on viscosity had been studied because this property is important for the behavior of the polymer solution in electrospinning (Table 4.1).

Table 4.1 Viscosities of PES solutions in NMP at room temperature.

PES (%)	Viscosity (Pa s)
9	0.10
15	0.53
22	3.82

Figure 4.1 shows SEM images of PES electrospun nanofiber membranes from different solutions, using the same processing conditions, with stationary substrate set-up and PET nonwoven served as the substrate. The solution with 22% PES in NMP can be electrospun into well-defined nanofiber membranes (cf. Figure 4.1(c)) and the image analyses gave a mean fiber diameter of 489 ± 142 nm. As shown in Figure 4.1 (a) and (b) for PES concentration of 9% and 15%, respectively, the overall morphology of the web obtained is changed from a fiber network into spherical particles connected by fibers with the decrease of the polymer concentration in the solution used for electrospinning. This coincides with the results of previous works in literature review [14-22,25-29].

The results could be explained in terms of the viscosity of the solution effect (cf. section 2.2.1.1). As clearly seen in Table 4.1, it was presented that the viscosity of the 22% PES electrospinning solution (3.82 Pa s) was higher than those of 9% PES (0.10 Pa s) and 15% PES (0.53 Pa s) electrospinning solutions. However, increasing the polymer concentration led to increasing the viscosity of the polymer solution, an increased in the concentration results in greater polymer chain entanglements of the solution that is essential to maintain the continuity of the jet during electrospinning [15]. Furthermore, the chain entanglement of polymer had a significant impact on whether resultant jet breaks up into electrospun nanofibers [15,16].

4.1.2 Influence of spinneret-to-collector distance

The nanofiber membranes surface morphology with variation of distance between spinneret-to-collector are presented in Figure 4.2

(a)

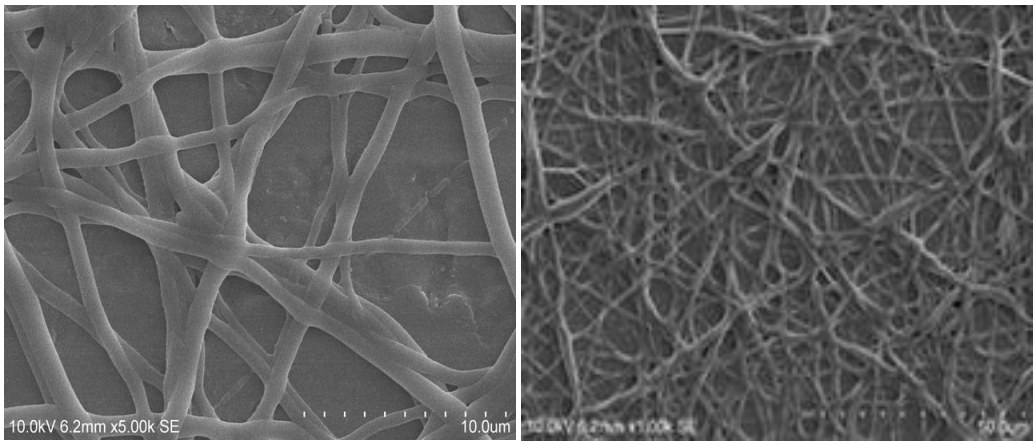
10.0kV 6.2mm x5.00k SE
10.0um

(b)

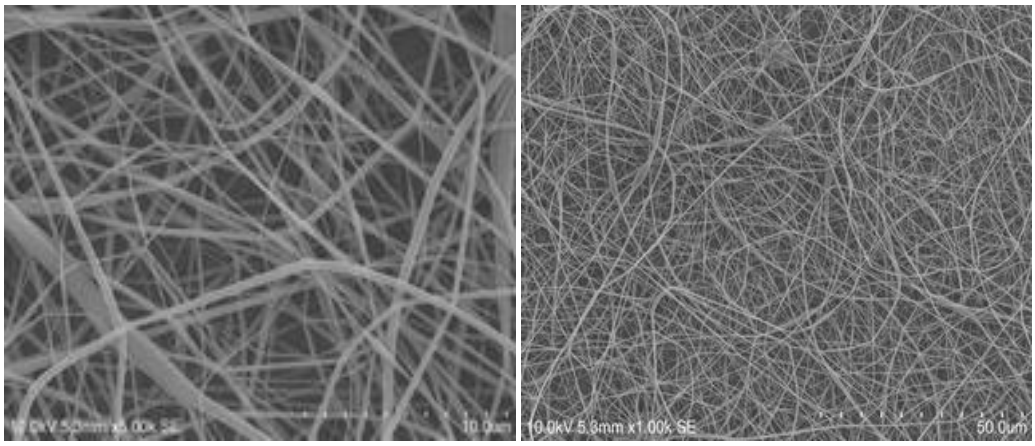
10.0kV 5.3mm x1.00k SE
50.0um

(c)

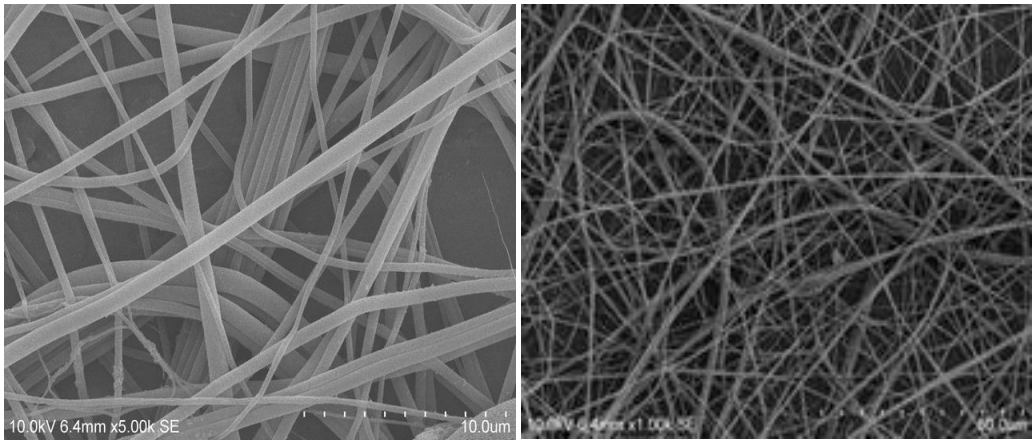
10.0kV 6.4mm x5.00k SE
10.0um

(d)

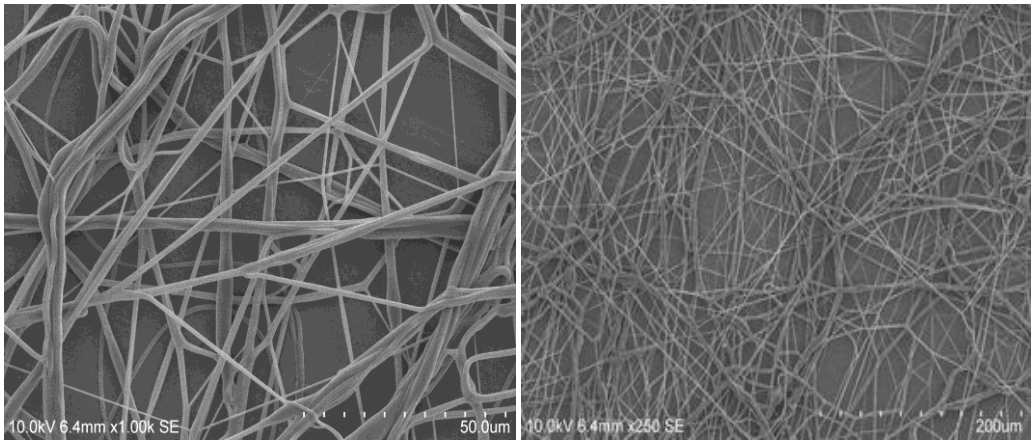

Figure 4.2 SEM micrographs of nanofiber membranes obtained by electrospinning from 22% PES in NMP using the conditions, i.e., an applied voltage of 30 kV, a flow rate of 20 µL/min, a spinneret diameter of 0.8 mm, stationary substrate set-up and PET nonwoven served as the substrate, but with different distance between spinneret -to-collector: (a) 5 cm, (b) 10 cm, (c) 15 cm and (d) 20 cm.

Figure 4.2 shows the SEM micrographs of nanofiber membranes obtained by electrospining from 22%PES in NMP by electrospinning, using same process conditions, with stationary substrate set-up and PET nonwoven served as the substrate, but with different spinneret-to-collector distance. For the nanofiber membranes which were electrospun at a distance of 5 cm, the overall morphology of fiber showed a thick ribbon shape and the surface of fiber was adhesive. The structure of the nanofiber membranes was a film-like. Homogeneous and regular fibers, without ribbon shape, were achieved when the distance between spinneret-to-collector increased from 5 cm to 10 cm (cf. Figure 4.2 (b)). As shown in Figure 4.2 (c) and (d) for distance between spinneret-to-collector of 15 cm and 20 cm respectively, the electrospun fibers seem to be closely jointed or even slightly fused together, when distance increased from 10 cm to 15 and 20 cm respectively. This means that the tip-to-collector distance affected the structure and morphology of electrospun fibers because of their influences complementing on the deposition time, evaporation rate of polymer solution and the electric field strength. For fibers to form, the electrospinning jet must have enough time for the evaporation of the solvent from polymer solution. Thereby, increasing the distance in electrospinning process resulted in a decrease of the average fiber diameter. Nevertheless, when the distance was too large resulted ribbon shaped morphology due to lower stretching force on the jet [41].

4.1.3 Influence of substrate in electrospun nanofibers

The morphology of nanofiber membranes which were electrospun from the same PES solutions under identical conditions onto different substrates are shown in Figure 4.3

(a) (b)

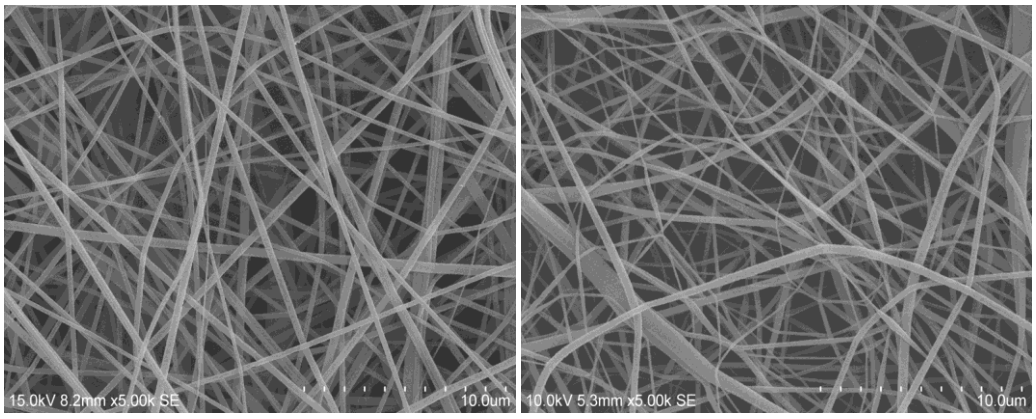

Figure 4.3 SEM images of nanofiber membranes obtained by electrospinning from 22% PES in NMP onto: (a) aluminum foil, and (b) PET nonwoven, as the substrates and using the conditions, i.e., a spinneret-to-collector distance of 10 cm, an applied voltage of 30 kV, a flow rate of 20 µL/min, a spinneret diameter of 0.8 mm and with stationary substrate set-up.

Figure 4.3 shows the SEM micrographs of nanofiber membranes obtained from solution of 22% PES in NMP by electrospinning using same processing conditions, the stationary substrate set-up, but with different substrates. Because the morphologies are identical, it can be concluded that these PES solutions can also be directly electrospun onto a porous PET nonwoven support which will enable the straight forward characterization of trans-membrane pore structure and filtration properties.

4.1.4 Influence of parameters in process on membranes structure

The photo of nanofiber membrane structure that was electrospun from the same PES solutions under identical conditions as in section 4.1.3 is presented in Figure 4.4.

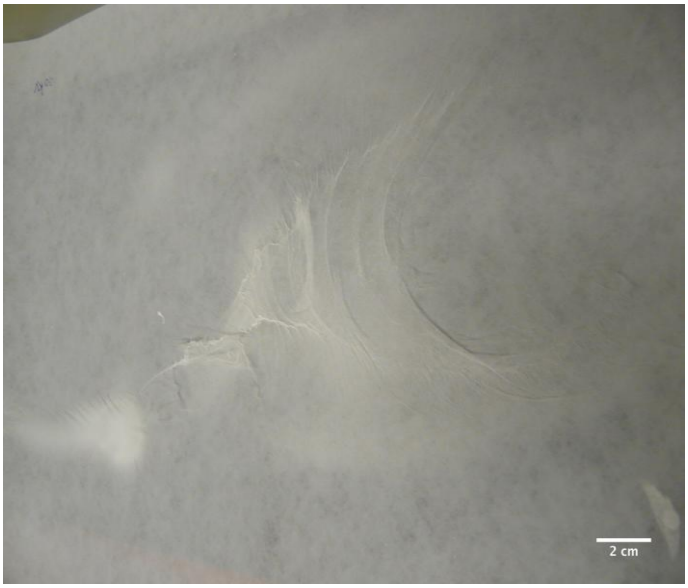

Figure 4.4 Photo image of nanofiber membranes obtained by electrospining from 22% PES in NMP using the conditions, i.e., a spinneret-to-collector distance of 10 cm, an applied voltage of 30 kV, a flow rate of 20 µL/min, a spinneret diameter of 0.8 mm, stationary substrate set-up and PET nonwoven served as the substrate.

Figure 4.4 shows the photo image of nanofiber membranes structure obtained from solution of 22% PES in NMP by electrospinning using processing conditions with stationary substrate set-up. Although the overall morphology of nanofiber in membrane shows homogeneous and regular fibers (cf. Figure 4.3 (a)). Nevertheless, membrane structure result indicated a 3-dimensional fiber web and discontinuous membrane sheet on substrate. This is because of static electric field in process and high charge on the material.

4.2 Optimization of PES nanofiber membranes

The 22% PES solution can be electrospun into well-defined nanofiber web by using the processing conditions, i.e., a spinneret-to-collector distance of 10 cm, an applied voltage of 30 kV, a flow rate of 20 µL/min, and a spinneret diameter of 0.8 mm, with stationary substrate set-up and using PET nonwoven as substrate and image analyses gave a mean fiber diameter of 489 ± 142 nm but the resulting conditions lead to a 3-dimensional fiber web on the substrate (cf. Figure 4.4). Therefore, in this section a moving substrate was used and it will be investigated the influence of parameters such as humidity, electrical potential, spinneret-to-collector distance on electrospinning process in order to produce the homogeneous layer membrane sheet. The morphology of nanofiber membranes was firstly observed.

4.2.1 Influence of relative humidity in electrospinning process

The nanofiber membranes were electrospun from 22% PES in NMP using same condition as before, but with different relative humidity conditions. The morphology of nanofiber membranes are presented in Figure 4.5.

(a)

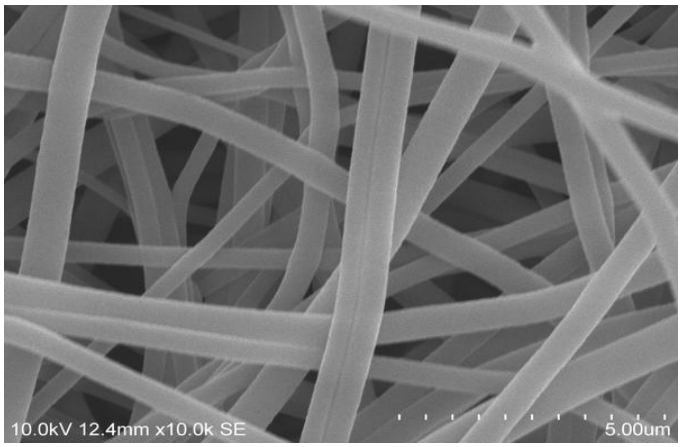

(b)

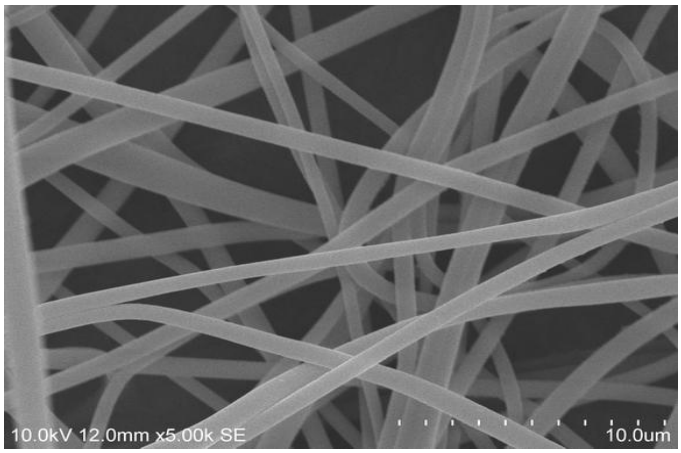

(c)

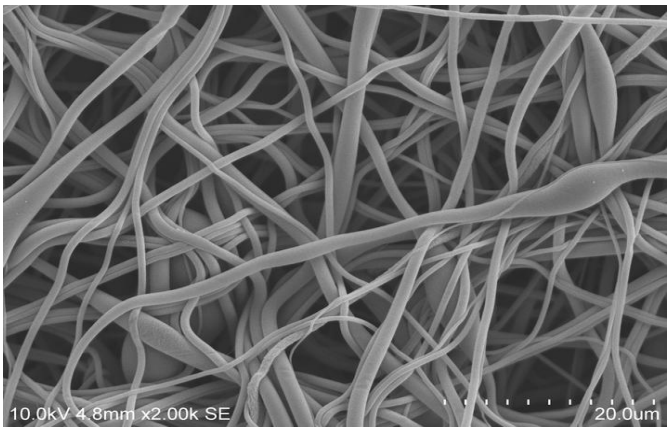

Figure 4.5 SEM images of nanofiber membranes obtained by electrospinning condition, i.e., a spinneret-to-collector distance of 10 cm, an applied voltage of 30 kV, a flow rate of 20 µL/min, and a spinneret diameter of 0.8 mm, a speed of substrates moving of 2.2 cm/min and PET nonwoven served as the substrate but different relative humidity conditions: (a) 50%, (b) 65% and (c) 80%.

Figure 4.5 shows the SEM micrographs of nanofiber membranes obtained from solution of 22% PES in NMP by electrospinning using processing conditions, where PET nonwoven served as the substrate. Optimum results were obtained, when the 22% PES solution was electrospun at a relative humidity of 65%. At higher humidity (>80%) resulted in irregular fiber formation, e.g., varying thickness, or even droplets. Low humidity yielded good fiber geometry; however, solidification appeared not to be finalized. This is assumed to be due to too little uptake of water in proto-membrane. Tang et al. [24], Medeiros et al. [42] and Wang et al. [43], reported that higher humidity led to increase the conductivity of this region between the tip and collector, therefore, changing the properties of the electric field strength in electospinning process due to the polarization of water molecules. Hence, the electrospun fiber became thick-diameter fiber due to weak electric field strength and smaller draw-down force at higher humidity.

4.2.2 Influence of electrical potential in electrospinning process

The nanofiber membranes surface and cross section morphology with variation of apply voltage are presented in Figure 4.6.

(a)

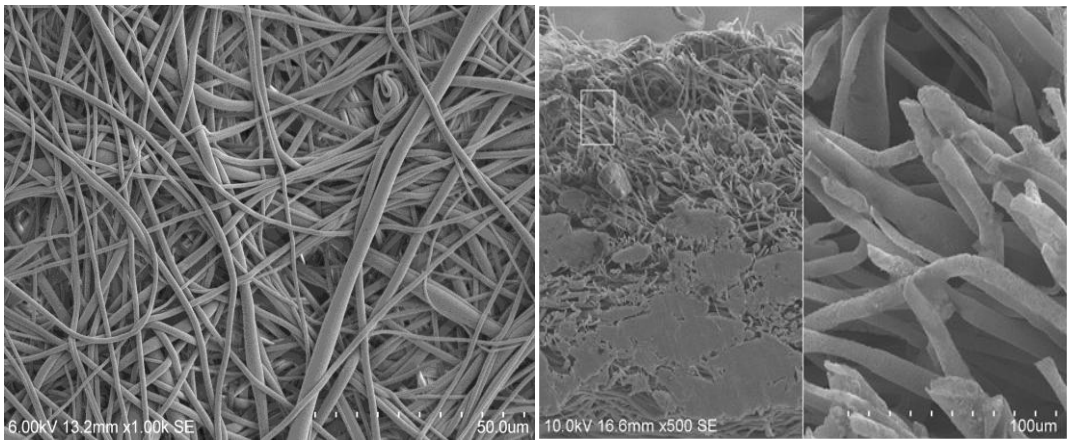
6.00kV 13.2mm x1.00k SE
50.0um
10.0kV 16.6mm x500 SE
100um

(b)

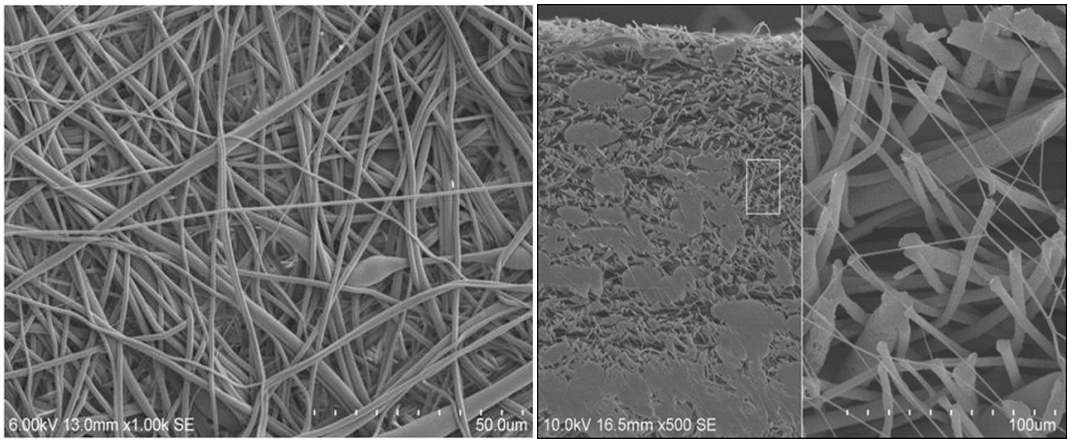
6.00kV 13.0mm x1.00k SE
50.0um
10.0kV 16.5mm x500 SE
100um

(c)

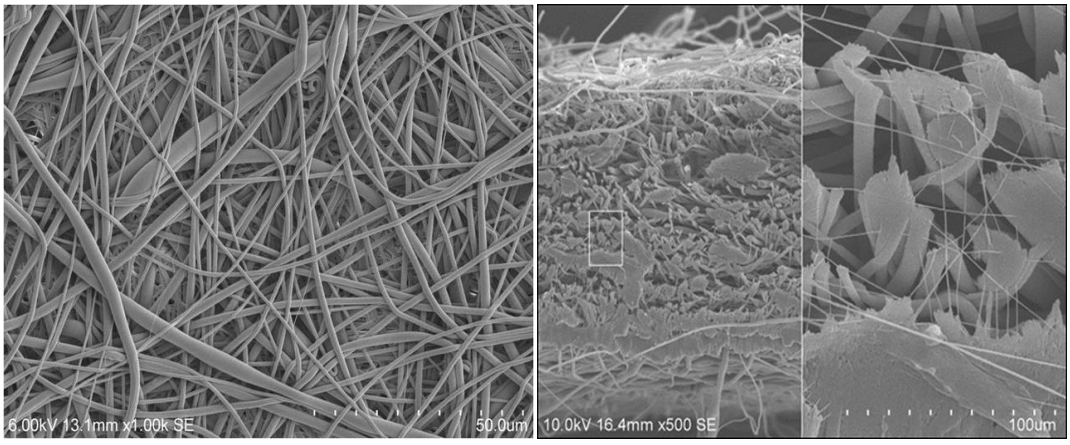
6.00kV 13.1mm x1.00k SE
50.0um
10.0kV 16.4mm x500 SE
100um

(d)

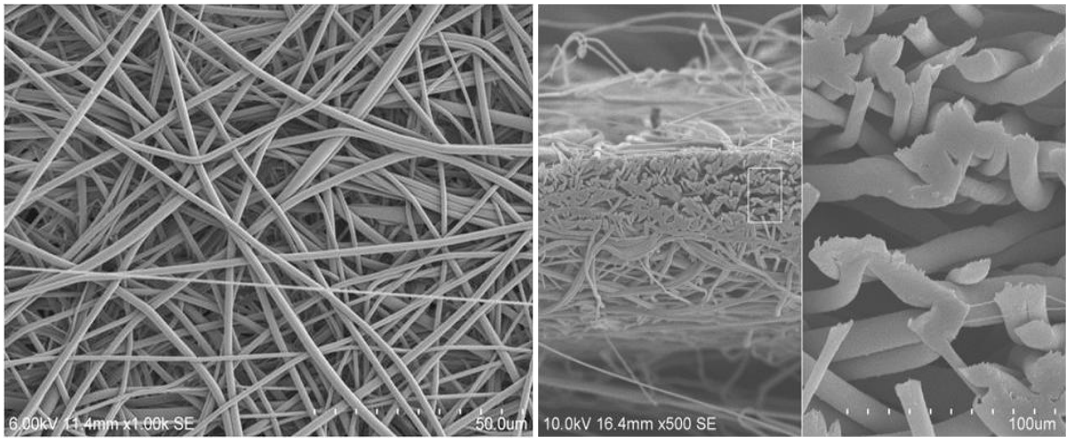

Figure 4.6 SEM images of the nanofiber membranes surface and cross section with variation of applied voltage: (a) 8 kV, (b) 10 kV, (c) 15 kV and (d) 18 kV, using processing conditions, i.e., a spinneret-to-collector distance of 10 cm, a flow rate of 20 µL/min, a spinneret diameter of 0.8 mm, 65% RH, a speed of substrates moving of 2.2 cm/min and PET nonwoven served as the substrate.

Nanofiber membranes surface morphology as well as cross-section structure, which were electrospun from solution of 22% PES in NMP by using a speed of substrates moving of 2.2 cm/min and PET nonwoven as the substrate, which were visualized by using SEM. The overall surface morphology of nanofiber membranes were electrospun with applied voltage of 8 kV resulted a beaded-fiber and thicker fiber as well as the nanofiber membranes were electrospun with applied voltage lower than 18 kV, as seen from the images in Figure 4.6 (a)-(c). However when the 22% PES in NMP solution was electrospun at an applied voltage of 18 kV, it yielded a more regular fiber formation (as shown in Figure 4.6 (d)). Nevertheless cross section images of all electrospun membrane revealed the super fine fibers in between the nanofibers.

Fiber diameter data which was measured by using engage software program are summarized in Table 4.2.

Table 4.2 Fiber diameter of electrospun membranes with variation of applied voltage in process (note: the length of the membrane is 30 cm in all cases).

Applied Voltage (kV)	Diameter of fiber (nm)			Avg. width of membranes (cm)
	Average	Max	Min	
8	1047 ± 348	2353	598	15
10	2218 ± 1587	5858	534	15
12	1039 ± 224	1635	470	15
14	993 ± 264	1554	399	15
15	992 ± 312	3142	598	15
16	909 ± 236	2225	548	15
18	875 ± 156	1179	400	15

From Table 4.2 can be seen that the electrospun membranes which were prepared with an applied voltage of 18 kV exhibited the finest fiber diameter (875 nm), when compared with nanofiber membranes that were prepared of lower applied voltage. As seen in Table 4.2, it indicated that decreasing of applied voltage could increase the diameter of fiber (cf. SEM, Figure 4.6). As the results, it was found that the diameter of electrospun fibers decreases with increasing electric field. These results accord with the results of Buchko et al. [14], Fong et al. [19] and Park et al. [39]. The thin nanofibers obtained in the electrospinning process are produced as a result of spiral motion and elongation of a polymer jet driven by stronger stretching force at higher electrical potential between the polymer solution in capillary and the collector. When the electrostatic force in the polymer jet become large enough to overcome the cohesive force within the jet, then the spiral motion and elongation of the polymer jet in process with higher electric field strength become more active, and consequently finer nanofibers are achieved [14,39].

4.2.3 Influence of spinneret-to-collector distance

The surface morphology of electrospun membranes with variation distance between spinneret-to-collector are shown in Figure 4.7.

(a) (b)

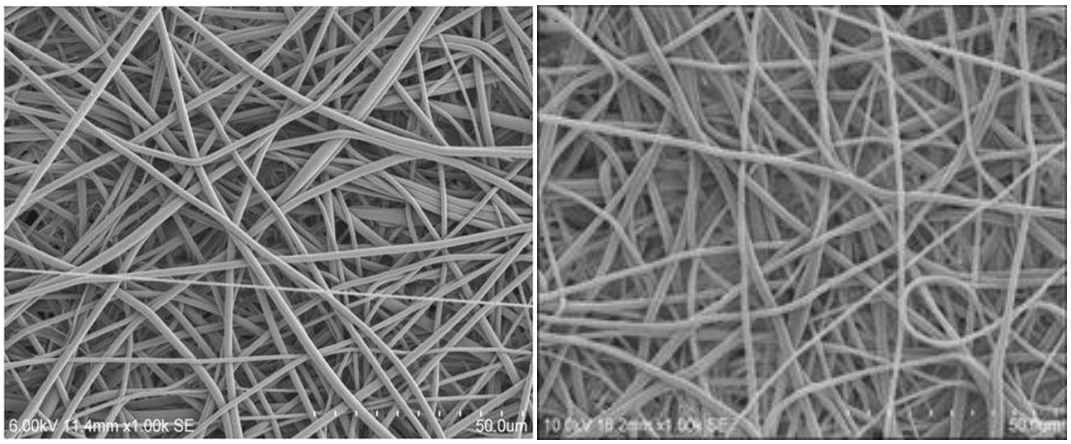

(c) (d)

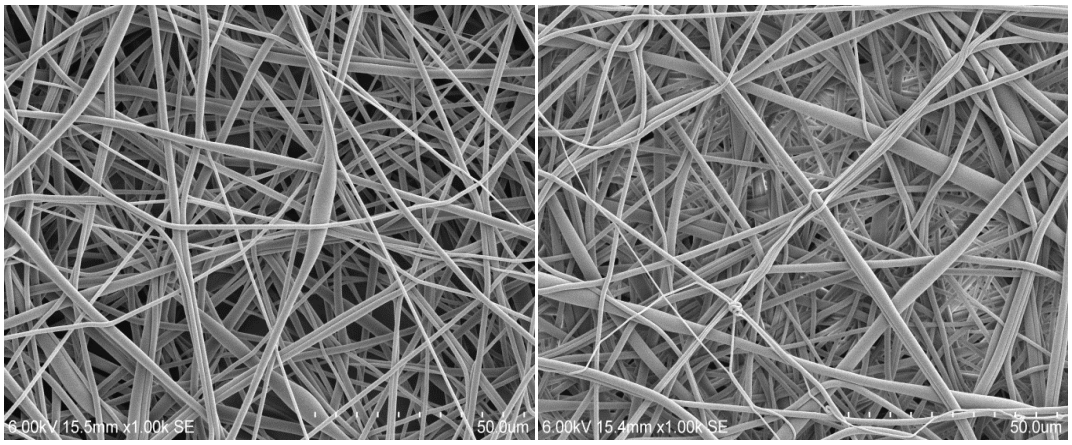

Figure 4.7 SEM images of electrospun membranes using the process condition, i.e., an applied voltage of 18 kV, a flow rate of 20 µL/min, a spinneret diameter of 0.8 mm and 65% RH, a speed of substrates moving of 2.2 cm/min and PET nonwoven served as the substrate but with variation of distance between spinneret-to-collector; (a) 10 cm, (b) 12 cm, (c) 14 cm and (d) 15 cm.

Figure 4.7 shows the influences of variation distance between spinneret- to – collector on the PES electrospun membrane morphology, which were electrospun by using a speed of substrates moving of 2.2 cm/min and PET nonwoven served as the substrate. As clearly seen in Figure 4.7 (a), when 22% PES was electrospun at 10 cm resulted homogeneous and well-defined nanofiber membranes. From Figure 4.7 (b), a few bead fibers appeared when the distance between spinneret-to-collector was 12 cm. Nevertheless at higher distance between spinneret-to-collector (14 and 15 cm), beaded and thicker fiber were formed on structure of electrospun membranes (Figure 4.7 (b)-(d).

In addition, fiber diameter data, which was measured by using engage software program, are summarized in Table 4.3.

Table 4.3 Fiber diameter of electrospun membranes with variation of distance between spinneret-to-collector in process (note: the length of the membrane is 30 cm in all cases).

Distance (cm)	Diameter of fibers (nm)			Avg. width of membranes (cm)
	Average	Max	Min	
10	875 ± 156	1179	400	15
12	896 ± 204	1342	579	17
14	1010 ± 312	1987	468	18
15	973 ± 334	1814	148	19

Table 4.3 showed the influence of distance between spinneret-to-collector variations on the fiber diameter of electrospun membranes. It was seen that when membranes were electrospun at distance spinneret-to-collector of 10 cm led to lowest average fiber diameter, which the image analyses gave an average fiber diameter of 875 nm. Whereas the electrospun membranes were prepared at higher distance between spinneret-to-collector of 12, 14 and 15 cm, the image program analyses gave the average diameter of fiber of 896, 1010 and 973 nm, respectively. It can be concluded that decreasing of spinneret-to-collector distance leads to decreasing diameter of the fibers because of increasing electric field strength in electrospinning process due to stronger stretching force on the jet. Furthermore, increasing of spinneret-to-collector distance leads to increasing size of the electrospun membranes. The influences of variation distance between spinneret-to-collector in process were discussed by many researchers (see section 2.2.3).

4.2.4 Homogeneity of PES electrospun membranes

The photo of electrospun membrane structure that was prepared from the 22% PES solutions under the same conditions with a speed of substrates moving of 2.2 cm/min, 65% RH and using PET nonwoven as substrate, is presented in Figure 4.8.

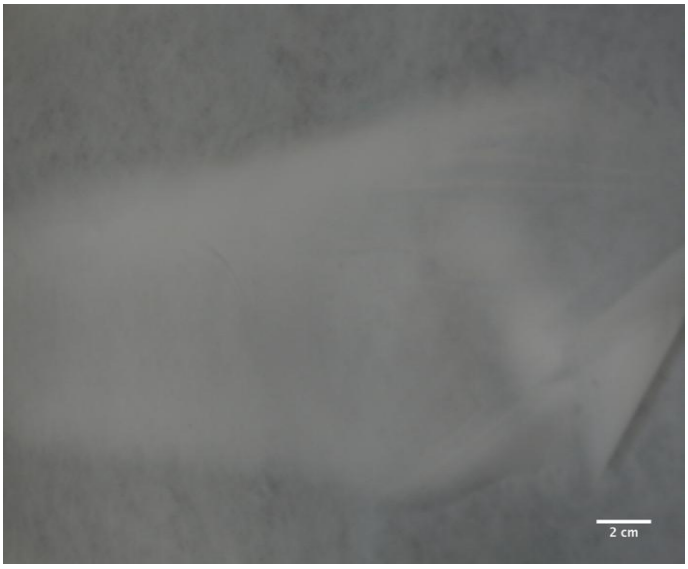

Figure 4.8 Specimen of 22% PES electrospun membrane, which was prepared under conditions, i.e., an applied voltage of 18 kV, a spinneret-to-collector distance of 10 cm, a flow rate of 20 µL/min, a spinneret diameter of 0.8 mm, a speed of substrates moving of 2.2 cm/min, 65% RH and using PET nonwoven as the substrate.

As presented in Figure 4.8, when the 22% PES solution was electrospun membrane using a spinneret diameter of 0.8 mm, a speed of substrates moving of 2.2 cm/min, 65% RH and served the PET nonwoven as the substrate yielded a more planar membrane compared to the membrane which was electrospun using same condition (cf. Figure 4.4), but with different applied voltage condition (30 kV).

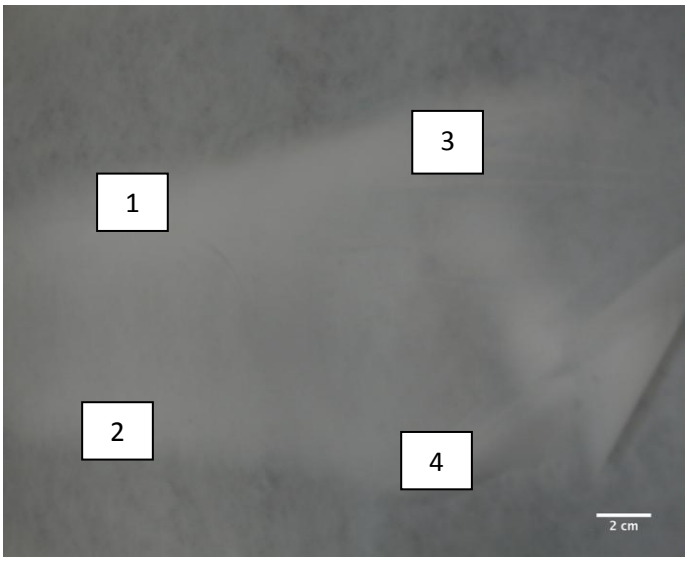

(a) (b)

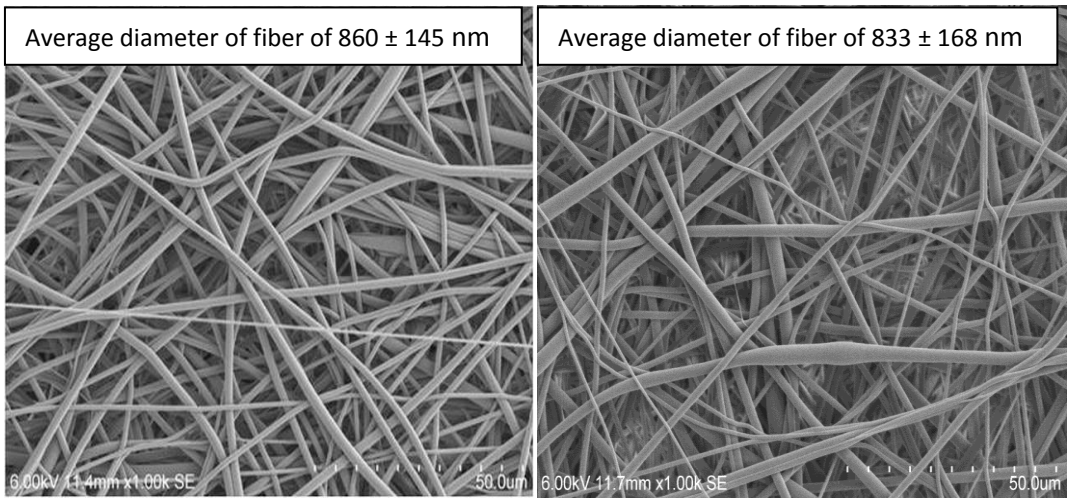

(c) (d)

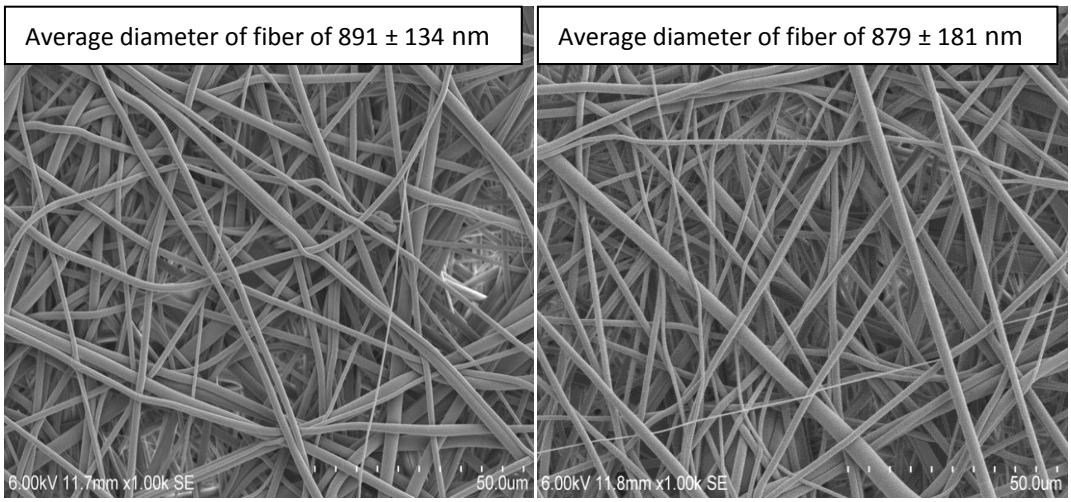

Figure 4.9 SEM images and fiber diameter with different position on electrospun membranes obtained by using the same electrospinning condition as Figure before; (a) position 1, (b) position 2, (c) position 3 and (d) position 4.

From SEM images of electrospun membranes which was obtained by using electrospinning condition same as Figure 4.8, the overall surface morphology of all position on electrospun membranes resulted in good fiber geometry formation and the whole electrospun membrane looked uniform, e.g., without droplets, or even thicker fiber formation. Furthermore, the average fiber diameter showed the nearby values, which were ranging from 833-891 nm. Overall all data indicated that electrospun membranes were homogeneous.

4.2.5 Influence of post-treatment conditions on fiber surface of electrospun membranes

The proto-membranes formed by electrospinning were treated under different conditions in order to investigate the influence of post-treatment conditions on surface morphology of membranes. The morphology of electrospun membranes are presented in Figure 4.10.

(a) (b)

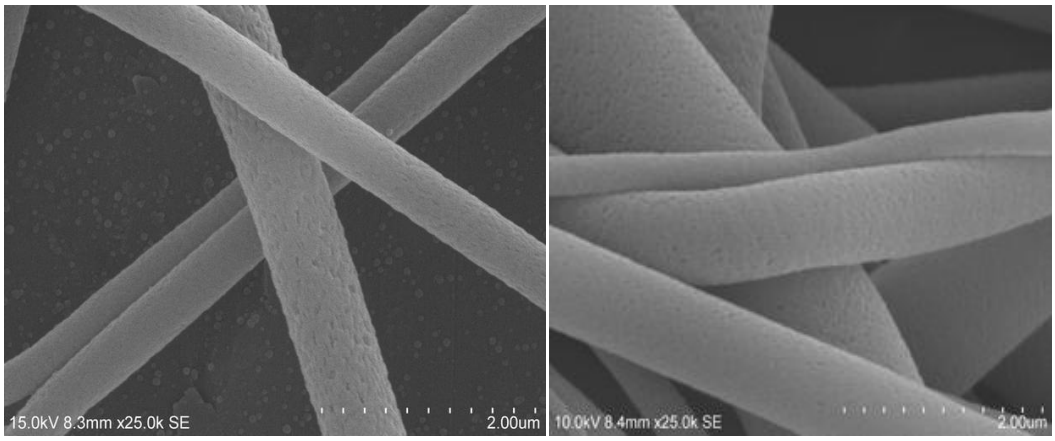

Figure 4.10 SEM micrographs of nanofiber membranes obtained by electrospinning from 22% PES in NMP using an applied voltage of 18 kV, a spinneret-to-collector distance of 10 cm, a flow rate of 20 µL/min, a spinneret diameter of 0.8 mm, a speed of substrates moving of 2.2 cm/min, 65% RH and using PET nonwoven as the substrate with different treatment conditions: (a) immersion in an aqueous coagulation bath and (b) drying at 65 ± 5% RH and 20 °C.

Figure 4.10 shows the SEM micrographs of fiber surface obtained from solutions of 22% PES in NMP by electrospinning using same processing conditions but with different treatment conditions. It is clearly seen in Figure 4.10 (a) that the proto-membrane which had been treated by immersion into the water bath leads to a pronounced porosity on the fiber surface as compared to the another treatment condition (cf. Figure 4.10 (b)). It is assumed that this is due to a phase separation induced by the exchange of the residual solvent NMP in the proto-membrane with water in the aqueous coagulation bath, acting as non-solvent for PES.

4.3 Properties of PES electrospun membranes

PES solutions were electrospun by using various conditions in the process. Thereafter, they were tested with respect to the properties such as thickness, porosity, basic weight, pore size, mechanical property and contact angle.

4.3.1 Thickness of electrospun membrane

The thickness of electrospun membranes are shown in Figure 4.11.

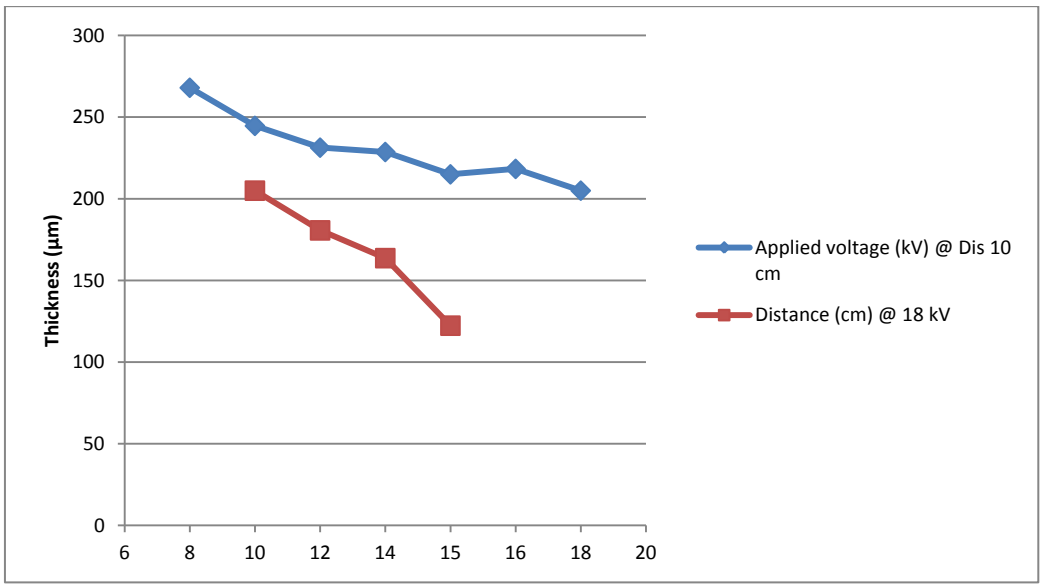

Figure 4.11 Thickness of electrospun membranes by using the condition, a flow rate of 20 µL/min, a spinneret diameter of 0.8 mm, a speed of substrates moving of 2.2 cm/min, 65% RH and using PET nonwoven as the substrate with different applied voltage and distance between a spinneret-to-collector in process.

As clearly seen in Figure 4.11, the thickness of electrospun membranes tended to decrease slightly when the applied voltage and distance between spinneret-to-collector in process increased.

4.3.2 Porosity of electrospun membranes

The calculated porosity of electrospun membranes are summarized in Figure 4.12.

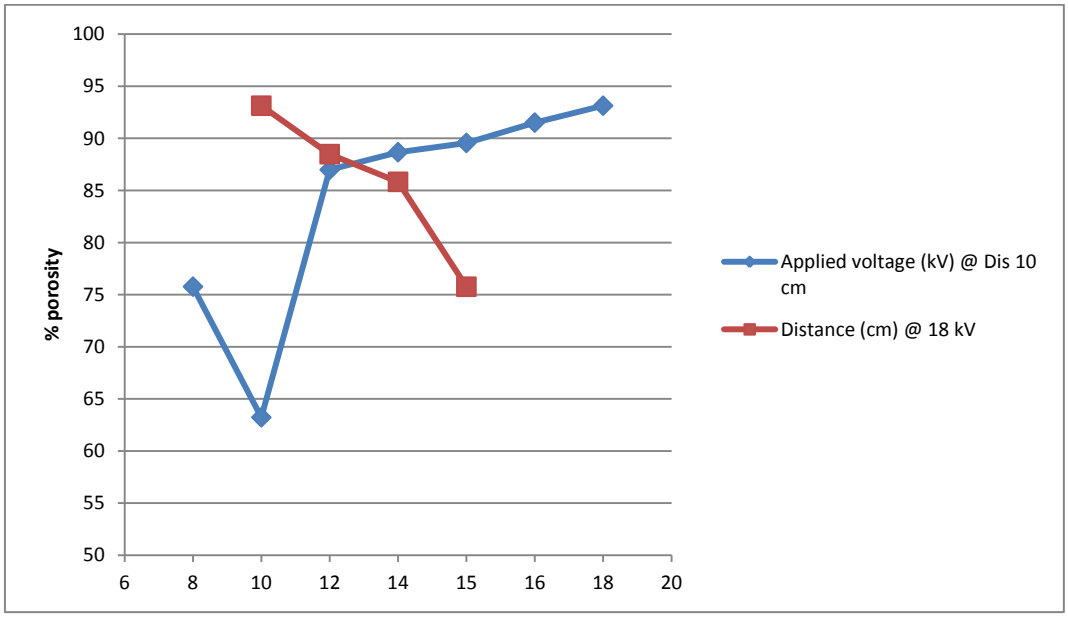

Figure 4.12 Porosity of electrospun membranes by preparing under conditions, a flow rate of 20 µL/min, a spinneret diameter of 0.8 mm, a speed of substrates moving of 2.2 cm/min, 65% RH and using PET nonwoven as the substrate but with varying applied voltage and distance between spinneret-to-collector in electrospinning process.

Figure 4.12 showed the porosity of electrospun membranes at varied applied voltage and distance between spinneret-to-collector. The porosities of electrospun membranes are high for membranes prepared by high applied voltage and at low spinneret-to-collector distance. The electrospun membranes were prepared with an applied voltage of 18 kV presented the highest porosity of 93%, when compared with electrospun membranes that were prepared of lower applied voltage. It can be explained that increasing of applied voltage could decrease the diameter of fiber and then led to decreasing mean pore size of membranes (cf. Figure 4.6 and Figure 4.16). From these phenomenon led to increasing porosity of electrospun membranes (cf. Figure 5.13).

Figure 4.12 also showed the effect of distance between spinneret-to-collector variations on porosity of electrospun membranes. The calculated results showed that when membranes were electrospun at distance spinneret-to-collector of 10 cm led to highest porosity of electrospun membrane of 93%. While the

electrospun membranes were prepared at higher distance between spinneret-to-collector, the porosity was slightly decreased. As the result, it was found that the porosity of electrospun membranes decreased with increasing distance between spinneret-to-collector. Correlating these results with the mean pore size as well as fiber diameter (cf. 4.2.3) of the electrospun membranes in Figure 4.13, it clearly indicated that the mean pore size is the crucial parameter to determining the porosity of the electrospun membranes. Increasing of mean pore size leads to decreasing porosity of electrospun membranes [cf. 105, 106].

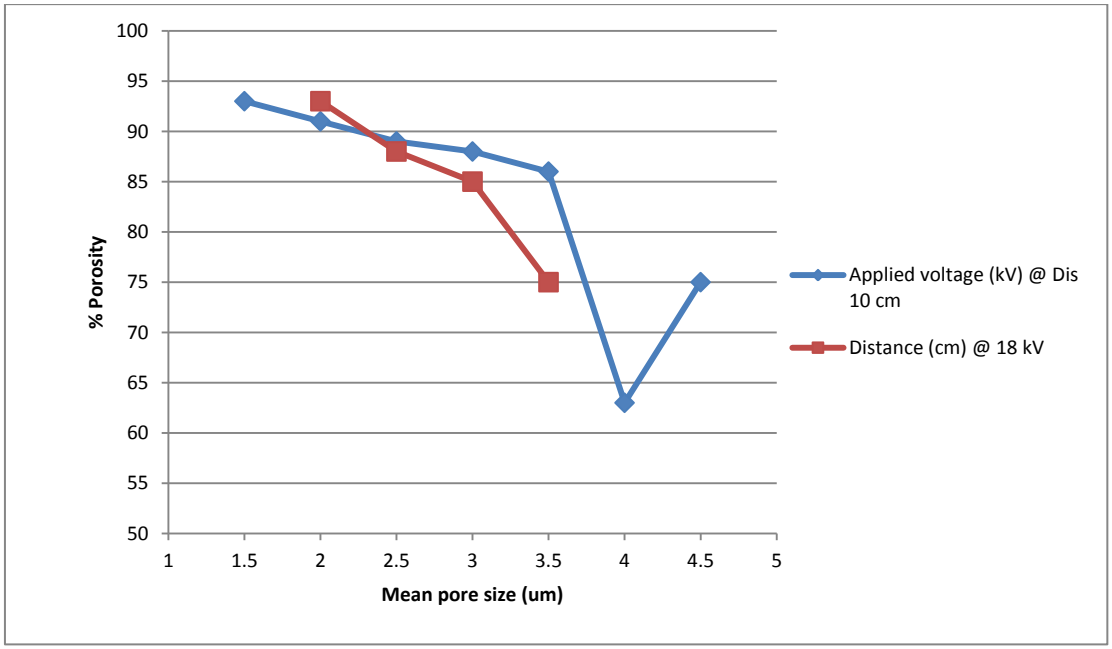

Figure 4.13 Correlation between mean pore size with porosity of electrospun membranes tunable by preparation conditions.

4.3.3 Basic weight of electrospun membranes

Since spinning parameters were found to have an effect on membrane size, thickness and porosity, it was important to try and establish the basic weight, which is a major parameter of a membrane. The delicate handling and problematic sample preparation, the basic weight was not measured but estimated on the basic of other process or sample parameters. Two different approaches for this calculation were chosen (cf. 3.2.3.5). Based on the mass flow during spinning and the spinning time, the total maximum mass spread over the membrane area was calculated and related to the membrane area. The calculated basic weight of electrospun membranes are presented in Table 4.4 and Figure 4.14.

The data in Table 4.4 shows that area increased with increasing spinneret-to-collector, whereas thickness and basic weight decreased. This is logic, as the same amount of polymer has to cover an increasing area or size of membrane; hence the (mean) thickness decreases. The model assumes a uniform deposition of fiber over the area. This simple assumption obviously does not relate to the actual geometry of the membrane, where the thickness changes across the membrane roughly according to a Gaussian shape.

Table 4.4 Correlation between area and thickness with basic weight of electrospun membranes tunable by preparations condition (note: the length of the membrane is 30 cm in all cases).

Distance spinneret-to-collector (cm)	**Width of membrane (cm)**	**Thickness (µm)**	**Basic weight (mg/cm^2)**
10	15	205	0.169
12	17	180	0.149
14	18	163	0.141
15	19	122	0.134

The influence of varying distance between spinneret-to-collector and applied voltage on the calculated basic weight of electrospun membrane is shown in Figure 4.14. It can be seen that when membranes were electrospun at distance spinneret-to-collector of 10 cm led to highest basic weight of 0.169 mg/cm^2. Moreover, it was found that the basic weight of electrospun membranes decreased with increasing distance between spinneret-to-collector. While the electrospun membranes with varying of applied voltage showed similar the calculated basic weight.

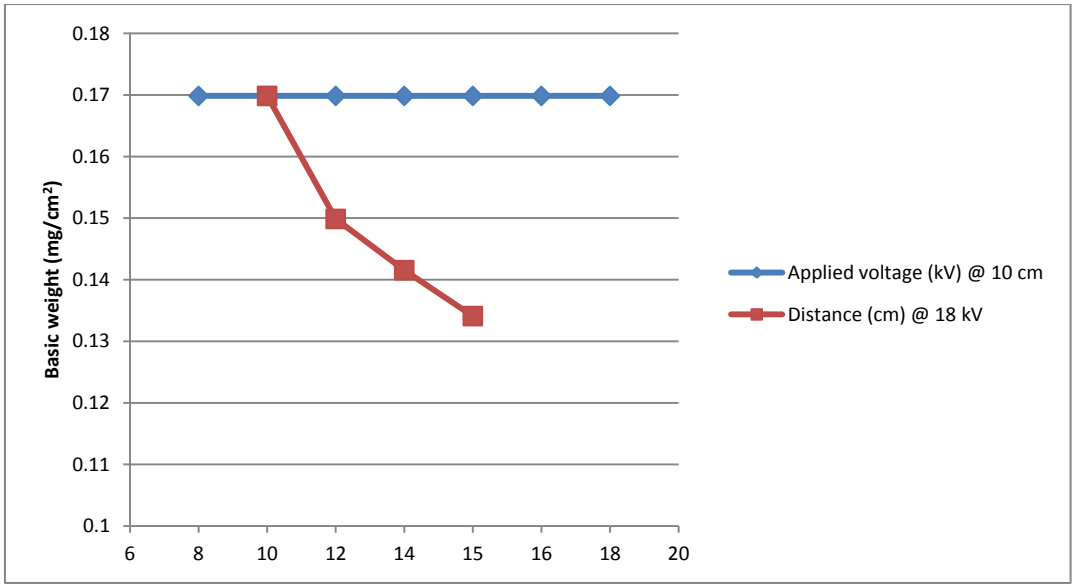

Figure 4.14 Calculated basic weight of electrospun membranes by using the condition, a flow rate of 20 µL/min, a spinneret diameter of 0.8 mm, a speed of substrates moving of 2.2 cm/min, 65% RH and using PET nonwoven as the substrate with different applied voltage and distance between a spinneret-to-collector in process.

In a second approach to estimate the basic weight, the specific volume of fibers in a unit area (1 cm^2) was calculated from the measured (mean) thickness and the porosity, which was determined in section 3.2.3.5 (cf. eq. 3.3). The basic weight was then calculated using the PES density of 1.37 g/cm^3. The resulting numbers are given in Table 4.5.

Table 4.5 Correlation between thickness and porosity with basic weight of electrospun membranes tunable by preparations condition.

Distance spinneret-to-collector (cm)	Thickness (µm)	Porosity (%)	Basic weight (mg/cm^2)
10	205	93	1.9
12	180	88	3.0
14	163	85	3.3
15	122	75	4.1

It is clearly seen that there is no agreement the basic weight calculated by the two models. The actual values differ by one order of magnitude, and the estimated weight follows an opposing trend in dependence on distance between

spinneret-to-collector. In order to judge the significance of both models (see eq. 3.2 and 3.3), several aspects shall be discussed.

First, it has to be noted that in the above calculations, the thickness was an average value derived from multiple measurements over the whole membrane, the stated porosity (cf. Table 4.5) characterizes the central area of the membrane. This is due to the necessary size of the samples for the determination of the porosity in the chosen way. Again, one has to point out that at least the membrane thickness is not constant and varies from edge to central area to edge. It may be assumed that the stated porosity will not be significant for the edge portions of the membrane.

Second, if we make use of the weight values derived from mass flow and as stated in Table 4.4 to calculate membrane porosity using eq. 3.3, we obtain porosities of the order of 99% for all of four samples.

Third, typical porosities of technical textiles and nonwovens made of micro-fibers with diameter of 5 µm and larger area of the order of 90%. Given this background, it is reasonable to assume far higher porosities for nanofibrous membranes, whereas values like 85 or 75% as given in Table 4.5 are highly unlikely.

It has to be concluded that the basic weight value in Table 4.4 are quite representative, but also that the chosen way to characterize porosity (cf. 3.2.3.4) may be doubtful in the case of these specific samples.

4.3.4 Mean pore size of electrospun membranes

The mean pore size of the electrospun membranes is a factor for determining the filtration performance of the membranes. Basically, smaller pore size leads to higher aerosol collection efficiency or particle separation efficiency, both of which are the most critical performance criteria of air filtration and water filtration, respectively [30]. The measured mean pore sizes are presented in Figure 4.15 and the correlation between diameters of nanofibers with mean pore size of electrospun membranes tunable by preparations condition is shown in Figure 4.16.

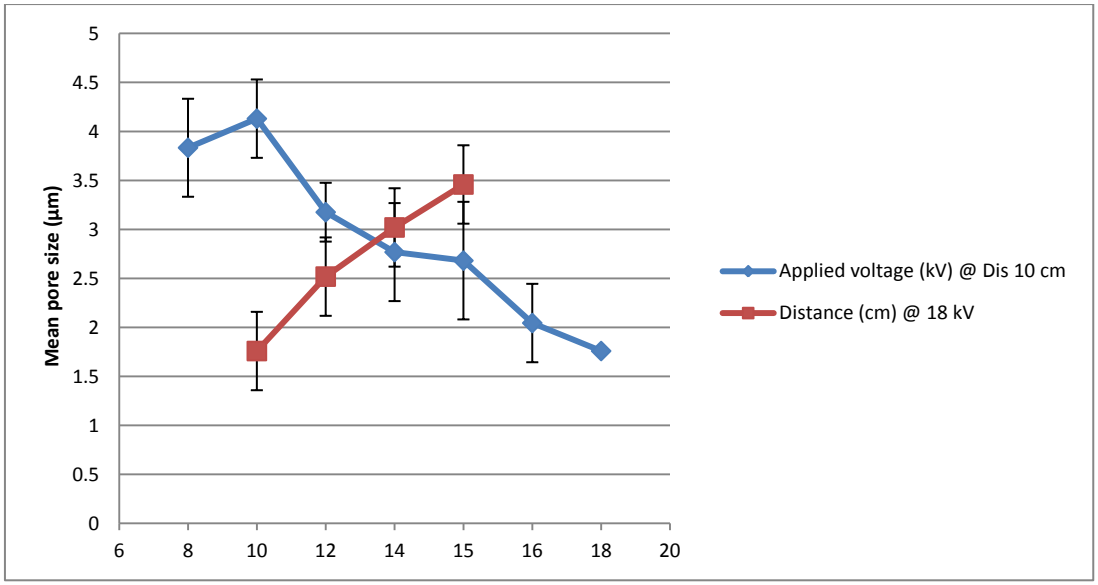

Figure 4.15 Effect of varying applied voltage and distance between spinneret- to-collector in electrospinning process on the mean pore size of electrospun membranes by preparing under conditions with a flow rate of 20 µL/min, a spinneret diameter of 0.8 mm, a speed of substrates moving of 2.2 cm/min, 65% RH and using PET nonwoven as the substrate.

It can be seen in Figure 4.15 that increasing applied voltage and decreasing distance in the electrospinning process leads to decreasing mean pore size of membranes. The mean pore size of electrospun membranes by preparing at high applied voltage is lower than electrospun membranes by preparing at low applied voltage. The electrospun membranes were prepared with an applied voltage of 18 kV exhibited the pore size of 1.7 µm, when compared with nanofiber membranes were prepared of lower applied voltage. As seen in Figure 4.15, it indicated that increasing of applied voltage could decrease the diameter of fiber (cf. Table 4.2) and hence mean pore size of membranes decrease (cf. Figure 4.16).

The influence of varying distance between spinneret- to- collector on the mean pore size of electrospun membranes also is shown in Figure 4.15. It was seen that when membranes were electrospun at distance spinneret-to-collector of 10 cm led to lowest mean pore size of 1.7 µm. Besides, it found that the mean pore size of electrospun membranes increased with increasing distance between spinneret-to-collector. Correlating these results with the fiber diameter of the electrospun membranes in Figure 4.16, it could be seen that the fiber diameter is the crucial parameter to determining the mean pore size of the electrospun membranes. Increasing of fibers diameter leads to increasing mean pore size of electrospun membranes. This result was similar to the results of Park et al. [39].

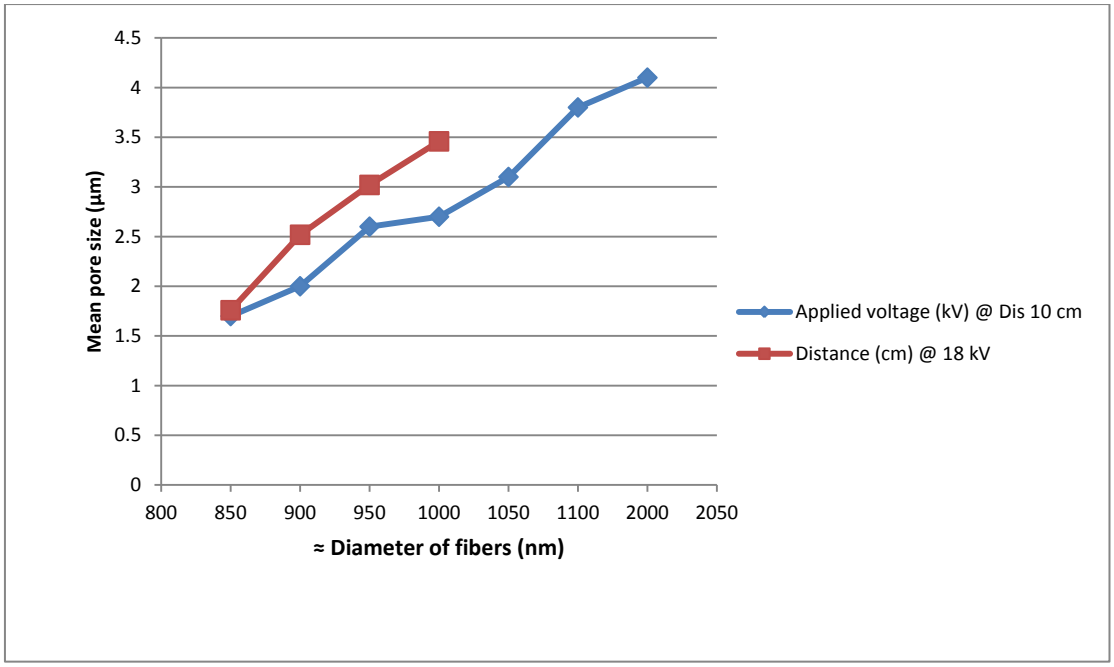

Figure 4.16 Correlation between diameters of nanofibers with mean pore size of electrospun membranes tunable by preparations condition.

4.3.5 Mechanical property of electrospun membranes

The electrospun membranes were tested for their tensile strength and elongation at break. The results are reported in Table 4.6.

Table 4.6 Tensile strength and elongation at break of electrospun membranes which were prepared under conditions, a spinneret-to-collector distance of 10 cm, a flow rate of 20 µL/min, and a spinneret diameter of 0.8 mm, a speed of substrates moving of 2.2 cm/min, 65% RH and using PET nonwoven as the substrate but with variation of applied voltage in electrospinning process.

Applied voltage (kV)	Porosity (%)	Thickness (µm)	Fiber diameter (nm)	Tensile Strength (N)	Elongation (%)
14	88	228	993	6.9 ± 1.0	7.2 ± 1.7
16	91	218	909	4.7 ± 1.3	7.9 ± 1.8
18	93	205	875	4.6 ± 1.2	14.8 ± 1.2

The tensile strength and elongation at break properties testing results of electrospun membrane samples preparing under the conditions but with variation of applied voltage are shown in Table 4.6. It was found that tensile strength of electrospun membrane that was prepared by an applied voltage of 14 kV exhibited

the highest tensile strength (6.9 N), when compared with the electrospun membranes prepared under applied voltage of 16 and 18 kV (4.7 and 4.6 N, respectively). While, the elongation at break showed an increasing trend. However, the relations between the porosity and tensile strength of electrospun membranes also are shown in Table 4.6. It indicated that the tensile strength of electrospun membranes decreased with increasing porosity as well as decreasing fiber diameter and membrane thickness.

4.3.6 Contact angle of electrospun membranes

Sessile water drop static contact angle (CA) of electrospun membranes are presented in Figure 4.17.

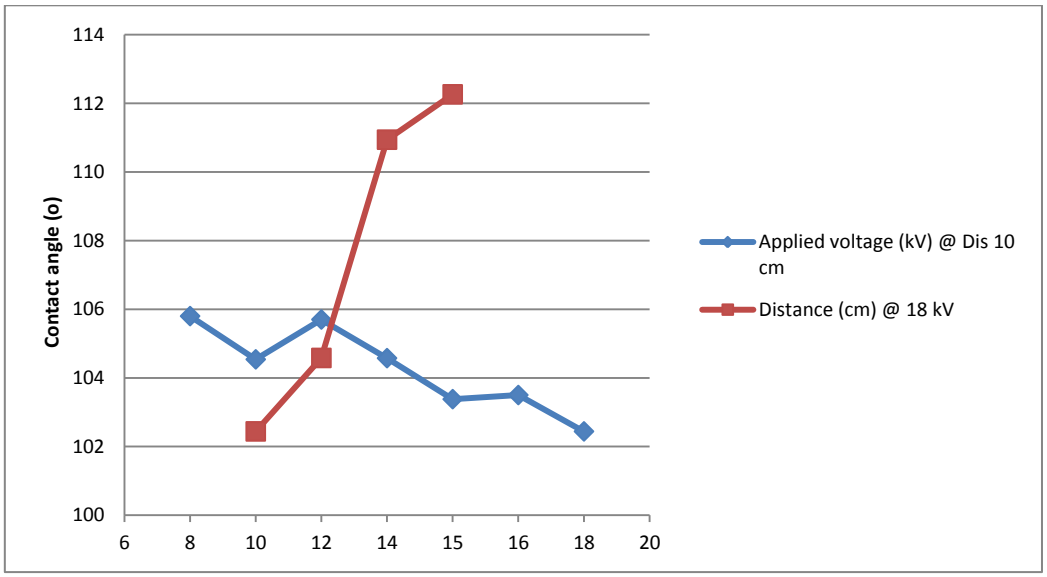

Figure 4.17 Contact angles of membranes by preparing under electrospinning conditions, a flow rate of 20 µL/min, a spinneret diameter of 0.8 mm, a speed of substrates moving of 2.2 cm/min, 65% RH and using PET nonwoven as the substrate but with varying applied voltage and distance between spinneret-to- collector.

As clearly seen in Figure 4.17, all membranes prepared as electrospun nanofiber-web shows similar and high contact angle. The contact angles of electrospun membranes are ranging from 102° to 112°, while the typical nonporous PES film has ≈70° [4]. The observed high CA of the electrospun nanofiber membranes in comparison with that of the nonporous PES film should be a result of the surface roughness that is introduced multiple contacting points on the water

surface such that the interface area between the water droplet and the nanofiber membranes surface becomes smaller. However, correlation of contact angle of rough surfaces relation to the normal smooth surface have been proposed by using contact angle model for explanation regarding those phenomenon, which the well known is the Cassie-Baxter's model. The assumption of the Cassie-Baxter's model (see Figure 4.18) is when measuring contact angle on the highly rough surface such as a hydrophobic electrospun nanofiber membrane, the liquid drop is rested upon a composite surface of polymer fiber and air gaps between them [cf. 107,108]. This could be also explained because the PES electrospun membrane had high surface porosity (see Figure 4.6 and 4.7).

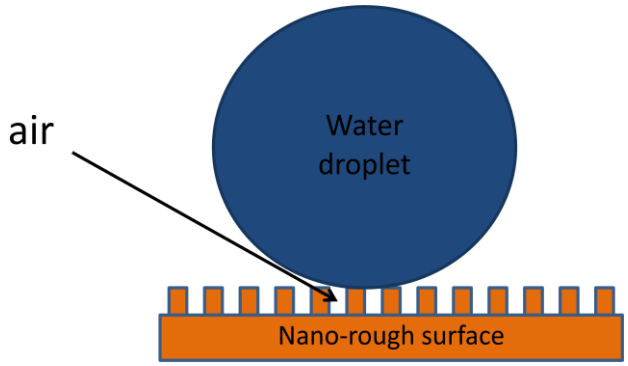

Figure 4.18 Schematic of the Cassie-Baxter's model.

4.4 Performance of PES electrospun membranes

4.4.1 Gas permeability

Gas permeability of electrospun membranes are summarized in Figure 4.19.

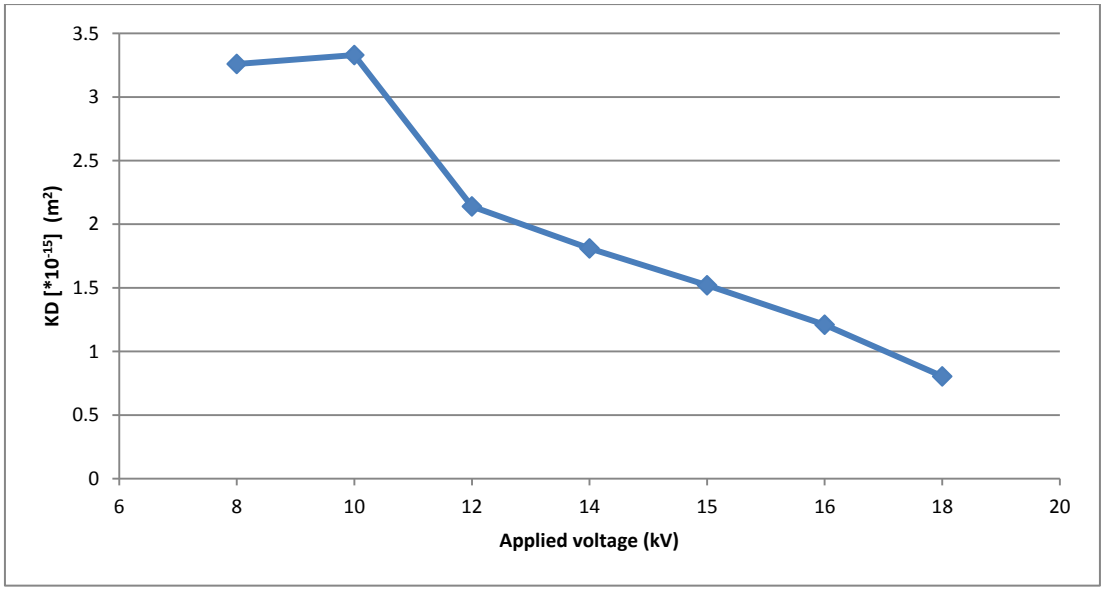

Figure 4.19 N_2 gas permeability of PES electrospun membranes prepared by using conditions, a spinneret-to-collector distance of 10 cm, a flow rate of 20 µL/min, a spinneret diameter of 0.8 mm, 65% RH, a speed of substrates moving of 2.2 cm/min and using PET nonwoven as the substrate, but with variation applied voltage in process.

Gas flow through electrospun membranes could be explained with the theory that assumes that porous media is a bundle of cylindrical tubes passing from one surface of the membranes to the other surface, and not necessarily perpendicular to the surface [84]. Figure 4.19 showed that increasing applied voltage led to decreased gas permeability of electrospun membranes. It is to be noted here that there is a close relationship between the applied voltage and fiber diameter and also mean pore size of membranes. As the diameter of electrospun fibers decreases with increasing electric field, hence the mean pore size also decreases. Consequently, the mean pore size has affected the gas permeability that decreasing of mean pore size leads to decreasing gas permeability of electrospun membranes as well (see Figure 4.20). In addition, decreasing of thickness (see Figure 4.11) and increasing of porosity (see Figure 4.12) also lead to decreased gas permeability of electrospun membranes.

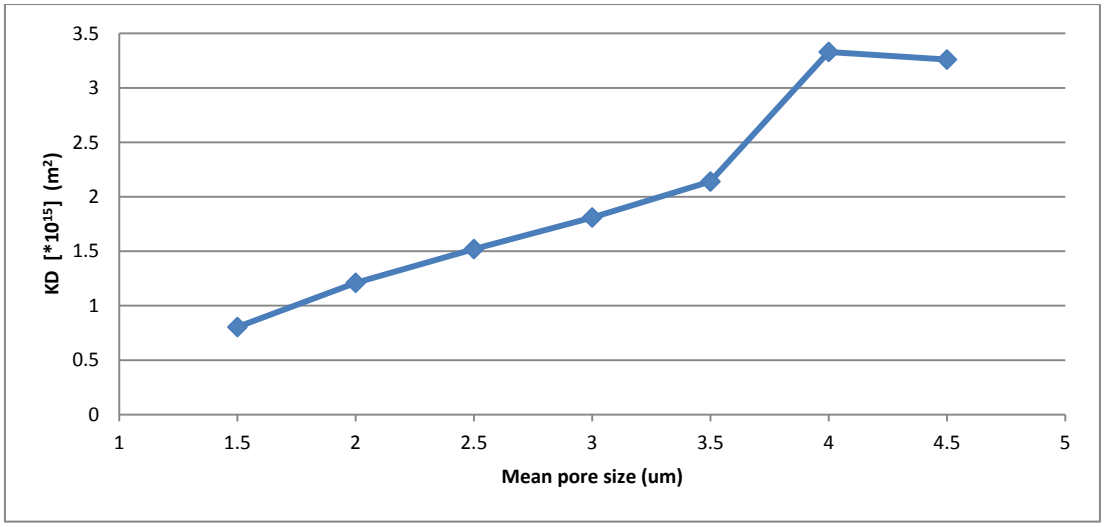

Figure 4.20 Correlation between mean pore size with N_2 gas permeability of electrospun membranes tunable by preparations condition.

4.4.2 Air filtration performance

The air filtration data of PES electrospun membranes are presented in Figure 4.21.

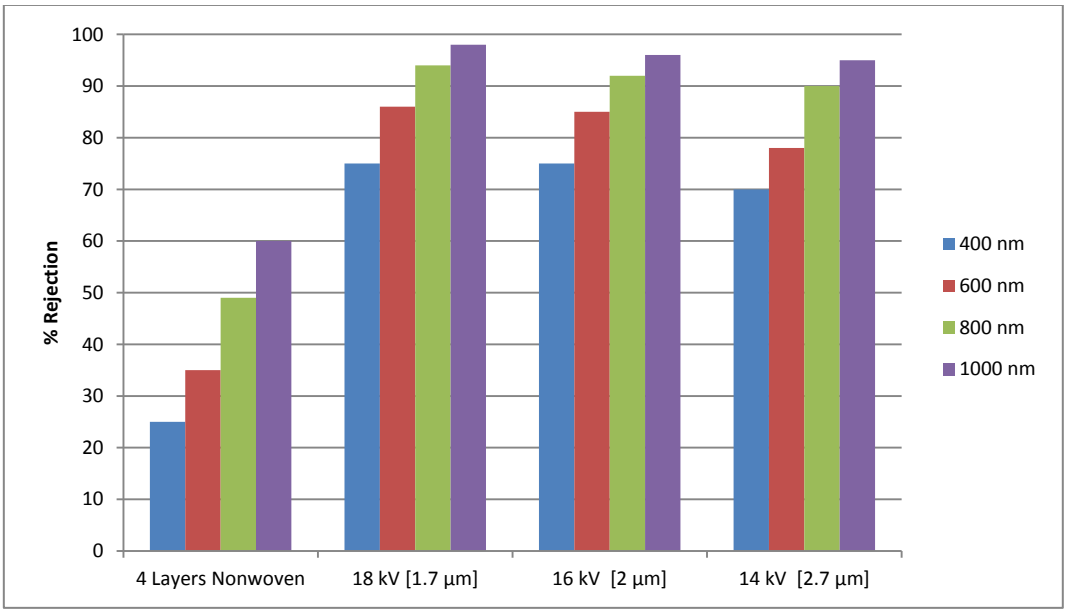

Figure 4.21 Aerosol (DEHS) collection efficiency of electrospun nanofiber prepared by using conditions, a spinneret-to-collector distance of 10 cm, a flow rate of 20 µL/min, a spinneret diameter of 0.8 mm, a speed of substrates moving of 2.2 cm/min, 65% RH and using PET nonwoven as the substrate, but with variation applied

voltage, compared with commercial nonwoven (Novatexx 2429) at average pressure drop of 350 Pa.

The efficiency of the DEHS particles collection (in the size-range from 400 – 1000 nm) passing through the 4 layers commercial nonwoven (Novatexx 2429) with pore size of 8 µm and thickness of 150 µm and a single electrospun membrane with the backing layers, i.e. nonwoven-electrospun nanofiber-nonwoven, are shown in Figure 4.21. The aerosol (DEHS) filtration performance of electrospun nanofiber web was much greater than that of the 4 layers commercial nonwoven. This, the 4 layers commercial nonwoven is able to reject the DEHS nano particles only about 25% of 400 nm, 35% of 600 nm, 48% of 800 nm and 60% of 1000 nm. While, the electrospun nanofiber, with the highest applied voltage of 18 kV (pore size 1.7 µm), is able to reject the DEHS nano particles more than 70% of 400 nm, 85% of 600 nm, 90% of 800 nm and 98% of 1000 nm. This result clearly demonstrated the potential of electrospun nanofiber in the development of filter material against aerosol nanoparticles. However, Figure 4.21 also shows that aerosol (DEHS) collection efficiency of electrospun nanofiber is dependent of the applied voltage in the process, that the electrospun nanofiber prepared by applying higher voltage has higher aerosol rejection than electrospun nanofiber prepared with lower voltage. It should be noted that the electrical potential makes a pore size significant influence on the aerosol (DEHS) collection efficiency of electrospun nanofiber. These results can be also explained by using the diameter of fiber and the mean pore size data. Reduced diameter of nanofibers led to decreasing mean pore size of electrospun filter (cf. Figure 4.16). In addition, increased fiber diameter web also induces increased specific surface area of the web, which enables the probability of particle deposition on the fiber surface to be increased [39]. Moreover, the mechanisms of particles removal are captured by the large particles are blocked on the filter surface due to the sieve effect and the particles which are smaller than the surface-pores would penetrate into the nanofibers filter, as collected by fibers, via either interception or impaction, or static electrical attraction. Therefore, very fine particles could be collected due to the Brownian motion effect [5,39,58].

4.4.3 Water flux

The PES electrospun membranes were tested in the water filtration to check the performance. Water flux is summarized in Figure 4.22.

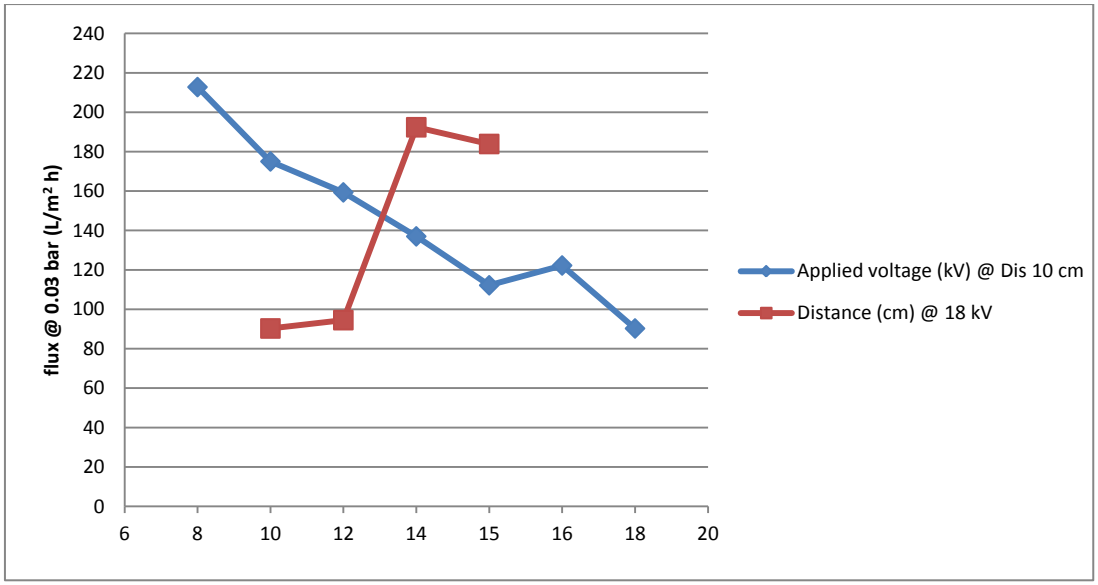

Figure 4.22 Water flux of PES electrospun membranes prepared by using conditions, a flow rate of 20 µL/min, a spinneret diameter of 0.8 mm, a speed of substrates moving of 2.2 cm/min, 65% RH and using PET nonwoven as the substrate with variation applied voltage and distance between spinneret-to-collector in process.

According to the water flux profile shown in Figure 4.22, the electrospun membranes prepared by applying higher voltage have lower flux than membranes prepared with lower voltage. At the applied voltage of 8 kV, the water flux was very high at 212 L/m^2 h. As the applied voltage in process was increased from 10 kV to 18 kV, the water flux of the electrospun PES membrane was decreased from 175 to 90 L/m^2 h. This can be explained in term of the decreased pore size of the electrospun PES membrane.

Figure 4.22 also showed the water flux profile of PES electrospun membranes prepared by variation of distance between spinneret-to-collector in process. It was seen that the electrospun membranes prepared by increasing distance between spinneret-to-collector leads to increasing water flux of membranes, when membranes were electrospun at distance spinneret-to-collector of 15 cm led to highest water flux (183 L/m^2 h). Whereas, the water flux of electrospun membranes reduced from 183 to 94 L/m^2 h, when the distance between spinneret-to-collector was decreased from 14 cm to 10 cm.

The mean pore size of the electrospun PES membrane, (cf. Figure 4.15), by preparing at high applied voltage is lower than electrospun membranes by preparing at low applied voltage. Furthermore, the result in Figure 4.15, it was found that the mean pore size of electrospun membranes increased with increasing distance between spinneret-to-collector. Correlating these results between mean pore size with water flux of electrospun membranes are shown in Figure 4.23, it could be explained that the mean pore size of electrospun membranes are the crucial

parameter to measuring the water flux of the electrospun membranes, that is decreasing of mean pore size leads to decreasing water flux of electrospun membranes. Similarly, such a performance has been reported by other researchers [5,6,86-109].

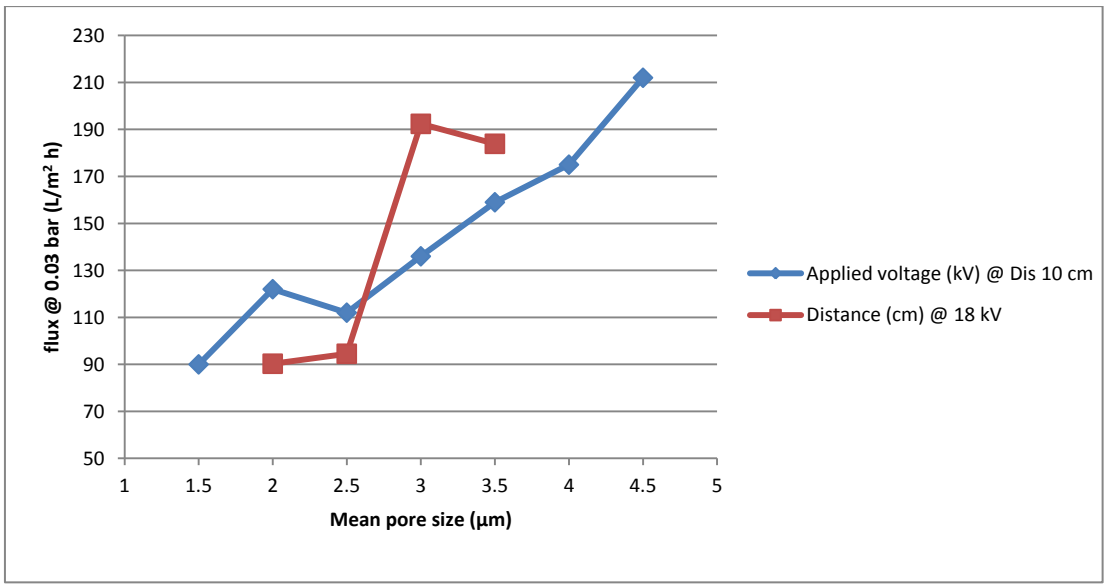

Figure 4.23 Correlation between mean pore size with water flux of electrospun membranes tunable by preparations condition.

4.4.4 Water filtration performance

Figure 4.24 shows filtrate flux during the measurement of rejection efficiency with silica nanoparticles (size 35 nm) and feed solution concentration of 1.5 %wt/v.

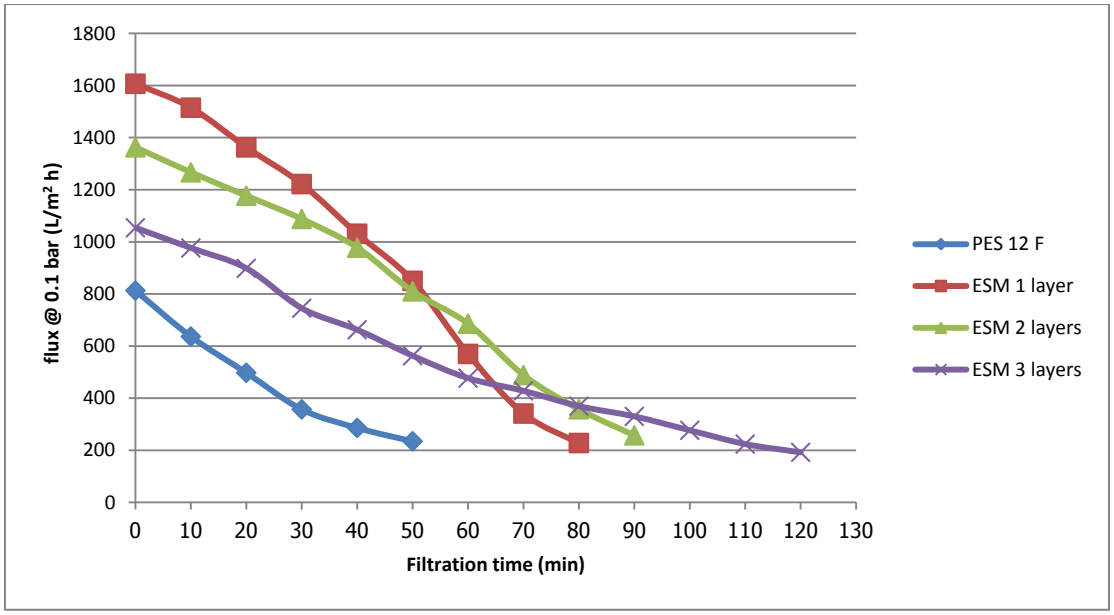

Figure 4.24 Filtrate flux during the measurement of rejection efficiency with silica nanoparticles (size 35 nm) for PES electrospun membranes by using conditions, applied voltage of 18 kV, a spinneret-to-collector distance of 10 cm, a flow rate of 20 µL/min, a spinneret diameter of 0.8 mm, a speed of substrates moving of 2.2 cm/min, 65% RH and served the PET nonwoven as the substrate, compared with commercial membrane (PES 12F Membrana).

As clearly seen in Figure 4.24, the fluxes through the commercial membrane (PES 12F) dropped very rapidly in the beginning of filtration for silica nanoparticles. The filtrate fluxes of commercial membrane (PES 12F Membrana) were much smaller than the filtrate fluxes of PES electrospun membrane. It should be noted that the mean pore size (1 µm) and porosity (65%) of the commercial membrane were smaller than PES electrospun membrane. However, the filtrate fluxes of varying layer of PES electrospun membrane were in the following order: ESM 1 layer > ESM 2 layers > ESM 3 layers. This indicated that the thickness of electrospun membrane increased, lower flux was obtained. Such phenomenon had been observed in the previous reported literature [95]. The 3 layers electrospun membrane also showed the longest filtration time to reach the value of 200 L/m^2 h at 0.1 bar (120 min) compared to the 2 layers (90 min), 1 layer (80 min) of electrospun membrane and commercial membrane (50 min), respectively.

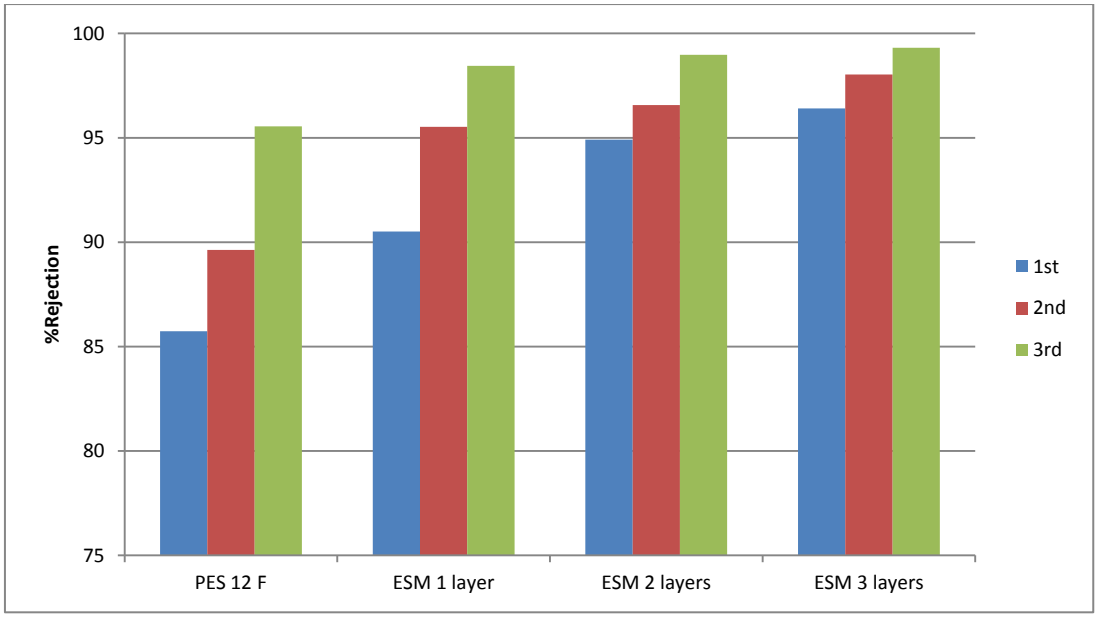

Figure 4.25 Rejection tests of membranes investigated by measuring three retention values, for the first, the second and the third of 5 ml permeate.

In general, rejection data presented in Figure 4.25 show that the PES electrospun membranes had the higher particles rejection than PES commercial membrane. Besides, the rejections of electrospun membranes were well above 90%, while commercial membrane rejected the nanoparticles of 85% at the first measuring retention. This implies that the PES electrospun membranes were successful in rejecting these nanoparticles. However, the rejection of varying layer of PES electrospun membrane was in the following order: ESM 3 layers > ESM 2 layers > ESM 1 layer. At the end of rejection experiment run, the PES electrospun membranes exhibited the rejection above 98%. Because of the nanoparticles are small, they were able to pack closely together, reducing the effective pore size of the electrospun membrane significantly at the surface. This dense “cake layer” acted as the separating layer for the electrospun membrane. However similar phenomenon is found in many previously reported works [5,6,100].

Furthermore, the water flux profile before and after silica nanoparticles separation is shown in Figure 4.26.

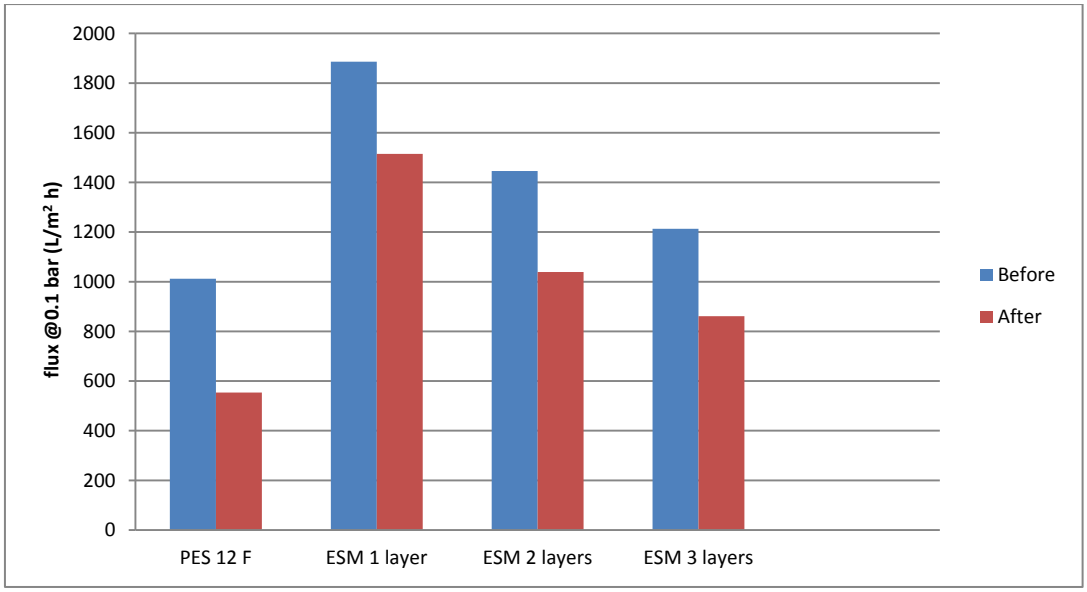

Figure 4.26 Pure water flux of membranes before and after silica nanoparticles separation.

Overall, PES electrospun membrane showed greater water flux than commercial membrane both before and after separation. The layer increase leads to decreasing water flux of electrospun membranes. Importantly, it is clearly shown that the water flux before particles separation of all membrane was higher than the water flux after particles separation. As the nanoparticles were small, they were able to pack closely together giving a so-called "layer effect", and hence reducing the effective pore size of electrospun membrane after particles separation. Consequently, the water flux of electrospun membrane after particles separation would result in lower flux. Moreover, as the data shows in Table 4.7, it indicated that PES electrospun membranes, which were achieved in this work, are competitive with a state-of-art of microfiltration membranes with similar pore diameter.

Table 4.7 Properties and filtration performance of PES electrospun membranes by using conditions, applied voltage of 18 kV, a spinneret-to-collector distance of 10 cm, a flow rate of 20 µL/min, a spinneret diameter of 0.8 mm, a speed of substrates moving of 2.2 cm/min, 65% RH and served the PET nonwoven as substrate, compared to commercial membrane (PES 12F Membrana) and other electrospun membranes in literature review.

Polymer	Fiber diameter (nm)	Pore size (µm)	Thickness (µm)	Permeability (l/m^2.h.bar)	Filtration performance (%)	Particle size (µm)	Ref.
PES	875	1.7	205	18860	98	0.035	this work
PES 12F	(film)	1	110	10000	85	0.035	this work
PES	280	2.0	200	2080	98	1.0	[92]
PSU	470 ± 150	2.1	135	13333	94	1.0	[6]
PVDF	380 ± 106	4.1	300	4000	91	5.0	[7]
PAN-PET	100	0.22	200	2189	97	0.5	[58]

Chapter 5
Conclusions and Outlook

5. Conclusions and outlook

5.1 Conclusions

Through this work, nanofiber membranes were produced from polyethersulfone (PES) by means of electrospinning process. The effect of 5 processing variables, including polymer concentration, applied voltage, spinneret-to-collector distance, substrate and humidity, were thoroughly investigated. The first results demonstrated that with a voltage of 30 kV, a spinneret-to-collector distance of 10 cm and a PES solution concentration of 22%, the formation of uniform nanofibers without any beads could be achieved in a stationary substrate set-up. Remaining process parameters were constant with a flow rate of 20 µL/min and a spinneret diameter of 0.8 mm. A PET nonwoven served as the substrate. Electrospun nanofibers with fiber diameter as small as 489 nm were produced.

The ambient humidity proved to be of major importance, which can be explained by its influence on solvent evaporation. In contrast to other polymer systems, the optimum electrospinning conditions were given at a high humidity of the order of 65% RH.

Actual nanofiber membranes could be manufactured by electrospinning PES on moving substrates as, e.g., PET nonwoven. Compared to the stationary experiment, the spinning conditions had to be further adapted to produce fibers of constant diameter. Namely, the voltage had to be decreased further. Typical spinning conditions were a voltage of 18 kV and a spinneret-to-collector distance of 10 cm. Under these spinning conditions, electrospun membranes with a mean fiber diameter of 875 ± 156 nm, a thickness of 205 µm and a calculated basic weight of 0.169 mg/cm^2 were obtained. The mean pore size was found to be 1.7 µm, and a porosity of 93% was determined by water emersion test. The tensile strength of the membrane was 4.6 N and contact angles in excess of ≈102°.

By variation of voltage and distance the characteristics of the membranes could be controlled to a certain degree.

Filtration membrane properties, such as N_2 gas flow and the efficiency of the DEHS particles collection (in the size-range from 400 – 1000 nm) as well as the pure water flux, the filtrate flux and rejection of 35 nm silica nanoparticles were investigated.

With regard to air filtration, it was found that the PES electrospun membranes, which were prepared by increasing applied voltage, showed decreasing N_2 gas permeability with decreasing mean pore size. Besides, the aerosol (DEHS in the size-range from 400 – 1000 nm) filtration performance of PES electrospun

nanofiber web was much greater than that of the 4 layers commercial nonwoven with pore size of 8 µm (Novatexx 2429). This result clearly demonstrated the potential of electrospun nanofiber in the development of filter material against nano-sized particles and aerosols.

Water flux of the electrospun membranes can be controlled by the spinning conditions. Membranes prepared with higher voltage have lower flux than membranes prepared with lower voltage. The electrospun membranes, which were prepared at an increased distance between spinneret-to-collector, exhibited high water flux. Both effects can easily be explained by the influence on the spinning parameters onto pore size. The filtrate fluxes of PES commercial membrane with pore size of 1 µm (12F Membrana) was much smaller than the filtrate fluxes of all investigated PES electrospun membranes. Overall, PES electrospun membrane showed greater water flux than commercial membrane (12F Membrana) both before and after silica nanoparticles of 35 nm. In spite of their rather large pore sizes and the high water flux, the PES electrospun membranes had the higher particles rejection than PES commercial membrane (12F Membrana). At the first retention measurement, the rejection of PES electrospun membranes was well above 90%, while PES commercial membrane (12F Membrana) rejected the silica nanoparticles by 85%. Moreover, the PES electrospun membranes exhibited the rejection above 98% at the end of rejection experiment run. It can be concluded from these results that electrospun nanofiber PES membranes can be used in various applications such as removal of nano or micro-particles from waste-water, e.g., pre-filters to minimize contaminations and fouling prior to UF or NF. In summary, the results suggest that PES electrospun nanofiber membranes are excellent materials for high flux MF applications.

5.2 Outlook

Generally, high performance MF membranes can be made from PES but the main limitation of this material is that it is prone to fouling due to its relatively hydrophobic character (cf. section 4.3.6). Therefore, membrane modification is usually done to increase the membrane resistance towards fouling. Common methods used to manufacture low fouling membranes are blending membrane polymer with hydrophilic additive (e.g., PVP). Moreover, polymeric additives (usually hydrophilic polymers) in a casting solution are also used in order to increase both pore size and porosity (performing agent) and to suppress macrovoid formation and increases membrane hydrophilicity.

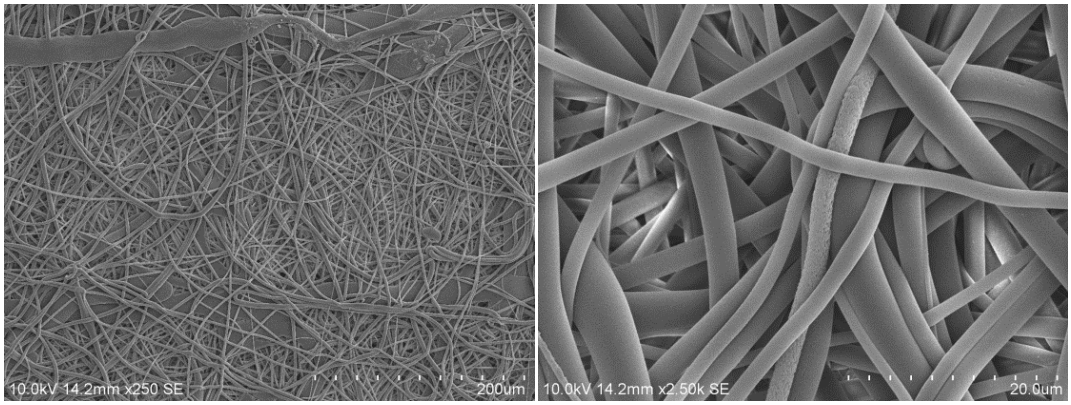

Figure 5.1 Morphology of electrospun membrane prepared from 22% PES with 5% Pluronic, using the processing condition, i.e., an applied voltage of 18 kV, a flow rate of 20 µL/min, a spinneret-to-collector distance of 10 cm, a spinneret diameter of 0.8 mm, moving speed of substrate of 2.2 min/cm, 65% RH and PET nonwoven served as the substrate.

A first experiment in this direction conducted as a proof of principle was performed in the further work of this research. 5% Pluronic (31R1) was added to a standard spinning solution and spun under same conditions as before. The result from SEM images (Figure 5.1) of the electrospun 22% PES and 5% Pluronic nanofibers membrane using the same processing condition as before and PET nonwoven served as substrate, exhibited in irregular fiber formation and the diameter of fibers were varying thickness. These results could be explained in term of the viscosity of the solution effect (cf. section 2.2.1.1). When the processing conditions, i.e., an applied voltage, a flow rate and a spinneret-to-collector distance, are varied and the resulting fiber diameter becomes into nano range. Then, the electrospun membranes would be expected to improve the wetability and filtration performance. Therefore, this work is worth continuous research.

References

[1] W.S. Winston Ho, K.K. Sirkar, Membrane handbook, Van Nostrand Reinhold, New York, 1992.

[2] M. Cheryan, Ultrafiltration and microfiltration handbook, Technomic Publishing Company Inc., Pennsylvania, 1998.

[3] R.W. Baker, Membrane technology and applications, 2nd ed., John Wiley & Sons, Ltd., Chichester, 2004.

[4] H. Susanto, M. Ulbricht, Characteristic, performance and stability of poly(ether sulfone) ultrafiltration membranes prepared by phase separation method using different macromolecular additive, J. Membr. Sci., 327 (2009) 125-135.

[5] F. Jian, N. Haitao, L. Tong and W. Xungai, Application of electrospun nanofibers, J. Chin. Sci. Bull., 53 (2008) 2265-2286.

[6] R. Gopal, S. Kaur, C. Y. Feng, C. Chan, S. Ramakrishna, S. Tabe and T. Matsuura, Electrospun nanofibrous polysulfone membranes as pre-filters: Particular removal, J. Membr. Sci., 289 (2007) 210-219.

[7] R. Gopal, S. Kaur, Z. Ma, C. Chan, S. Ramakrishna and T. Matsuura, Electrospun nanofibrous filtration membrane, J. Membr. Sci., 281 (2006) 581-586.

[8] T. Uyar, R. Havelund, Y. Nur and J. Hacaloglu, Molecular filters based on cyclodextrin functionalized electrospun fibers, J. Membr. Sci., 332 (2009) 129-137.

[9] http://www.nano.kku.ac.th

[10] M. Ziabari, V. Mottaghiable, A. K. Haghi, Application of direct tracking method for measuring electrospun nanofiber diameter, Braz. J. Chem. Eng., 26 (2009).

[11] Z. M. Huan, Y. Z. Zhan, M. Kotaki, S. Ramakrishna, A review on polymer nanofibers by electrospinning and their applications in nanocomposites, J. Comp. Sci., 63 (2003) 2223-2253.

[12] http://www.chromacademy.com/Electrospray-Ionization-ESI-for-LC-MS.asp

[13] N. G. McCrum, C. P. Buckley, C. B. Bucknall, Principles of polymer engineering, Oxford University Press, USA, 1997.

[14] C. J. Buchko, L. C. Chen, S. Y. Martin, Processing and microstructural characterization of porous biocompatible protein polymer thin films, D. C. Polym., 40 (1999) 7397.

[15] S. Ramakrishna, K. Fujihara, W. E. Teoteik, C. Lim, Z. Ma, An Introduction to electrospinning and nanofibers, World Scientific Publishing, 2005.

[16] S. L. Shenoy, W. D. Bates, H. L. Frisch, G. E. Wnek, Role of chain entanglements on fiber formation during electrospinning of polymer solutions: good solvent, non-specific polymer–polymer interaction limit, Polymer, 46 (2005) 3372-3384.

[17] X. Zong, K. Kim, D. Fang, S. Ran, B. S. Hsiao, B. Chu, Structure and process relationship of electrospun bioabsorbable nanofiber membranes, Polymer, 43 (2002) 4403-4412.

[18] M. Ma, G. C. Rutledge, Nanostructured electrospun fibers, Polym. Sci., 7 (2012) 187-208.

[19] H. Fong, D. H. Reneker, Elastomeric nanofibers of styrene-butadiene-styrene blocks copolymer, J. Polym. Sci. Pt. B-Polym. Phys., 37 (1999) 3488-3493.

[20] C. Mituppatham, M. Nithitanakul, P. Supaphol, Ultrafine electrospun polyamide-6 fibers: effect of solution conditions on morphology and average fiber diameter. Macromol. Chem. Phys., 205 (2004) 2327-2338.

[21] C. Yao, X. Li, K. G. Neoh, Z. Shi, E. T. Kang, Surface modification and antibacterial activity of electrospun polyurethane, J. Membr. Sci., 320 (2008) 259-267.

[22] K. Tan, S. K. Obendorf, Fabrication and evaluation of electrospun nanofiberrous antimicrobial Nylon 6 membrane, J. Membr. Sci., 305 (2007) 287-298.

[23] X. Li, X. Hao, D. Xu, G. Zhang, S. Zhong, H. Na, D. Wang, Fabrication of sulfonated poly(ether ether ketone ketone) membrane with high proton conductivity, J. Membr. Sci., 281 (2006) 1-6.

[24] Z. Tang, C. Qiu, J. R. McCutcheon, K. Yoon, H. Ma, D. Fang, E. Lee, C. Kopp, B. S. Hsiao, B. Chu, Design and fabrication of electrospun poly(ether sulfone) nanofibrous scaffold for high-flux nanofiltration, J. Polym. Sci. Pt. B-Polym. Phys., 47 (2009) 2288-2300.

[25] K. Nakata, S. H. Kim, Y. Ohkoshi, Y. Gotoh, M. Nagura, Electrospinning of poly (ether sulfone) and evaluation of the filtration efficiency, Society of Fiber Sci. and Technol. Japan, 63 (2007) 307-312.

[26] M. Kang, H.J. Jin, Electrically conducting electrospun silk membranes fabricated by adsorption of carbon nanotube, Coll. Polym. Sci., 285 (2007) 1163-1167.

[27] B. Wang, Y. Sun, H. Wang, Preparation and properties of electrospun PAN/Fe_3O_4 magnetic nanofibers, J. Appl. Polym. Sci., 115 (2010) 1781-1786.

[28] H. Fong, I. Chun, D. H. Reneker, Beaded nanofibers formed during electrospinning, Polymer, 40 (1999) 4585.

[29] J. Zeng, X. Xu, X. Chen, Q. Liang, X. Bian, L. Yang, X. ling, Biodegradable electrospun fibers for drug delivery, J. Contr., 92 (2003) 227-231.

[30] P. K. J. Baumgarten, Electrostatic spinning of acrylic microfibers, Colloid Interface Sci., 36 (1971) 71.

[31] S. Megelski, J. S. Stephens, D. B. Chase, J. F. Rabolt, Micro- and nano-structured surface morphology on electrospun polymer fibers, Macromolecules, 35 (2002) 8456-8466.

[32] K. H. Lee, H. Y. Kim, La, Y. M. Lee, N. H. Sung, Influence of a mixing solvent with tetrahydrofuran and N,N-dimethylformamide on electrospun poly(vinyl chloride) nonwoven mats, J. Polym. Sci.: Part B: Polym. Phys., 40 (2004) 2259.

[33] M, Bognitzki, W. Czado, T. Frese, A. Schaper, M. Hellwig, M. Steinhart, A. Greiner, H. Wendorff, Nanostructured fibers via electrospinning, Adv. Mater., 13 (2001) 70.

[34] S.V. Fridrikh, J.H. Yau, M.P. Brenner, G.C. Rutledge, Controlling the fiber diameter during electrospinning, Phys. Rev. Lett., 90 (2003) 144-502.

[35] T. Bahners, U. Schlosser, E. Schollmeyer, Field modification for optimized fiber production by electrospinning, Chem. F. Inter., 4 (2006) 246-249.

[36] G. Taylor, Disintegration of Water Drops in an Electric Field. Proc. R. Soc. Lond.,

280 (1964) 383-397.

[37] X. Zong, K. Kim, D. Fang, S. Ran, B. S. Hsiao, B. Chu, Structure and process relationship of electrospun bioabsorbable nanofiber membranes, Polymer, 43 (2002) 4403-4412.

[38] J. S. Lee, K.H. Choi, D. H. Ghim, S. S. Kim, D. H. Chun, H. Y. Kim, W. H. Lyoo, Role of molecular weight of a tactic poly(vinyl alcohol) (PVA) in the structure and properties of PVA nanofabric prepared by electrospinning, J. Appl. Polym. Sci., 93 (2004) 1638-1646.

[39] H. S. Park, Y. O. Park, Filtration properties of electrospun ultrafine fiber webs, Korean J. Chem. Eng., 22 (2005) 165-172.

[40] R. S. Barhate, C. K. Loong, S. Ramakrishna, Preparation and characterization of nanofibrous filtering media, J. Membr. Sci., 283 (2006) 209-218.

[41] S. L. Zhao, X. H. Wu, L. G. Wang, Y. Huang, Electrospinning of ethyl-Cyanoethyl cellulose/tetrahydrofuran solutions, J. Appl. Polym. Sci., 91 (2004) 242-246.

[42] E. S. Medeiros, L. H. C. Mattoso, R. D. Offeman, D. F. Wood, W. J. Can, J Chem., 86 (2008) 590-599.

[43] C. Wang, C. H. Hsu, L. H. Lin, Macromolecules, 39 (2006) 7662-7672.

[44] P. K. Baumgarten, Electrostatic spinning of acrylic microfibers, J. Colloid Interface Sci., 36 (1971) 71.

[45] R. Gopal, S. Kaur, Z. Ma, C. Chan, S. Ramakrishna, T. Matsuura, Electrospun nanofibrous filtration membrane, J. Membr. Sci., 281 (2006) 581-586.

[46] J. He, Y. Wan, J. Yu, Application of vibration technology to polymer electrospinning, Inter. J. Nonli. Sci. and Numer. Simul., 5 (2004) 253-262.

[47] V. Beachley, X. Wen, Polymer nanofibrous structures: Fabrication, biofunctionalization, and cell interactions, Prog. Polym. Sci., 35 (2010) 868-892.

[48] Z. Huang, Y. Z. Zhang, M. Kotaki, S. Ramakrishna, A review on polymer nanofibers by electrospinning and their applications in nanocomposites, Composites Sci. and Technol., 63 (2003) 2223-2253.

[49] http://www.smartsynthetics.com/amsoil-filters

[50] http://www.downdraft.com/filters/filters.htm

[51] http://www.freedm.ncsu.edu

[52] http://www.stevens.edu

[53] http://www.nanowerk.com

[54] http://www.epa.gov

[55] K. Sutherland, Filters and filtration handbook, 5th, Elsevier, USA, 2008.

[56] http://www.lydallfiltration.com/

[57] http://www.filtsep.com/view/30721/

[58] R. Wang, Y. Liu, B. Lia, B. S. Hsiao, Electrospun nanofibrous membranes for high flux microfiltration, J. Membr. Sci., 392-393 (2012) 167-174.

[59] A. Holzmeister, M. Rudisile, A. Greiner, J. H. Wendorff, Structurally and chemically heterogeneous nanofibrous nonwovens via electrospinning, Euro. Polym. J., 43 (2007) 4859-4867.

[60] K. Yoon, B. S. Hsiao and B. Chu, Functional nanofibers for environmental applications, J. Mater. Chem., 18 (2008) 5326-5334.

[61] P. P. Tsaia, H. Schreuder-Gibson, P. Gibson, Different electrostatic methods for making electrets filters, J. Electrost., 54 (2002) 333-41.

[62] T. Bahners, E. Schollmeyer, Multi-layer deep bed filter for micron/submicron separation, Filtration, 8 (2008) 135-139.

[63] T. Bahners, E. Schollmeyer, Technische textilien, 44 (2001) 130.

[64] N. Fuchs, The mechanics of aerosols, Pergamon Press, Oxford, 1946.

[65] G. Pflueger, A. Bossman, W. Ringens, T. Bahners, H. Fissan, E. Schollmeyer, Textil Praxis Int., 40 (1985) 1300.

[66] T. Bahners, E. Schollmeyer, J. Aerosol Sci., 17 (1986) 191.

[67] T. Bahners, E. Schollmeyer, Staub-Reinh. Luft., 47 (1987) 115.

[68] V. Thavasi, G. Singh, S. Ramakrishna, Electrospun nanofibers in energy and environmental applications, Energy Environ. Sci., 1 (2008) 205-221.

[69] http://www2.donaldson.com

[70] R. W. Baker, Membrane Technology and Applications, 2nd ed., Wiley, 2004.

[71] W. C. Hinds, Aerosol technology, 2nd ed., Wiley, New York, 1999.

[72] K. M. Yun, C. J. Hogan, Y. Matsubayashic, M. Kawabec, F. Iskandara, K. Okuyama, Nanoparticle filtration by electrospun polymer fibers, Chem. Eng. Sci., 62 (2007) 4751-4759.

[73] A. Podgórski, A. Bałazy, L. Grado´n, Application of nanofibers to improve the filtration efficiency of the most penetrating aerosol particles in fibrous filters, Chem. Eng. Sci., 61 (2006) 6804-6815.

[74] A. Patanaika, V. Jacobsa, Rajesh, D. Anandjiwala, Performance evaluation of electrospun nanofibrous membrane, J. Membr. Sci., 352 (2010) 136-142.

[75] J. Pich, Theory of aerosol filtration by fibrous and membrane filters, in: C. N. Davies (Ed.), Aerosol Science, Academic Press, London, (1966) 223-283.

[76] Q. Zhang, J. Welch, H. J. Park, C. Yuwu, W. Sigmund, C.M. Marijnissen, Improvement in nanofiber filtration by multiple thin layers of nanofiber mats, J. Aero. Sci., 41(2010) 230-236.

[77] K. Soukup, D. Petrs, P. Kluson, O. Solcov, Nanofiber membranes evaluation of gas transport, Catalysis Today, 156 (2010) 316-321.

[78] S. Fotovati, H. V. Tafreshi, B. Pourdeyhimi, Influence of fiber orientation distribution on performance of aerosol filtration media, Chem. Eng. Sci., 65 (2010) 285-5293.

[79] W. W. F. Leung, C. H. Hung, Investigation on pressure drop evolution of fibrous filter operating in aerodynamic slip regime under continuous loading of submicron aerosols, Sep. Purif. Technol., 63 (2008) 691-700.

[80] W. W. F. Leung, C. H. Hung, Skin effect in nanofiber filtration of submicron aerosols, Sep. Purif. Technol., 92 (2012) 174-180.

[81] H. W. Lia, C. Y. Wua, F. Tepperb, J. H. Leea, C. N. Leec, Removal and retention of viral aerosols by a novel alumina nanofiber filter, Aero. Sci., 40 (2009) 65-71.

[82] A. D. Vaisniene, J. Ktunskis, G. Buika, Electrospun PVA nanofiber for gas filtration applications, Fiber&Textile in East. Euro., 77 (2009) 40-43.

[83] W. W. F. Leung, C. H. Hung, P. T. Yuen, Effect of face velocity, nanofiber packing density and thickness on filtration performance of filters with nanofibers coated on a substrate, Sep. Purif. Technol., 71 (2010) 30-37.

[84] M. A. Hassan, B. Y. Yeom, A. Wilkie, B. Pourdeyhimi, S. A.Khan, Fabrication of nanofiber meltblown membranes and their filtration properties, J. Membr. Sci., 427 (2013) 336-344.

[85] M. H. V. Mulder, Basic Principles of Membrane Technology, 2nd ed., Kluwer Academic Publishers, 1996.

[86] S. Kaur, Z. Ma, R. Gopal, G. Singh, S. Ramakrishna, T. Matsuura, Plasma-induced graft copolymerization of poly(methacrylic acid) on electro spun poly(vinylidene fluoride) nanofiber membrane, Langmuir, 23 (2007) 13085-13092.

[87] X. Zhuang, L. Shi, K. Jia, B. Cheng, W. Kang, Solution blown nanofibrous membrane for microfiltration, J. Membr. Sci., 429 (2013) 66-70.

[88] A. M. Bazargan, M. Keyanpour-rad, F. A. Hesari, M. E. Ganji, A study on the microfiltration behavior of self-supporting electrospun nanofibrous membrane in water using an optical particle counter, Desalination, 265 (2011) 148-152.

[89] B. Veleirinho, J. A. Lopes-da-Silva, Application of electrospun poly(ethylene terephthalate) nanofiber mat to apple juice clarification, Proc. Biochem., 44 (2009) 353-356.

[90] A. Cooper, R. Oldinski, H. Ma, J. D. Bryers, M. Zhang, Chitosan – based nanofibrous membranes of antibacterial filter applications, Carbohydrate Polymer, 92 (2013) 254-259.

[91] S. Sh. Homaeiogohar, K. Buhr, K. Ebert, Polyethersulfone electrospun nanofibrous composite membrane for liquid filtration, J. Membr. Sci., 365 (2010) 68-77.

[92] S. Sh. Homaeiogohar, J. Koll, E. T. Lilleodden, M. Elbahri, The solvent induced interfiber adhesion and its influence on the mechanical and filtration properties of poly(ether sulfone) electrospun nanofibrous microfiltration membranes, J. Membr. Sci., 98 (2012) 456-463.

[93] K. Yoon, K. Kim, X. Wang, D. Fang, B. S. Hsiao, B. Chu, High flux ultrafiltration membranes based on electrospun nanofibrous PAN scaffolds and chitosan coating, Polymer, 47 (2006) 2434-2441.

[94] W. J. Wrasidlo, K. J. Mysels, J. Parentral Sci. Technol., 38 (1984) 24.

[95] F. G. Paulsen, S. S. Shojaie, W. B. Krantz, Effect of evaporation step on macro-void for formation in wet-cast polymeric membranes, J. Membr. Sci., 91 (1994) 265

[96] R. S. Barhate, S. Ramakrishna, Nanofibrous filtering media: Filtration problems and solution from tiny materials, J. Membr. Sci., 296 (2007) 1-8.

[97] T. Eugene Cloete, M. D. Kwaadsteniet, M. Botes, Nanotechnology in water treatment applications, Caister Acadamic Press, Norfolk, UK, 2010.

[98] H. You, Y. Yin, X. Li, K. Zhanga, X. Wang, M. Zhua, B. S. Hsiao, Low pressure high flux thin film nanofibrous composite membranes prepared by electrospraying technique combined with solution treatment, J. Membr. Sci., 394– 395 (2012) 241-247.

[99] Z. Tang, J. Wei, L. Yung, B. Ji, H. Ma, C. Qui, K. Yoon, F. Wan, D. Fang, B. S. Hsiao, B. Chu, UV-cured poly(vinyl alcohol) ultrafiltration nanofibrous membrane based on electrospun nanofiber scaffolds, J. Membr. Sci., 328 (2009) 1-5.

[100] D. Aussawasathien, C. Teerawattananon, A. Vongachariya, Separation of micron to sub-micron particles from water: Electrospun Nylon-6 nanofibrous membranes as pre-filters, J. Membr. Sci., 315 (2008) 11-19.

[101] N. N. Bui, M. L. Lind, E. M. V. Hoek, J. R. Mccutcheon, Electrospun nanofiber supported thin film composite membranes for engineered osmosis, J. Membr. Sci., 385-386 (2012) 10-19.

[102] T. J. Sill, H. A. von Recum, Electrospinning: Applications in drug delivery and tissue engineering, Biomaterials, 29 (2008) 1989-2006.

[103] Y. Liu, R. Wang, H. Ma, B. S. Hsiao, B. Chu, High-flux microfiltration filters based on electrospun poly(vinyl alchhol) nanofibrous membranes, Polymer, 54 (2013) 548-556.

[104] Z. Ma, M. Kotaki, S. Ramakrishna, Electrospun cellulose nanofiber as affinity membrane, J. Membr. Sci., 265 (2005) 115-123.

[105] A. I. Gopalan, P. Santhosh, K. M. Manesh, J. H. Nho, S. H. Kim, C. G. Hwang, K. P. Lee, Development of electrospun PVdF-PAN membranes-based polymer electrolytes for lithium batteries, J. Membr. Sci., 325 (2008) 683-690.

[106] J. R. Kim, S. W. Choi, S. M. Jo, W. S. Lee, B. C. Kim, Electrospun PVdF-based fibrous polymer electrolytes for lithium ion polymer batteries, Electrochem. Acta., 50 (2004) 69.

[107] P. Roach, N. J. Shirtcliffe, M. I. Newton, Progress in super-hydrophobic surface development, The Royal Society of Chem., 4 (2008) 224-240.

[108] J. M. Lim, G. Y. Yi, J. H. Moon, C. J. Heo, S. M. Yang, Super hydrophobic films of electrospun fibers with multiple-scale surface morphology, Langmuir., 23 (2007) 7981-7989.

[109] S. Sh. Homaeiogohar, J. Koll, E. T. Lilleodden, M. Elbahri, The solvent induced interfiber adhesion and its influence on the mechanical and filtration properties of poly(ether sulfone) electrospun nanofibrous microfiltration membranes, J. Membr. Sci., 98 (2012) 456-463.

Appendix-1

List of Abbreviations

µL	microlitre
µm	micrometer
Avg	average
DEHS	di-ethyl-hexyl-sebacat
DMF	dimethylformamide
ESM	electrospun membrane
HEPA	high efficiency particulate air
kV	kilovolts
MF	microfiltration
N_2	nitrogen
NF	nanofiltration
nm	nanometer
NMP	n-methyl-2-pyrrolidone
Pa s	pascal-second
PAN	polyacrylonitrile
PCL	polycaprolactone
PDLA	polylactic acid
PEO	polyethylene oxide
PES	polyethersulfone
PET	polyethylene terephthalate
PLLA	poly-L-lactide acid

PS	polystyrene
PSU	polysulfone
PU	polyurethane
PVA	polyvinyl alcohol
PVC	polyvinyl chloride
PVDF	polyvinylidene fluoride
RH	relative humidity
SEM	scanning electron microscope
St	stokes number
TFNC	thin film nanocomposite
Tg	glass-transition temperature
THF	tetrahydrofuran
Tm	melting temperature

Appendix-2

List of Conferences

2011	International Congress on Membranes and Membrane Processes (ICOM) , Amsterdam, Netherlands.
	"Preparation of Electrospun Polyethersulfone Nanofiber Membranes" (poster paper)
2011	International Conference The World's Most Established Textile and Garment Machinery Technology Exhibition (ITMA), Barcelona, Spain
2010	Aachen- Dresden International Textile Conference, Dresden, Germany
	"Preparation of Electrospun Polyethersulfone Nanofiber Membranes" (poster paper)
2009	Aachen- Dresden International Textile Conference, Aachen, Germany

Appendix-3

Curriculum Vitae

Personal information:

Name	Bintasan KWANKHAO	Place of Birth	Trang, Thailand
Birth Date	February 27,1979	Nationality	Thai

Education:

2009-2013	Doctoral study at the University of Duisburg-Essen, Lehrstuhl für Technische Chemie II, Germany
2002-2004	Master of Science (Applied Polymer Science and Textile Technology), Chulalongkorn University, Thailand
	Thesis: Changes of Color and Physical Properties of Fabrics after UV Protection Finishing
1998-2002	Bachelor of Engineering (Textile Engineering), Rajamangala Institute of Technology, Thailand
	Project: A Study of Possibility of Bagasse Paper Pulp to Made Textile Fiber

Related job experience:

April 2005 – Current	Lecturer, Department of Textile Engineering, Faculty of Engineering, Rajamangala University of Technology Thanyaburi, Thailand
2003 – 2004	Assistant researcher, Center of Excellence in Textiles, Department of Material Science, Faculty of Science, Chulalongkorn University, Thailand

Research:

2007 – 2009	Co-researcher, “A Study of Producing Bullet Proof Vest from Man Made Fiber for Commercial Purposes”, Thailand Textile Institute, Ministry of Industry (in patent)

Training:

April – May, 2008	Swiss Textile College, Zurich and Wattwil, Switzerland